SCUOLA NORMALE SUPERIORE - PISA

Interaction of rotavirus nonstructural protein NSP5 with the viral replication complex

Thesis submitted for the degree of Doctor Philosophiae
(Perfezionamento in Genetica Molecolare e Biotecnologie)

Candidate:
Francesca Arnoldi

Supervisor:
Dr. Oscar Burrone

Academic Year 2007/2008

CONTENTS

ABSTRACT

Rotavirus morphogenesis starts in intracellular inclusion bodies called viroplasms, where synthesis of the11 dsRNA genome segments and their packaging in new viral particles take place. RNA replication is mediated by several viral proteins, of which VP1, the RNA-dependent RNA polymerase, and VP2, the core scaffolding protein, were shown to be sufficient to provide replicase activity *in vitro*. *In vivo*, however, viral replication complexes also contain the nonstructural proteins NSP2 and NSP5, which were shown to be essential for replication, to interact with each other and to form viroplasm-like structures (VLS) when coexpressed in uninfected cells.

In order to gain a better understanding of the intermediates formed during viral replication, this work focused on the interactions of NSP5 with VP1, VP2 and NSP2. We constructed a tagged form of VP1 and by coimmunoprecipitation experiments we demonstrated that VP1 and NSP5 interact in virus-infected cells as well as in the absence of other viral proteins or viral RNA in cotransfected cells. Using deletion mutants of NSP5 or different fragments of NSP5 fused to EGFP, we identified the 48 C-terminal amino acids as the region essential for interaction with VP1. On the other hand, removal of the C-terminal 15 amino acids from tagged VP1 resulted in a less efficient coimmunoprecipitation with NSP5, suggesting an involvement of the C-terminus of VP1. Interaction of NSP5 with VP2 was investigated by coexpression of the two proteins in uninfected cells, which resulted in a strong hyperphosphorylation of NSP5 and in the formation of VLS, that we named VLS(VP2i) to distinguish them from those induced by NSP2, here designated as VLS(NSP2i). VLS(VP2i) were shown to assemble independently of the phosphorylation degree of NSP5 and to recruit the viroplasm-resident proteins NSP2, VP1, VP2 and VP6 (the protein forming the middle

layer of the virion). Attempts to coimmunoprecipitate NSP5 and VP2 failed both from infected and cotransfected cells.

Tagged VP1 was found to localize in VLS (both VP2i and NSP2i) and in viroplasms, and to be able to replace wild-type VP1 structurally by being incorporated into progeny viral particles. Coexpression of different combinations of tagged VP1, NSP5, NSP2 and VP2 showed that the interaction of VP1 with NSP5 is not affected by the other viral proteins and is stronger than the interaction with NSP2. In addition, an inhibitory effect of VP1 on the levels of NSP5 hyperphosphorylation induced by both NSP2 and VP2 was observed.

Altogether, these data confirmed an important role for NSP5 in replication, related with the interactions with the two structural proteins essentially involved in viral genome synthesis, and suggested that NSP5 plays a key role in architectural assembly of viroplasms and in recruitment of the other viroplasmic proteins.

LIST OF ABBREVIATIONS

3D	three-dimensional
aa	amino acids
ATP	adenosine triphosphate
bp	base pair
CPE	cytopathic effect
C-terminal	carboxy-terminal
DLP	double-layered particle
DMEM	Dulbecco's modified Eagle's medium
DMSO	dimethylsulfoxide
DSP	Dithiobis(succinimidylpropionate)
dsRNA	double-strand RNA
EDTA	ethylenediamine tetraacetic acid
EGFP	enhanced green fluorescent protein
EM	electron microscopy
ER	endoplasmic reticulum
ERGIC	ER-Golgi Intermediate Compartment
FCS	foetal calf serum
FITC	fluorescein isothiocyanate
GST	glutathione-S-transferase
HA	hemagglutinin
HIT	histidine triad
HRP	horseradish peroxidase
IPTG	isopropyl-β-D-thiogalactopyranoside
λ-PPase	lambda-phosphatase
MOI	multiplicity of infection
NSP	nonstructural protein
nt	nucleotides
N-terminal	amino-terminal
ORF	open reading frame
PAGE	polyacrylamide gel electrophoresis
PBS	Phosphate buffered saline
p.i.	post infection
p.t.	post transfection
RdRp	RNA-dependent RNA polymerase
RITC	rhodamine isothiocianate
RNase	Ribonuclease
siRNA	small interfering RNA
sn	supernatant
ssRNA	single-strand RNA
TBS	Tris buffered saline
TLP	triple-layered particle
UTR	untranslated region
UV	ultraviolet
VLP	virus-like particle
VLS	viroplasm-like structures

INTRODUCTION

Rotavirus was identified as a cause of human acute gastroenteritis (AGE) in 1973, when it was found in duodenal biopsies from children with acute non-bacterial gastroenteritis (25, 99), and then it has been recognized as the major etiologic agent of gastroenteritis in infants and young children worldwide. According to data collected until 2006, rotavirus is responsible for 500,000-600,000 deaths every year, 80% of which occur in developing countries, and in addition represents a significant cause of morbidity in developed countries (203). Two oral, live-attenuated vaccines have been shown to be effective and safe in several clinical trials and were licensed by many countries worldwide (73, 91). Several post-marketing surveillance studies are now under way to monitor the impact of these vaccines. Moreover, since human rotaviruses exhibit a huge genomic and antigenic diversity and since the pressure of anti-rotavirus vaccine-specific antibodies might select novel strains, many studies are aimed at evaluating the present geographical distribution of the different strains and its variations over time (73).

Studies on the molecular biology of rotavirus have so far led to a large but not exhaustive knowledge of the mechanisms, by which the virus replicates inside the host cell. One of the main limits is the lack of a universal reverse genetics system that enables to manipulate the virus genome and to identify roles and functions of the different viral proteins. In fact, for several of them the essential involvement in viral replication has been clearly demonstrated, but the exact function remains unknown, representing the goal of many research works.

1. VIRUS CLASSIFICATION

Rotaviruses are classified as a genus within the family *Reoviridae*, which includes non-enveloped viruses with segmented, double-stranded RNA (dsRNA) genomes. The name is derived from Latin "rota", meaning "wheel", and is due to the wheel-like appearance of the virion observed by electron microscopy. A triple-layered icosahedral protein capsid encloses 11 genome segments (91).

Rotaviruses are classified serologically into groups: viruses sharing cross-reacting antigens detectable by serologic tests with different monoclonal and polyclonal antibodies against VP6 (the protein forming the middle layer) belong to the same group. Five groups have been firmly established (A to E) and two more groups (F, G) are likely to exist; group A rotaviruses are those of major medical interest. Viruses within group A are classified further either into serotypes by cross-neutralization studies or into genotypes by sequence comparison. Serotypes are defined in a binary classification system by VP4 and VP7, which are the components of the external layer and are targets of neutralizing antibodies: serotypes determined by VP7 are termed G (which stands for glycoprotein) and those defined by VP4 are named P (which stands for protease-sensitive protein). Genotypes are based on identities between sequences of cognate genome segments. So far, 16 different G genotypes and 27 P genotypes have been detected. Whilst for G serotypes and G genotypes the correlation is practically complete, there is no concordance between P serotypes and P genotypes and they are still designated separately (the serotype in open Arabic numbers and letters and the genotype in Arabic numbers in squared brackets: for example, the human Wa strain is classified as G1P1A[8]) (91). A new classification system has recently been proposed based on the sequences of all 11 genome

segments and phylogenetic analyses, which allow to identify in a comprehensive fashion distinct genotypes and reassortment events (175, 176).

2. DESCRIPTION OF THE VIRION

2.1. OVERVIEW

Structural studies using cryoelectron microscopy and computer image reconstruction have provided a description of the virion as an icosahedral particle of 75nm diameter and consisting of three concentric capsid protein layers (235, 300). The complete viral particle (= the infectious virion) is called triple-layered particle (TLP), a particle where the outer layer is missing is named double-layered particle (DLP) and a subviral particle containing only the innermost layer is designated as a single-layered particle or "core". The genome consisting of 11 segments of double-strand RNA (dsRNA) is packaged within the inner layer, together with two proteins involved in transcription and genome replication: the RNA-dependent RNA polymerase (RdRp), VP1, and the capping enzyme, VP3. The inner layer is formed by 120 molecules of VP2, the middle layer by 260 trimers of VP6 and the outer layer by 780 molecules (260 trimers) of VP7 and 60 trimers of VP4 (Fig. 1) (91). The entire structure has a left handed T=13 icosahedral symmetry and is perforated by 132 aqueous channels of three types (I-III). The type I channels play an important role in viral transcription as through them the newly formed messenger RNA (mRNA) exits into the cytoplasm. A detailed description of the virion 3D structure and of the genome organization is provided in the following paragraphs (91).

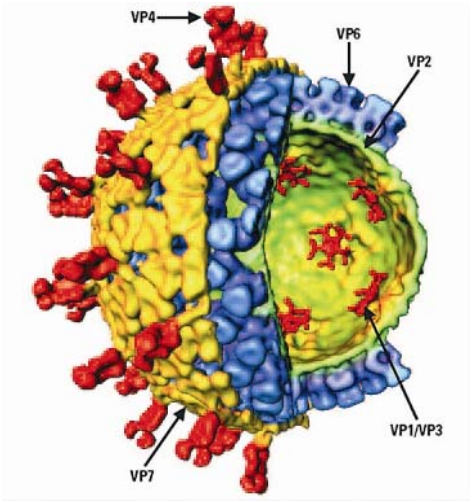

FIG. 1: cut-away view of the rotavirus TLP showing the outer layer (VP7 in yellow and VP4 in red), the middle layer (VP6 in blue) and the inner layer (VP2 in green) surrounding the enzymes VP1 and VP3 (in red), which are anchored to the inside of the VP2 layer at the five-fold axes (From Jayaram et al, 2004).

2.2. SPATIAL ORGANIZATION OF THE TRIPLE-LAYERED PARTICLE

The outer layer of the TLP is formed by the major protein VP7, which is uniformly distributed giving rise to a smooth outer surface. The 780 molecules of VP7, organized as trimers, form a T=13l (l for levo) icosahedral lattice defining the different types of aqueous channels (235). Sixty VP4 projections are anchored near the type II channels surrounding each 5-fold vertex (232, 299). The VP4 spikes protrude for about 100-120Å and present a bi-lobed head at the distal end (232, 300). Recent structural studies suggest that the each spike is a VP4 trimer, in which two VP4 molecules are associated and form the visible spike and the third VP4 molecule is flopping and not visible by cryo-EM (see Fig. 5 in chapter 3) (81). VP4 interacts with both VP7 and the middle layer protein VP6 and through these interactions plays an important role in maintaining the precise geometric arrangements between the outer and the middle layer (299).

The intermediate layer is composed of 780 VP6 polypeptides organized in 260 trimers on a T=13 lattice, which produce the typical bristle-like structure of DLPs (235, 300) (Fig. 2). VP6 trimers contain conserved peptides for interactions with the inner layer protein VP2 on the inside and with VP7 and VP4 at the outside. While the lateral interactions between VP6 trimers are not sufficient to make a closed icosahedral structure, the interactions with VP2 drive the assembly of correctly sized rotavirus particles (48, 174). The arrangements of the VP6 trimers and their contacts with the VP7 trimers are such that the aqueous channels in the outer and in the middle layers lye in register; however, VP7 induces a slight displacement of the VP6 trimers flanking the 5-fold axis, which is responsible for the different diameter of the type I channels in the two layers (156, 162).

The inner layer is a thin, relatively smooth spherical structure formed by 120 molecules of VP2 assembling to 60 asimmetric dimers, which are arranged in a T=1 icosahedral simmetry (160, 234). Since VP2 is the only protein capable to form stable virus-like particles when expressed alone in insect cells or also with various combinations of VP6, VP4 and VP7 (62), it has been considered the rotavirus scaffolding protein (62, 153). Although VP2 forms a relatively smooth shell, a small portion extends further inward at the 5-fold axes to form a pentagonal structure (234) (Fig. 2). Small pores surrounding the 5-fold axes pass through the VP2 layer connecting the core environment with the outside (233, 234).

The aqueous channels are classified in three types based on their position on the icosahedral structure (235). All channels are about 55Å wide at the outer surface, with the exception of type I channels that have a narrower opening (about 40Å), constrict then further and widen again to reach the maximum width in proximity of the inner shell (235). Their depth through the two outer shells is about 140Å (235). Nascent mRNA transcripts exit the DLPs through type I channels, which run down the

icosahedral 5-fold axes, suggesting an important role for these channels in viral transcription (159).

Inside the core, positioned at each of the 12 pentameric edges of the VP2 lattice, there are complexes formed by one molecule of VP1 and one of VP3, which means that 12 copies of VP1 and VP3 are contained in each viral particle (234). Even if the exact position of the genome segments has not been determined yet, the dsRNA genome was visualized as an ordered dodecahedral structure, in which the dsRNA helices are packed around the VP1-VP3 complex (234) (Fig. 2).

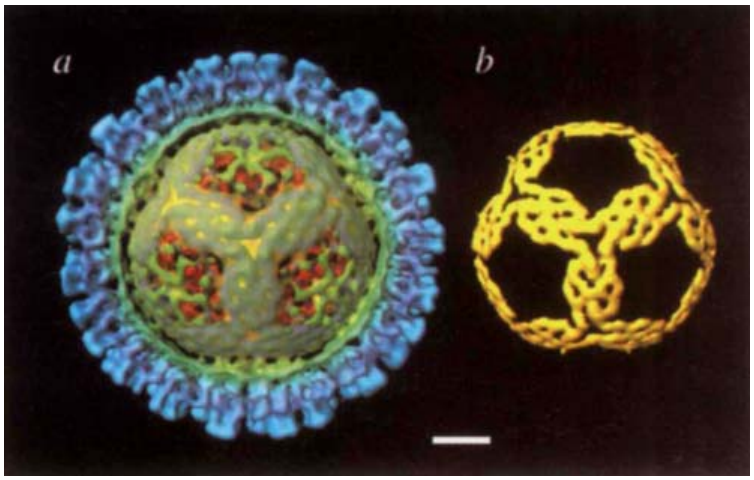

FIG. 2: Structural organization of RNA inside rotavirus. a) cut-away view of the rotavirus DLP showing internal organization: VP6 is represented in shades of blue, VP2 in shades of green; the VP1-VP3 complex at the 5-fold axes is shown in red and portions of VP2 at the 5-fold in green. The dodecahedral shell of the ordered RNA, shown also separately in b), is represented in yellow. (From Prasad et al, 1996).

2.3. THE VIRAL GENOME

Rotavirus genome consists of eleven segments of dsRNA, each encoding one protein, with the exception of segment 11 of some strains that encodes two (NSP5 and NSP6). The RNA segments can be extracted from purified or semipurified virus and resolved by polyacrylamide gel electrophoresis (PAGE), showing a migration pattern of eleven different bands (Fig. 4). The nucleotide sequence of all segments is known for several rotavirus strains. All are between 660 and 3300 bp in size and share the following general features (91):

- lack of a poly(A) tail;
- 5′ cap structure $m^7GpppG^{(m)}GPy$ on the positive-sense strand;
- uncapped minus-strand;
- high content of A+U (58-67%);
- complete complementarity of both RNA strands;
- one single ORF (except for segment 11 of some strains).

On one side the different genome segments share sequence signals in order to be transcribed and replicated by the same RdRp, on the other they contain signals to be distinguished from one another during packaging. While assembly and encapsidation signals remain still unknown, some of the signals for transcription and replication have been identified in both untranslated regions (UTRs) (76). In particular, for the medically important group A rotaviruses the plus-strand RNAs start with the consensus sequence 5′-GGC$(A/U)_{6-8}$-3′ and end with the consensus sequence 5′-UGUGACC-3′ (76) (Fig. 3). The conserved sequence at the 3′UTR has been identified as a signal promoting minus-strand RNA synthesis (215, 294). In particular, the 3′-terminal CC have been shown to be crucial for the formation of the initiation complex of RNA replication (51, 53). However, they are dispensable for specific

binding of the RdRp, which instead requires the four nucleotides 5'-UGUG-3' of the 3'-terminal consensus sequence and also other signals positioned in non-conserved regions positioned upstream (280). Within the same conserved sequence, the last four nucleotides 5'-GACC-3' function as translation enhancers (56). The conserved sequence within the 5'-UTR, in particular the second G, has also been shown to play a role in the attachment of the RdRp and cofactors into a stable initiation complex for minus-strand RNA synthesis (281) (Fig. 3). Based on computer modelling, the 5' and 3' UTRs are predicted to stably anneal to form a panhandle structure, from which the 3'-terminal conserved sequence extends as un-base-paired tail (54, 206) and this structure has been proposed to be stabilized by the RdRp (281).

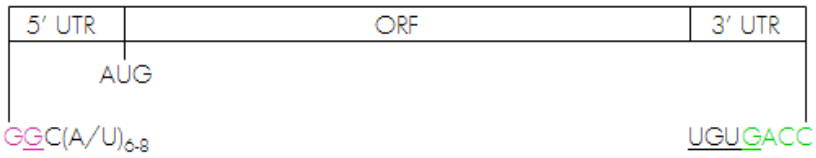

FIG. 3: Schematic representation of a group A rotavirus plus-strand RNA. The conserved sequences at the 5' and 3' ends are indicated. Both sequences were shown to be essential for the formation of the minus-strand initiation complex. They are predicted to stably base-pair forming a panhandle structure. The dinucleotide GG indicated in purple is conserved within all groups of rotaviruses and the second G was shown to be essential for specific recognition by the polymerase VP1. Another recognition signal for VP1 is at the 3'UTR. Both signals are underlined. The sequence indicated in green is a translation enhancer.

Rotavirus genomes (better investigated for group A rotaviruses) show an extensive diversity, which is essentially due to the following mechanisms (135):

- accumulation, sometimes fixation, of point mutations (genomic drift);
- genome segment reassortment (genomic shift): a dual infection with two co-circulating human strains or a human and an animal strain leads to a viral progeny containing novel assortments of genome segments;
- gene rearrangements (75): considerable tracts of sequence within a single genome segment may be altered by deletions or duplications. Most gene rearrangements involve segment 11 and consist in a partial head-to-tail duplication of the dsRNA sequence (113).

2.4. GENE-PROTEIN ASSIGNMENT

The genome segments code for six structural proteins found in virus particles (VP1, VP2, VP3, VP4, VP6, VP7) and five or six nonstructural proteins (NSPs) found in infected cells but not in mature virus particles (NSP1-NSP6; as mentioned above, some strains have only a single ORF in segment 11 and lack NSP6) (91). Some NSPs are found in subcellular locations, some others in cytoplasmic viral inclusion bodies called viroplasms and considered sites of viral genome replication and packaging (91).

Comparative studies of the electrophoretic pattern of genome segments deriving from different strains have shown that the relative migration order of the eleven genes can differ (91). Therefore, the gene-protein assignment is specific for each strain (Fig. 4). Table 1 lists the RNA segments and their protein products for the simian rotavirus SA11 strain. All functions reported in literature for rotavirus proteins are also summarized. A more detailed description of their properties and functions is provided in the following chapter.

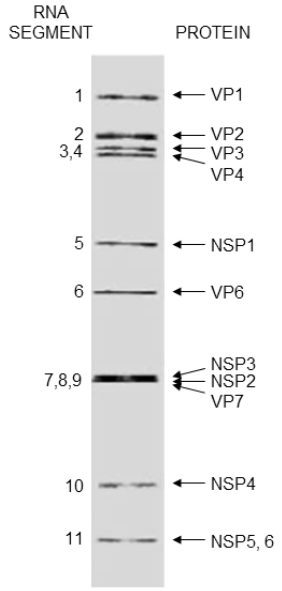

FIG. 4: PAGE gel showing the 11 dsRNA genome segments of the rotavirus SA11 strain. The genome segments are numbered on the left and the encoded proteins are indicated on the right. Segment 11 of this strain has also an alternative ORF encoding the nonstructural protein NSP6.

RNA SEGMENT		PROTEIN PRODUCT					
no.	Size (bp)	Protein name	Deduced MW (KDa)	Location (oligomeric state)	Post-translational modif.	Enzymatic activities and functions	Binding properties
1	3302	VP1	125	Inner core		RNA-dependent RNA-polymerase	ssRNA; NSP2; NSP5; complex with VP3; VP2?
2	2690	VP2	94	Core	Myristylation	Required for replicase activity of VP1	ssRNA and dsRNA; VP6; NSP5
3	2591	VP3	88	Inner core		Guanylyl-methyl transferase	ssRNA; complex with VP1; VP2?
4	2362	VP4	86.8	Outer layer (trimer)	Proteolitic cleavage to VP5* and VP8*	Cell attachment; protease-enhanced infectivity; neutralization antigen; virulence	VP7; sialic acid or sialic acid derivatives; several integrins; Hsc70; TRAF2; Rab-5 and PRA-1; complex with VP7 and NSP4
5	1611	NSP1	58.7	Nonstructural		Virulence (antagonizing innate immune response)	RNA; IRF-3; IRF-5; IRF-7
6	1356	VP6	44.8	Middle layer (trimer)	Myristylation	Required for transcription; neutralization antigen	VP7; VP4; VP2; NSP4
7	1059	NSP3	34.6	Nonstructural (dimer)		Inhibitor of host cell translation; role in viral translation?	ssRNA; eIF4GI; RoXaN
8	1104	NSP2	36.7	Nonstructural (octamer)		NTPase/RTPase, NDP kinase, helicase activities; role in replication and possibly in packaging; viroplasm formation	ssRNA; NTPs; NSP5; VP1; tubulin
9	1062	VP7	37.4	Outer layer (trimer)	Cleavage of signal sequence; glycosylation	Cell entry; neutralization antigen	VP4; VP6; Ca^{2+}; some integrins; complex with NSP4 and VP4;
10	751	NSP4	20.3	Nonstructural	Glycosylation	Intracellular receptor for DLPs; role in linking packaging and morphogenesis, in morphogenesis and in regulation of transcription and calcium homeostasis; enterotoxin; viroplasm maturation	VP6; microtubules; laminin-β3; fibronectin; complex with VP4 and VP7; α1β1 and α2β2 integrins; caveolin-1
11	667	NSP5	21.7	Nonstructural (dimer?)	O-glycosylation Phosphorylation	Role in replication; viroplasm formation; ATPase activity	ssRNA and dsRNA; NSP2; VP1; VP2; tubulin; NSP6
		NSP6	12	Nonstructural		Regulation of NSP5 multimerization?	ssRNA and dsRNA; NSP5

TAB. 1: Genes, gene protein assignments and published functions of proteins of group A rotavirus SA11 strain.

3. ROTAVIRUS PROTEINS

VP1

VP1 is the viral RNA-dependent RNA polymerase (RdRp) acting as both, the transcriptase (for mRNA synthesis) and the replicase (for minus-strand RNA synthesis). Several lines of evidence indicate that VP1 is the viral RdRp: (i) VP1 contains sequence motifs that are shared by RdRps of other RNA viruses (188); (ii) VP1 has NTP-binding activity and, when cross-linked with the nucleotide analog 8-azido-ATP, inhibits RNA transcription (284); (iii) VP1 specifically recognizes multiple functionally distinct elements at the 3' end of viral plus-strand RNAs (53, 207, 280); (iv) recombinant VP1 can direct template-dependent minus-strand synthesis *in vitro* in the presence of VP2 (212, 308). To date, regions of VP1 responsible for specific recognition of the templates and the enzymatic activity have not been identified and this is in part due to the lack of a solved 3D structure. Based on a bioinformatic programme comparing shared motifs of different viral RdRps, an overall structural conservation has been identified in the middle of the sequence, whereas the N- and C-termini have been predicted as unique regions (288), which could be related to unique functions of VP1 or to interactions with specific rotavirus proteins. Interactions of VP1 with NSP2 (145) and NSP5 (2, 8) have been described by coimmunoprecipitation experiments from extracts of both infected and transfected cells. Moreover, VP1 may interact with VP2 because: (i) they form virus-like particles (VLPs) when coexpressed in insect cells (307, 308); (ii) purified recombinant VP1 and VP2 can drive synthesis of dsRNA in template-dependent assays only when both are present (212, 280); (iii) far-Western blot analysis showed a binding between VP1 and VP2 involving the N-terminus of VP2 (aa 1 to 25) (307).

VP2

VP2 is the major scaffolding component of rotavirus core: 120 molecules of VP2 form the innermost capsid layer of rotavirus enclosing the genomic dsRNA (153). Since VP2 is the only protein capable to form stable VLPs when expressed alone in insect cells or also in various combinations with VP6, VP4 and VP7, it has been considered the rotavirus scaffolding protein (62, 153). However, VP2 shell has both a structural and a functional role: interactions with trimers of VP6 (forming the intermediate particle layer) are responsible both for the stability of DLPs and for mRNA synthesis and transcript extrusion (48, 162); VP2 binds to genomic dsRNA, as demonstrated by UV cross-linking experiments (152), and its higher affinity for ssRNA than for ds nucleic acids (35) suggests a possible role in the encapsidation of ssRNAs used as templates for dsRNA synthesis; in fact, VP2 is required by VP1 in *in vitro* replication assays to achieve the replicase activity directing minus-strand synthesis (212, 280).

The N-terminus of VP2 is responsible for both its nonspecific RNA binding activity (35, 152) and the proper assembly of VP1 and VP3 into the core (307) forming a complex located on the inner surface of the VP2 layer at the icosahedral fivefold axes (234). More in detail, deletion of the first 26 amino acids completely abolished the RNA binding activity, indicating that either the first 26 amino acids contain the binding site(s) or they allow VP2 to fold in such a way that RNA binding can occur through several other RNA binding sequences identified in the first 132 amino acids (152). Baculovirus recombinant-mediated co-expression of N-terminally truncated forms of VP2 and VP1 and/or VP3 showed that the N-terminal 92 aminoacids are essential for incorporation of VP1 and VP3 in virus-like particles (VLPs), although they are not for VP2-VLP formation (307). Moreover, far-Western blot analyses using a series of truncated VP2 forms showed that full-length VP2 binds to VP1, any N-

terminal truncation lacking amino acids 1 to 25 fails to bind VP1 and a C-terminal 296-aa truncation maintains the ability to bind VP1 (307).

By cryoelectron microscopy and image reconstruction of VLPs formed either by full-length VP2 or by the truncation lacking the N-terminal 92 amino acids, it has been proposed that the 120 molecules of VP2 are arranged as dimers, each extending between neighbouring fivefold axes, and that the N-termini are located near the icosahedral vertices (159). Interestingly, previous cryoelectron microscopy experiments on native DLPs had shown significant interactions between the inner surface of VP2 layer and the genomic dsRNA near the icosahedral fivefold axes and minor interactions along the icosahedral twofold axes (234), supporting the idea of VP2 having an important role in organizing the genomic dsRNA within the core.

While the N-terminal region of VP2 seems to be essential for the spatial architecture of the core, it does not seem to be involved in interactions with VP6 and with the nonstructural protein NSP5. It has been reported that both full-length VP2 and a VP2 deletion mutant lacking the N-terminal 92 amino acids can form VLPs incorporating VP6 (49) and both coimmunoprecipitate with NSP5 and form aggregate structures in insect cells with NSP5 and VP6, and with either of them (23). Moreover, it has been shown that an insect cell lysate containing recombinant baculovirus-derived NSP5 dislodges VP6 from purified VLPs formed by VP2 and VP6, but not from purified DLPs (23). Since the differences between the two types of purified particles are the presence of genome segments and the stronger interaction between VP2 and VP6 in DLPs, it has been proposed that the interaction between the VP2 core and NSP5 occurs at early times to prevent the VP6 binding and thus the formation of defective particles until the set of genomic RNA segments inside core is complete (23).

VP3

VP3 is a basic protein responsible for capping rotavirus mRNAs through its guanylyl-transferase and methyl-transferase activities (52, 164, 225). It is one of the minor components of the core (163), a component of early replication intermediates and, together with VP1, seems to be the first protein to associate with viral (+)ssRNAs during packaging and RNA replication (104), possibly through its unspecific affinity for ssRNA (209). Together with VP1 and ssRNA, VP3 interacts with the N-terminus of VP2 (307) and this association might have a role in RNA replication. In fact, it has been shown that the presence of a functional VP3 is important for RNA replication (286) and that in *in vitro* replication assays VLPs containing VP1, VP2 and VP3 synthesize minus-strand RNAs more efficiently than VLPs formed only by VP1 and VP2 (308). The exact role of VP3 in this context is unclear. It has been proposed that VP3 increases the rate at which the components of the replicase complex assemble into functional structures (212).

VP4

VP4 is one of the two proteins of the outer layer of rotavirus. It is a non-glycosylated protein with essential roles in virus attachment and penetration. Antibodies against VP4 can neutralize by blocking cell entry and protect against rotavirus gastroenteritis (201, 244). In virions uncleaved with trypsin, molecules of VP4 are distributed on the surface of the VP7 shell as flexible stalks occupying each of the 60 symmetry-equivalent positions. In the gut lumen trypsin cleavage of VP4 maximises rotavirus infectivity (94, 98): this cleavage generates two fragments, VP5* (60KDa) and VP8* (28KDa), which remain associated with virions and confer the spike appearance of VP4 observed by cryoelectron microscopy in trypsin-cleaved virions (260, 299). VP8* forms the "heads" of the spikes and binds cellular receptors in the virus attachment phase (82); VP5*, together with the N-terminus of VP8*, forms the spike

"body", which is linked by an asymmetric "stalk" to a "foot" buried beneath the VP7 shell (81) and interacting with VP6 (299). The VP5* residues in the spike body are involved in membrane penetration and integrin binding (83, 120, 171). It appears that each spike is indeed a VP4 trimer (81) and that the rearrangement induced by trypsin cleavage allows a switch from a flexible structure into rigid spikes (64, 81), where two primed VP4 molecules are associated and present the VP8* core for receptor binding and the third primed VP4 molecule is flopping and not visible by cryo-EM (81) (Fig. 5A). It has been proposed that a second rearrangement event occurs during cell entry, in which two VP5* subunits fold back on themselves and join a third VP5* subunit to form a tightly associated trimer, shaped like a folded umbrella, from which VP8* dissociates (81) (Fig. 5B). This second rearrangement is thought to occur to unmask the membrane interaction region of VP5* allowing cell penetration (81). To support this VP4 rearrangement model, there is the evidence that a globular domain of VP5* containing the potential membrane interaction region has the intrinsic molecular property of alternatively forming dimers and trimers (301). As a further confirmation, it has been observed that at elevated pH the VP4 spike undergoes an irreversible conformational change from a bilobed structure to a distinctly stunted trilobed structure (217).

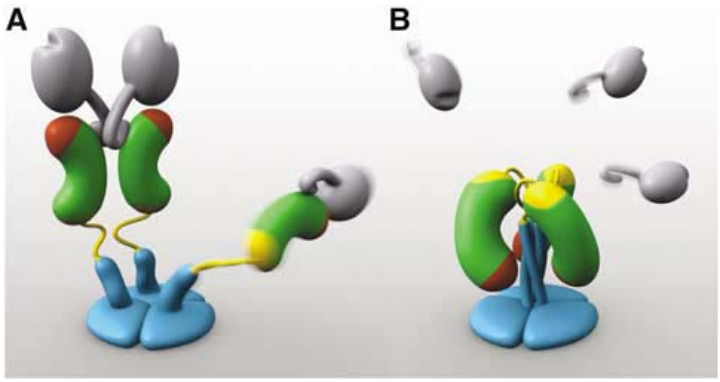

FIG. 5: Models of two VP4 conformations. (A) The primed state. Two rigid subunits form the spike visible in electron cryomicroscopy image reconstructions of trypsin-primed virions. A third subunit is flexible. VP8* is represented in gray, VP5* in green bean-shape, with a red membrane interaction region. (B) The putative post-membrane penetration state. VP8* has dissociated and the VP5* antigen domain has folded back. From Yoder et al, 2006.

VP8* contains a sialoside-binding region within a shallow groove on its surface, which is involved in sialic acid binding and hemagglutination in sialidase-sensitive rotavirus strains (82, 98). However, the capacity of VP8* of binding sialic acid derivatives has also been recognized for some sialidase-insensitive strains (28), and new carbohydrate binding regions in VP8* are being discovered in both types of strains (28, 82, 127). Interestingly, the VP8* sialic acid binding domain has a galectin fold, which might be responsible for features shared by VP4 and galectins, like the translocation to the plasma membrane via a Golgi-independent pathway or the capacity of activating the TRAF2-NF-kB-inducing kinase signalling pathway (155). The binding of VP8* to TRAF2, a member of a family of adapter proteins involved in transducing signals generated by ligands of Tumor Necrosis factor (TNF), and the consequent activation of NF-kB, which in turn causes the secretion of selected chemokines, suggests a role for VP4 in determining cell-specific responses to rotavirus infection (155).

VP5* is involved in cell attachment (304, 305) and is considered the main part of the molecule responsible for cell entry through a hydrophobic fusion domain that was shown to be able to permeabilize membranes in the absence of other rotavirus proteins (72). Since it was found that VP5* cannot permeabilize lyposomes or bacteria, it has been proposed that it has a selective permeabilizing activity, possibly by forming transient pores that could allow the decrease of calcium levels in the proximity of the plasma membrane or in endosomes (83, 107). VP5*, together with VP7, is also responsible for integrin binding, which is important not only for cell attachment and entry (involving mainly $\alpha 2$ integrins), but also for facilitating virus spread or host immune response modulation (involving mainly $\alpha 4$ integrins) (119, 129, 304): through its peptide sequence DGE, VP5* interacts with $\alpha 2\beta 1$ integrin (120, 121, 128) and it is likely to be involved in binding to $\alpha 4\beta 1$ and $\alpha 4\beta 7$ integrins through its peptide sequence YGL (119). Furthermore, VP5* has been shown to bind Hsc70 (303) in a post-attachment step important for cell entry (124).
The role of VP4 in the morphogenesis of rotavirus has been studied by experiments of RNA interference silencing VP4 expression (65, 67). The formation of spike-less TLPs in rotavirus-infected cells transfected with an siRNA against VP4 suggested that VP4 is not required for virus assembly (67). Since these spike-less TLPs have larger diameter than wild-type TLPs, it has been proposed that VP4 tightens the structure of the viral particle (67). Interestingly, VP4 silencing reduces the association of rotavirus particles with rafts and causes an accumulation of non-enveloped particles in the endoplasmic reticulum (ER) (65), suggesting a role for VP4 in trafficking newly synthesized particles. Many reports indicate that VP4 is indeed associated with rafts (68, 252), which are dynamic microdomains in cellular membranes enriched in cholesterol and sphingolipids and exert critical roles in membrane trafficking. However, the role of VP4 in virion assembly and release remains still unclear. During rotavirus infection the

newly synthesized VP4 seems to be localized both in the cytosol and in the plasma membrane, starting early after infection. More precisely, it has been detected in an area between viroplasms and ER (220), colocalizing in the ER proximity with NSP4 (108), with which it might interact (10), also because of the recognized ability to form heterotrimers with NSP4 and VP7 (170). It has also been identified in the ER-Golgi Intermediate Compartment (ERGIC) (65), in transiently enveloped particles (229) and in the plasma membrane in lipid rafts, associated with microtubules and exposed on the external face of the apical plasma membrane (69, 196, 252). The data from RNA interference experiments, the VP4 cellular distribution, the described interactions [with NSP4/VP7 and with the ER chaperone grp78 (296)], and the fact that VP4 needs to be added before VP7 to reconstitute *in vitro* infectious TLPs from non-infectious DLPs (283), support the idea that VP4 assembly into particles occurs inside or in the vicinity of the ER and not at a later time point when VP7-coated particles are already formed. However, since rafts are considered to be absent in the ER and the block of enveloped particles in the ER induced with chemical reagents does not correlate with a reduced cell surface targeting of VP4, it has been proposed that VP4 assembly in viral particles occurs as a post-ER event (69). Thus, two pools of VP4 might exist, one associating with viral particles in the ER and the other independently targeted to the plasma membrane (65). Further experiments are needed to prove this assumption. Finally, an involvement in localization and trafficking of the free cytosolic VP4 in infected cells has been suggested for two cellular proteins, Rab-5 and PRA1, both participating in vesicular trafficking and able to form complexes with free VP4 at late steps of infection (88).

VP6

VP6 is the major capsid protein of rotavirus. It forms 260 trimers that constitute the intermediate layer (91, 114, 250). The structure of the VP6 trimer consists of an

elongated, tower-like molecule, where the three subunits wrap around a central 3-fold axis with a right-handed twist. The VP6 monomer consists of two domains (H and B) positioned along the long dimension of the tower-like molecule and both involved in intra-trimer interactions. Each trimer contains conserved surfaces for interactions with other structural proteins, at the bottom for binding to VP2, at the top for contacting VP7, at the sides of domain H for binding to VP4 and at the sides of domain B for lateral interactions with other VP6 trimers. These inter-trimer interactions do not contain all the information to form a closed icosahedral shell, since interactions with the VP2 inner layer are also required for a correct assembly. A model for assembly has been proposed, in which the center of each of the twenty faces of the VP2 layer acts as a nucleation point for the growth of the middle layer and the driving force for assembly propagation appears to be the inter-trimer interactions rather than interactions with the VP2 layer (1, 174). A Zn^{2+} ion is located at the center of the VP6 trimer coordinated by three histidines, one for each VP6 monomer (174). Mutation of the Zn^{2+} coordination site renders the trimer more sensitive to proteases, but has no effect on the interaction with VP2 or on the DLP transcription activity (89). When coexpressed in insect or mammalian cells, VP2 and VP6 can in fact form double-layered virus-like particles (Dl-VLPs) (62, 110). However, while recombinant VP2 is able to form core-like particles in insect cells by itself (153), VP6 forms only tubular or spherical structures in the absence of other viral proteins (161, 240). The spherical structures are larger than Dl-VLPs, highlighting the importance of VP2 in the assembly of viral particles (161). The main parameter affecting interactions between VP6 molecules, and consequently the formation of spheres or tubes, is pH: at pH 3.5-5.5 these interactions generate spherical particles, at pH 5.5-7.0 large tubes and at pH above 7.0 small tubes (161). These observations suggested that the protonation state of VP6 is critical for assembly, probably affecting lateral inter-trimer contacts (161).

By connecting the outer layer and the inner layer, VP6 has a fundamental role in the structure of the virion as a physical adapter between the biological functions exerted by the two linked layers: cell entry and genome packaging (233). Moreover, VP6 seems to play an active role in transcription, because in its absence the process does not take place (24). In particular, it has been shown that: (i) hydrophobic interactions at the interface with VP2 are responsible for the DLP stability and subtle electrostatic interactions in the same area influence transcription and transcript extrusion (48); (ii) structural changes induced by anti-VP6 antibodies (97, 156) or the geometrical orientation of the trimers induced by interaction with VP7 (162) inhibit transcriptional activity. VP6 might also have a role in the budding of newly formed DLPs in the ER: in fact, during viral infection VP6 is localized at the periphery of viroplasms and in close proximity of the ER (220) and is thought to interact with the cytoplasmic tail of NSP4 (180, 275, 277), which is the viral ER-transmembrane protein mediating the budding of viral particles into the ER (9, 10, 19). Interestingly, NSP4 silencing experiments showed a drastic change of the VP6 distribution in infected cells: instead of being localized in viroplasms, in the absence of NSP4 VP6 forms filaments not colocalizing with tubulin, actin or vimentin (165). Furthermore, the same phenotype was observed when the expression of another nonstructural protein was silenced: NSP5 (166). However, at present there is no evidence of an interaction between VP6 and NSP5. On the contrary, it has been shown that NSP5 does not bind DLPs and that VP6 hinders the interaction between NSP5 and VP2 (23).

VP7

VP7 is a protein organized in 260 trimers forming the outer layer of rotavirus (300), in which VP4 molecules are inserted. In most rotavirus strains, but not in all of them, VP7 is N-glycosylated. It has a high content of conserved cysteines that form disulfide bonds important for the correct folding of the protein and the maturation of viral

particles (185). During the replicative cycle the newly synthesised VP7 is inserted in the ER membrane with a luminal orientation (143). The VP7 targeting to the ER is due to two hydrophobic regions located at the N-terminus, which are cleaved off after insertion of VP7 in the ER membrane, but are still necessary for the retention of VP7 in the ER (169, 231, 266, 295). The C-terminus is thought to be protruding into the cytoplasm and have important roles for the assembly of mature particles (60).

The conformation and stability of VP7 are calcium-dependent (79); in particular, the trimerization of VP7 requires calcium (80). In fact, many lines of evidence indicate that both the loss of the outer layer during cell entry and the formation of the same layer during virus assembly are mediated by calcium-dependent conformational changes of VP7: *in vitro* calcium chelation triggers TLPs uncoating (61); the outer layer contains calcium (258); low concentrations of calcium induce a VP7 solubilization (103, 247) shown to be necessary for the permeabilizing activity of the protein (47); in the absence of calcium, VP7 cannot interact with VP4 and NSP4 in the heterotrimeric complex formed during virus assembly (170, 230).

VP7 has an important role during cell entry, not only because of its membrane permeabilizing activity (47), but also because of its binding to $\alpha v\beta 3$ (306) and $\alpha x\beta 2$ integrins (120). VP7 also has a regulatory role in transcription, because it appears to induce a structural change of VP6 (156) and a reorganization of the VP6 trimer around the particle 5-fold axes (162) that inhibit the DLP transcriptional activity; moreover, it causes a steric hindrance that blocks the exit of nascent mRNAs through the type I channels (159). VP7 silencing experiments also revealed an important role of VP7 in removing the transient envelope during virus morphogenesis (165) and a contribution of VP7 to the NSP4 function of regulating calcium homeostasis during infection (302).

NSP1

NSP1 is an RNA-binding nonstructural protein that accumulates in the cytoplasm of infected cells in association with the cytoskeleton (132). It is the least conserved rotavirus protein; only the N-terminal zinc binding motif is completely conserved (189). This cystein-rich region has been shown to be essential for binding viral RNAs at the 5'UTR (37, 131) and it is important, but not sufficient, for allowing NSP1 binding to the cellular transcription factor IRF3 (Interferon Regulatory Factor 3) (117). This cellular protein is activated following virus infection and promotes the expression of IFNβ, which is secreted and induces the neighbouring uninfected cells to express another transcription factor, IRF7 (253). IRF7 is the main molecule responsible for the production of type I IFN (IFNα and β) in the anti-viral host response. NSP1 has been shown to target IRF3 to the proteasome (14), and it has been proposed to act as a E3 ubiquitin protein ligase based on the fact that the arrangement of the cysteine residues of the zinc binding motif resembles the RING fingers of the E3 ligase (116). However, NSP1 of some rotavirus strains does not have IRF3 as a target, despite having an intact zinc-binding domain (116). Furthermore, it has recently been shown that NSP1 induces the proteasome degradation of IRF7 (15). This is probably related with the ability of the virus to replicate in specialized trafficking cells (macrophages and dendritic cells) constitutively expressing IRF7 (11) and IRF5, which is another factor that upregulates IFNI expression and is involved in triggering apoptosis during viral infection (15). Therefore, NSP1 may be considered as a broad-spectrum antagonist of the innate immune response that limits the virus spread (15). Since truncated forms of NSP1 lacking portions at the C-terminus lose their ability of interacting with these IRF factors, the C-terminus seems to play an important role in this context and its sequence variability in strains infecting different animal species suggests that NSP1 may confer species specificity to different rotaviruses (15). NSP1

has thus an important role in virus spread, confirmed also by reassortment experiments that showed a strong correlation between the genome segment encoding NSP1 and virus virulence and spread (36) and by the demonstration that truncations of NSP1 are responsible for the formation of smaller plaques following rotavirus infection (214). However, NSP1 does not have a role in virus replication, since virus mutants encoding C-truncated forms of NSP1 replicate efficiently (214) and NSP1 silencing by RNA interference does not affect virus replication (261).

Interestingly, it has been shown that the stability of NSP1 is maintained by the other viral proteins, alone or in combination with viral RNA, since in their absence the proteasome-mediated degradation of NSP1 is significantly increased (222).

NSP2

NSP2 is a basic, conserved protein with an important role in virus replication. This role has been demonstrated both by analysis of cells infected with a temperature-sensitive (ts) mutant of SA11 rotavirus strain, tsE(1400), with a lesion in the genome segment encoding NSP2 (239) and by RNA interference experiments in which NSP2 expression was silenced (261). Both the growth of cells infected with tsE(1400) at a non-permissive temperature and the NSP2 silencing revealed a critical function of NSP2 in viroplasm formation, in genome replication and packaging and in the production of infectious viral progeny (239, 261). The requirement of NSP2 in viroplasm formation is also confirmed by the fact that NSP2 forms viroplasm-like structures (VLS) when transiently coexpressed with NSP5 in the absence of other viral proteins (96) (see Fig. 9 in chapter 4). Moreover, NSP2 has been found in early replication complexes (104, 211) and the immunoprecipitation with a monoclonal antibody against NSP2 of an extract of infected cells allowed to recover a viral complex with replicase activity (5).

The functional form of NSP2 is a doughnut-shaped octamer derived from self-assembly of NSP2 monomers and from tail-to-tail interactions of two tetramers (138, 139, 255, 273) (Fig. 6).

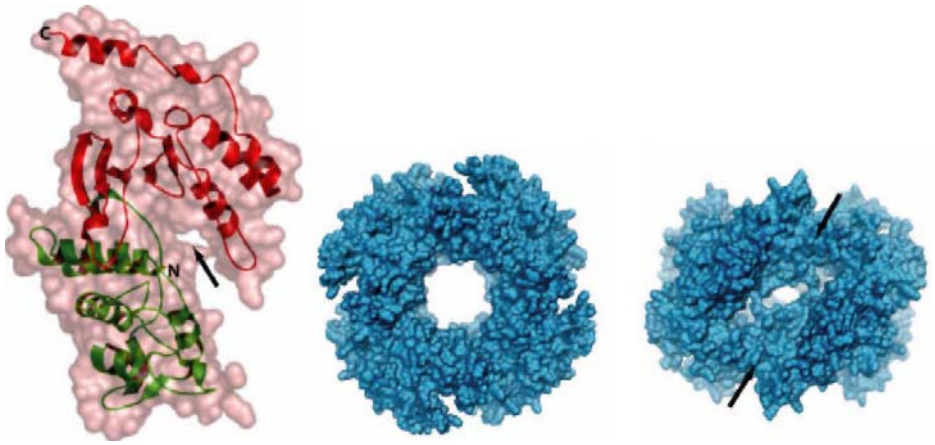

FIG. 6: NSP2 Structure. Structure of the NSP2 monomer (left), showing a deep cleft (arrow), which may be the site for NTP binding. Structure of the functional NSP2 octamer showing a view down the four-fold (middle) and a view down one of the two-fold axis in octamer (right). The deep grooves shown (right, arrows) are lined by basic residues and may be the sites for binding viral mRNA during genome replication and packaging. From Jayaram et al, 2004.

Each monomer has two distinct domains separated by an electropositive deep cleft that contains a histidine triad (HIT)-like motif (138) responsible for binding and hydrolysis of NTPs (46). The catalytic residue of this motif is a His in position 225, which becomes phosphorylated through the covalent attachment of the γP released after a Mg^{2+}-dependent hydrolysis reaction of the linkage between the γ and β phosphates (46, 151, 287). To catalyze this reaction, NSP2 can use both NTPs (270) and pppRNA (287) as substrates, thus exerting both NTPase and RTPase activities. Moreover, the NTPase activity has been shown to be associated with a phosphoryl-transfer function to NDPs similar to that of cellular NDP kinases (151). While the enzymatic activities of NSP2 can be attributed to the monomeric subunits,

its binding properties require the formation of the octamer. More in detail, it has been shown that NSP2 has a sequence-independent ssRNA binding (270) and a nucleic acid helix destabilizing activities (272) and it is able to bind NSP5 (2, 85, 139) and VP1 (8, 145); the 35Å central hole of the octamer, lined by neutral residues, was shown to be not involved in RNA and NSP5 binding, for which instead the four deep positively-charged grooves extending diagonally across the octamer are required (139). Interestingly, the binding sites of NSP2 with RNA and with a NSP5 mutant lacking the first 65 amino acids and the last 10 amino acids correspond, suggesting a competition between NSP5 and RNA for interaction with NSP2 (139). Furthermore, coimmunoprecipitation of NSP2 with NSP5 using anti-NSP5 antibodies was shown to require UV treatment, and to occur even after RNase digestion of the cellular extracts (2). Based on these findings, it has been suggested that NSP2-NSP5 interaction is not directly mediated by RNA and may be the consequence of a conformational change in NSP2 bound to RNA and/or nucleotides stabilised by the UV treatment (2).

The ssRNA binding and helix-destabilizing activities of NSP2 have been suggested to relax positive-strand RNA templates to facilitate genome replication (272) and the NSP5 binding seems to be important for viroplasm formation (96) and might regulate the NSP2-RNA interaction during genome replication (139). On the other hand, the roles of the enzymatic activities remain completely obscure. *In vivo* complementation studies have shown that the HIT-dependent enzymatic activities are necessary for dsRNA synthesis, but not for viroplasm formation, and it has been hypothesized that these activities are used only after establishment of cellular sites of replication and assembly (271). This could have something to do with the fact that the NTP binding causes a conformational change from a more relaxed to a more compact form of NSP2 (255) and also the RNA binding induces noticeable conformational changes,

whilst NSP5 binding does not (139). Moreover, it has been shown that a ssRNA molecule with a 5' γ-phosphate is preferred to NTPs as a substrate (287), suggesting that the hydrolytic activity of NSP2 may regulate the ssRNA binding activity or *vice versa*. Interestingly, the NSP5 binding activity does not interfere with the enzymatic activity of the HIT-like motif (287) and the catalytically inactive NSP2 mutant H225A supports VLS formation (46). Since NSP2 was found in early replication complexes, it has been proposed that the RTPase activity removes the γ-P from nascent negative-strand RNAs, but not from positive-strand RNAs because of the capping modification interfering with the RTPase function (287). However, dsRNAs are not substrates for the RTPase activity of NSP2 either and the role of this activity remains still obscure. For the NDP kinase activity, a role in the homeostasis of nucleotide pools has been suggested: NSP2 would guarantee sufficient levels of NTPs for transcription and replication and of ATP for processes requiring energy like transcription, NSP5 phosphorylation, RNA packaging and translocation (151), and the recently reported ATP-ase activity of NSP5 (13). Besides NDPs, also NSP5 had been proposed as a substrate for the phosphotransfer activity of NSP2 (290), however it has then been shown that the catalytic activity of NSP2 is not involved in the phosphorylation of NSP5, since NSP2 mutants that are NTP-ase defective still promote NSP5 hyperphosphorylation (46). Interestingly, and surprisingly, *in vitro* replication assays with recombinant VP1 and VP2 showed that NSP2 inhibits the initiation phase, but not the elongation phase, of the synthesis of dsRNA through its nonspecific RNA binding activity (291). More precisely, NSP2 does not block the recognition of the template by the polymerase, instead it interferes with the function of VP2 through an unknown mechanism, possibly by competing for binding to ssRNA (291).

NSP3

NSP3 is a slightly acidic protein, whose role in the viral replicative cycle is still not completely clarified. During virus infection, NSP3 is distributed diffusely throughout the cytoplasm, possibly associated with the cytoskeleton (177). NSP3 is composed of two functional domains separated by a dimerization domain (223). The N-terminal domain is required for sequence-specific RNA binding and the dimerization is necessary for the strong binding of a single molecule of RNA (74, 223). The sequence GACC within the consensus sequence at the 3'UTR of all viral mRNAs has been demonstrated as the shortest target recognized by NSP3 (227), and the binding of NSP3 to this sequence protects the 3' end from RNase digestion (226). Interestingly, NSP3 can recognize only mRNAs derived from the same serogroup, which could be one of the reasons why genomes of rotaviruses of different serogroups cannot reassort (227). The central domain of NSP3 is responsible for dimerization, forming a coil-coiled structure that confers to NSP3 dimer a heart shape (74, 223). By yeast two-hybrid assays, this domain has also been shown to be involved in interaction with RoXaN (Rotavirus X protein associated with NSP3), which is represented by two related proteins in mammalian cells (RoXaNI and RoXaNII) that might be important for translation regulation (292). In fact, RoXaNI can form a ternary complex with NSP3 and the other cellular ligand of NSP3: eIF4GI (eukaryotic Initiation Factor 4GI) (292). The NSP3 C-terminal domain is indeed involved in interaction with this cellular factor (223, 224), which is a scaffolding protein that binds the cap binding protein eIF4E, the RNA helicase eIF4A and the poly(A)-binding protein (PABP), in order to promote an efficient initiation of translation (134, 237, 274). NSP3 binds to eIF4GI in the same region recognized by PABP (224): it has been proposed that by bridging the cap-binding protein eIF4E via its binding to eIF4GI and the 3' end of viral mRNAs via its direct binding to the consensus

sequence, NSP3 promotes the circularization of viral mRNAs and their translation, while evicting PABP from eIF4GI impairs the translation of cellular mRNAs (224, 289). While there is a general agreement on the inhibitory activity of NSP3 on the synthesis of cellular proteins (191, 202, 224, 289), supported also by the recent observation that NSP3 causes a translocation of PABP to the nucleus (192), the role of promoting synthesis of viral proteins is now brought into question: in fact, RNA interference experiments that silenced NSP3 expression showed that NSP3 is not required for viral protein synthesis and, even more, its silencing correlates with an increased synthesis of viral RNA and with a concomitant increase in the yield of viral progeny (191). Furthermore, silencing the eIF4GI expression confirmed that its interaction with NSP3 is not required for viral protein synthesis (191). It has then been proposed that the interactions with eIF4GI and with the 3′ end of viral RNAs have two distinct functions: the first would help sequestering eukaryotic translation initiation complexes, thus inhibiting cellular protein synthesis, the second would prevent viral plus-strand RNAs from being selected for replication, thus ensuring a pool of transcripts available for translation, or would protect viral mRNAs from degradation (191).

NSP4

NSP4 is a multifunctional nonstructural glycoprotein (143) with key roles in virus transcription, morphogenesis and pathogenesis. It is the only nonstructural protein that does not bind to RNA. It is a 175 amino acid long, transmembrane protein targeted to the ER membrane by a signal sequence, which remains uncleaved. After insertion in the ER, most of the protein is exposed in the cytosol. NSP4 contains three predicted hydrophobic domains, H1, H2 and H3. H1 is a small domain, which is N-glycosylated in two sites and located in the ER lumen; H2 is a transmembrane domain and was initially thought to correspond to the signal sequence (19), until a

region in the cytosolic C-terminus downstream the H3 domain was shown to be involved in the ER retention (183); H3 is embedded in lipid bilayers on the cytoplasmic side of the ER (19) and is followed by a predicted amphipathic α-helix (AAH), which overlaps a folded coiled-coil region and is thought to mediate NSP4 oligomerization into dimers and tetramers stabilized by Ca^{2+} (32, 170, 277); finally, a hydrophilic C-terminus forms an extended cytosolic domain involved in binding of immature viral particles (DLPs) (31, 32, 143, 200, 277). Adjacent to the AAH region there is a microtubule-binding domain (297). Corresponding to the coiled-coil oligomerization domain there is also a region that binds two proteins of the extracellular matrix, laminin-β3 and fibronectin, with implications for the role of NSP4 in pathogenesis (30). In addition, the final part of the same domain contains two distinct integrin interaction motifs, shown to be responsible for binding to α1β1 and α2β1 integrins and for triggering signalling cascades important for the enterotoxin function of NSP4 (257). Furthermore, the same region is involved in a hydrophobic interaction with caveolin-1, a component of a subset of lipid raft microdomains called *caveolae*, which is thought to be involved in the intracellular transport of NSP4 (182, 204, 267). As already mentioned, the C-terminus of NSP4 acts as an intracellular receptor that binds newly made DLPs and mediates their budding into the ER lumen (9). More in detail, it has been shown that the extreme twenty residues of the C-terminus bind to VP6 (200), and that a region comprising part of the coiled-coil domain and part of the C-terminus contains sites important for VP4 binding (10). Upon budding of DLPs into the ER, NSP4 has been shown to hetero-oligomerize with VP4 and VP7 (170). The C-terminus of NSP4 has also enterotoxigenic properties: in fact, the region spanning amino acids 112–175 can be cleaved through a still unknown mechanism and secreted from rotavirus-infected cells to function as an enterotoxic peptide (309).

The two N-linked high-mannose oligosaccharide residues of NSP4 appear to be critical for the assembly function of NSP4, as treatment of infected cells with tunicamycin, a drug that blocks N-linked glycosylation, leads to the accumulation of enveloped particles in the ER (69, 218). The fact that the only other glycoprotein of rotavirus, VP7, is unglycosylated in some strains suggests that the oligosaccharides of NSP4 are those important for virus assembly. With this regard, glycosylation of NSP4 was reported to be not essential for NSP4 binding to DLPs or for oligomerization, but required for binding with the ER-associated molecular chaperon calnexin in an interaction shown to be not critical for virus assembly (184). The exact role of NSP4 glycosylation remains still unclear.

Three pools of NSP4 with different functions have been identified in infected cells:

- a first pool is represented by the NSP4 molecules localized in the ER membrane with the role of mediating the budding of immature viral particles into the ER, as described in paragraph 4.6 (91);
- a second pool comprises the NSP4 molecules localized in the ERGIC compartment and in the plasma membrane through their association to microtubules, lipid rafts or *caveolae*: these molecules might have a role in directing trafficking of vesicles carrying newly formed viral particles to the plasma membrane, as described in paragraph 4.7, or be simply detected there during their transit as "free NSP4 molecules" towards the plasma membrane and the extracellular environment. With this regard, there are reports in favor of a Golgi-independent pathway for trafficking NSP4 through the cell (142, 204, 267, 297, 309) and there is also a report showing that full-length NSP4 can be actively secreted through a Golgi-dependent pathway (40). This discrepancy has been attributed to the fact that the NSP4 molecules bypassing the Golgi network are involved in virus morphogenesis, while those

secreted through the Golgi-dependent pathway are involved in the enterotoxin function (40);

- the third pool includes NSP4 molecules distributed in cytoplasmic vesicular structures associated with the autophagosomal marker LC3 and with viroplasms; they have been proposed to promote the formation of large viroplasms by recruiting early viroplasms into putative "scaffold vesicles" (21).

Silencing NSP4 expression with siRNAs revealed the involvement of NSP4 in many aspects of the replicative cycle: regulation of calcium homeostasis (302), translocation of viroplasmic proteins (165, 262), viroplasm maturation (262), assembly of packaged particles (165, 262), association of rotavirus particles with rafts (65) and, finally, regulation of viral transcription by limiting plus-strand RNA accumulation (262). This latter function is thought to be exerted by NSP4 promoting conversion of transcriptionally active DLPs into quiescent TLPs (262).

NSP4 has also been identified as an enterotoxin (12, 137, 309). In fact, the delivery of purified recombinant NSP4 or synthetic NSP4 peptides into animal models causes age-dependent diarrhoea (12, 130). NSP4 is thought to exert its enterotoxigenic activity both after secretion as a truncated peptide (309) or as a full-length protein (40) and directly as soon as it is synthesized in infected cells (20, 38, 269). In both cases, an increase in calcium levels is observed, which has also been correlated with an age-dependent Cl^- secretion (193). However, in the first case, this calcium increase is mediated by the activation of signalling pathways involving phospholipase C (PLC) (78) or phosphoinositide-3-kinase (PI3K) (257) after interaction with receptors located in neighbouring cells. Among these, $\alpha 1\beta 1$ and $\alpha 2\beta 1$ integrins have recently been identified (257). In the second case, NSP4 modifies the plasma membrane permeability (197), increaseas the intracellular calcium levels through a PLC-independent mechanism (22) and alters the actin network organization in a

calcium-dependent manner by altering the phospohrylation status of the remodelling protein cofilin (20). Changes in subcortical actin dynamics can affect cellular processes like endo- and exocytosis, tight-junction biogenesis and ion transport, thus directly contributing to rotavirus pathogenesis (20, 39, 141, 199, 269).

NSP5

NSP5 is a highly conserved O-glycosylated phosphorylated nonstructural protein (112, 293) with affinity for ssRNA and dsRNA (290) and capable of forming homomultimers (109, 228). It plays a key role in the rotavirus replication cycle, as demonstrated by its silencing through siRNAs (45, 166). In fact, the lack of NSP5 in infected cells results in the significant reduction of viral proteins, viroplasms, viral transcripts, dsRNA genomes, and viral progeny (45, 166). Also the distribution of the viral proteins is affected, most of them appearing dispersed instead of concentrated in viroplasms, with the peculiarity of VP6 shifting from a viroplasm location to a fibrous array (166). The involvement of NSP5 in rotavirus replication is also suggested by its detection in early replication complexes (104), by its interaction with the two structural proteins essentially involved in genome replication, VP1 and VP2 (2, 8, 23), by its localization in viroplasms (220) and by the fact that it forms VLS when coexpressed with NSP2 in uninfected cells (96) (see Fig. 9 in chapter 4). However, the exact roles in rotavirus replication of NSP5, of its post-translational modifications and also of its interactions remain still unclear. NSP5 has been extensively studied both in the full-length format and in many truncated variants, which provided insight into the involvement of different NSP5 regions in processes like viroplasm formation, phosphorylation, capability of multimerizing and interactions with other viral proteins.

The NSP5 polypeptide consists of 196-198 amino acids (depending on the virus strain), has a high serine (21%) and threonine (4.5%) content and, after separation by

SDS-PAGE, displays several phosphorylated isoforms, of which the most abundant is the band at 28KDa, followed by the band at 26KDa; there is then a heterogeneous pattern of fainter bands of molecular weight ranging from 32 to 34KDa (3, 26, 228). All these bands were shown to correspond to phophorylated isoforms by labelling experiments (3, 26, 228), even the band at 26KDa that is resistant to phosphatase treatment (Fig. 7).

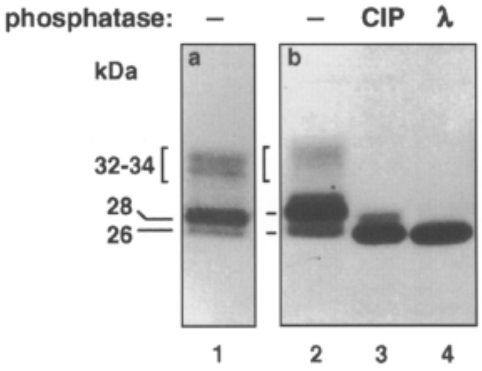

FIG. 7: SDS-PAGE analysis of NSP5. Lane 1: immunoblot analysis of extracts of SA11-infected MA104 cells (4h post-infection) reacted with anti-NSP5 serum. Lanes: 2-4: immunoprecipitation of NSP5 from virus-infected cells labelled in vivo with [^{35}S]-methionine and treated with phosphatases, as indicated. From Afrikanova et al, 1996.

As already mentioned, NSP5 is post-translationally modified by O-linked monomeric residues of N-acetylglucosamine (3, 112). Since lambda-phosphatase (λ-PPase) treatment of NSP5 labelled with [1,6-^{3}H]glucosamine showed that all bands can be converted into the 26KDa form with no loss of carbohydrate moieties, the addition of phosphates rather than O-glycosylation has been suggested to generate the different mobilities of the 26, 28 and 32-34KDa forms (3).

While the role of O-glycosylation is completely unknown, a lot of data, sometimes controversial, have been collected on multimerization and phosphorylation processes. NSP5 forms homomultimers through a region mapped to the 20 C-terminal amino acids, which have a predicted α-helical structure (256, 279). Consistent with this, mutants lacking the 10 C-terminal or the 18 C-terminal amino acids are unable to

multimerize (228, 279); in addition, the conserved cysteines in positions 170 and 173 have been shown to be not required for multimerization (279).

The mechanism leading to the NSP5 phosphorylation in infected cells is not yet completely elucidated. There are reports indicating that NSP5 expressed in bacteria, and thus free of contaminating kinases of mammalian cells, purified and incubated with [γ-^{32}P]ATP has a low level of auto-kinase activity *in vitro*, associated with a recently reported ATPase activity (13, 26, 290). However, the auto-kinase property is unlikely to be sufficient to generate a fully phophorylated state of NSP5 and the conversion from hypo- to hyperphosphorylated isoforms of NSP5 seems to be mediated by cellular casein kinase-like enzymes (43, 84, 87). Furthermore, a viral cofactor appears to be required to generate all the phosphorylated isoforms in the relative amounts observed in infected cells (3, 228). For instance, by coexpression experiments in uninfected cells NSP2 has been shown to be able to up-regulate the NSP5 hyperphosphorylation, most likely as a consequence of the interaction between the two proteins (2) and certainly not because of the NTPase activity of NSP2 (46). Thus, it is clear that many factors are involved in the hyperphosphorylation of NSP5, which appears to be a multi-step process (84). By the use of deletion and point mutants and siRNAs against the cellular kinase CK1α, it has been shown that the phosphorylation of serine 67 by CK1α and an intact C-terminus (84, 256, 279) are both required for initiating the cascade of NSP5 hyperphosphorylation (43, 84). Moreover, in the absence of other viral proteins, certain NSP5 deletion mutants lacking either the first 33 amino acids (Δ1) or the amino acids 81-130 (Δ3) can undergo hyperphosphorylation (87), probably because of an intact C-terminus able to multimerize and a conformation where serine 67 is available for phosphorylation; in addition, in the absence of other viral proteins, a mutant in which serine 67 is mutated to aspartic acid to mimic a phosphorylated residue is fully

hyperphosphorylated (84). It has then been proposed that the interaction with NSP2 induces a conformational change of NSP5 that renders serine 67 exposed and available for phosphorylation, but it was not predictable whether this phosphorylation occurs before or after NSP5 multimerization (84). Interestingly, and surprisingly, structural studies showed that a NSP5 mutant lacking the first 65 amino acids and the last 10 amino acids ($NSP5_{66\text{-}188}$) interacts with NSP2 as a dimer, and more precisely four NSP5 dimers bind to one NSP2 octamer (139). Since $NSP5_{66\text{-}188}$ was not expected to be able to dimerize because of the deletion at the C-terminus (279) and since it is known that NSP2 does not induce the hyperphosphorylation of mutants having a deleted C-terminus (96), it is possible that NSP5 needs to multimerize in complexes larger than dimers to be hyperphosphorylated.

Several lines of evidence indicate that an intact C-terminus is necessary but not sufficient not only for NSP5 hyperphosphorylation, but also for VLS and viroplasm formation: (i) NSP5 and NSP2 coexpressed in uninfected cells form VLS, but neither NSP5 expressed alone nor a NSP5 deletion mutant lacking the 18 C-terminal amino acids coexpressed with NSP2 do (85, 96); (ii) an NSP5 mutant containing only the 68 C-terminal amino acids cannot form VLS when expressed alone, but when it is transiently expressed in infected cells, it is recruited into viroplasms, probably as a consequence of its interaction with viral NSP5 (85, 87); (iii) in addition to an intact C-terminus, the presence of the 33 N-terminal amino acids was shown to be required for VLS formation in coexpression experiments with NSP2 (85); (iv) according to anticipated data in the Discussion section of ref. (13), the mutant $NSP5_{66\text{-}188}$ does not form VLS with NSP2 despite interacting with it. This latter observation negates the necessity of an interaction between NSP2 and NSP5 for VLS formation (85) and is consistent with the finding that N-tagged derivatives of NSP5 can form VLS when expressed alone in uninfected cells (190). It has then been proposed that the 10 C-

terminal amino acids of NSP5 may serve to promote viroplasm assembly through the mutual recognition, the multimerization and the consequent recruitment of already formed NSP5-NSP2 complexes (13); in this view, the contribution of NSP2, or of the tagging at the N-terminus, might consist in inducing a conformational change of NSP5 that renders the C-terminus accessible for the homo-multimerization of many NSP5 molecules. However, the role of NSP2 and the NSP5 N-terminus in VLS formation remains still little defined.

A controversial issue is the possibility of a link between NSP5 hyperphosphorylation and VLS or viroplasm formation: despite the frequently observed correlation between the hyperphosphorylation status of NSP5 and the viroplasm/VLS formation (96, 228), supported also by the fact that tagging NSP5 at the N-terminus renders the protein both capable of forming VLS by itself (190) and hyperphosphorylated (44), most evidence indicate that hyperphosphorylation is not required for viroplasm/VLS formation: in fact, (i) *in vivo* inhibition of phosphatases in cells transfected with an NSP5 encoding plasmid results in a fully phosphorylated NSP5, but not in VLS formation (27); (ii) NSP5 deletion mutants that are not phosphorylated are recruited into viroplasms of infected cells (87); (iii) an siRNA against CK1α, the kinase involved in the phosphorylation of serine 67, inhibits NSP5 hyperphosphorylation, but not viroplasm formation (43). It has been proposed that NSP5 hyperphosphorylation has a role in viroplasm maturation and possibly in replication since its inhibition by an siRNA against CK1α results in an altered viroplasm shape and a moderate decrease in dsRNA synthesis (43). Viroplasms have also been proposed as sites where NSP5 is protected by the action of cellular phosphatases (27) and NSP5 hyperphosphorylation would then be guaranteed by viroplasm/VLS formation. Hyperphosphorylation and viroplasm/VLS formation may also be independent processes triggered by a common event: the NSP5 multimerization.

It has recently been reported that calcium regulates VLS formation: in the absence of calcium VLS cannot form, but when two tandem DxDxD motifs located upstream and adjacent to the predicted C-terminal helix of NSP5 are mutagenized, VLS can form constitutively even in the absence of calcium (256). This is in agreement with the role of regulator of viroplasm maturation proposed for NSP4 (21), the viral protein that modifies the calcium homeostasis in rotavirus-infected cells.

With regard to the interaction of NSP5 with NSP2 (2, 85, 96, 139, 228), the N-terminus and the C-terminus of NSP5 have been initially identified by yeast two-hybrid and coimmunoprecipitation studies as the regions essential for binding (85). However, the cryo-EM structure of the complex NSP2-$NSP5_{66\text{-}188}$ suggests that those regions may also be dispensable (139). In the same report, a competition between $NSP5_{66\text{-}188}$ and RNA for binding to NSP2 is described, suggesting a role for NSP5 in regulating NSP2-RNA interaction during replication and/or packaging (139). Apart from interacting with NSP2, NSP5 also interacts with VP1 (2, 8) and VP2 (23), but the role of these interactions is at present completely obscure. As already mentioned, coexpression in insect cells of NSP5 and a deletion mutant of VP2 lacking the 92 N-terminal amino acids leads to the formation of a few and large inclusion bodies, into which VP6 is also recruited when coexpressed with the other two proteins (23). However, NSP5 was shown to affect the stability of VLPs formed by VP2 and VP6 and VP6 to hinder the NSP5-VP2 interaction (23). This suggests a competition between NSP5 and VP6 for binding to VP2.

An interaction of both NSP5 and NSP2 with tubulin has been found, suggesting a role for the two nonstructural proteins in anchoring viroplasms to microtubules (42).

NSP6

NSP6 is the smallest nonstructural protein of rotavirus, is encoded in an alternative ORF of the same segment encoding NSP5 (no. 11), is expressed at very low levels

and localizes in viroplasms (178, 238). It has a high rate of turnover, being completely degraded within two hours of synthesis (238). Some rotavirus strains of group A and all strains of group C do not encode NSP6 (115, 148), and the group A OSU strain encodes a truncated version of NSP6 (111), suggesting that this protein is not essential for the viral replication cycle. This view is strengthened by the fact that a cell line expressing NSP5 from OSU strain, and thus a truncated and possibly non-functional NSP6, transfected with an siRNA against NSP5 from SA-11 strain and infected with SA-11 strain, shows a wild-type phenotype of viral infection because of the complementation ability of the OSU-derived NSP5 and despite the absence of a full-length NSP6 (45). NSP6 was found to interact with the 35 C-terminal amino acids of NSP5, and since the removal of the 10 C-terminal amino acids from NSP5 abolishes the interaction, it has been proposed that NSP6 has a regulatory, but not essential, role in the self-association of NSP5 (279). However, the NSP5-NSP6 interaction has been described only in transfected cells and could never be detected in infected cells (279). Recently, it has been shown that similarly to NSP5, NSP6 has an unspecific affinity for both ss and dsRNA (238).

4. VIRUS REPLICATION

4.1. OVERVIEW

Most details of the rotavirus replicative cycle have been obtained from studies of cell culture-adapted rotavirus strains infecting monkey kidney cells (MA104). However, the natural cell host is the mature epithelial cell of the small intestine and

new data, sometimes in contrast with those derived from MA104 cells, are emerging from infection of differentiated human intestinal cell lines (Caco-2) (91).

The studies with MA104 cells allowed to define some general features of rotavirus replication (91):

- replication is totally cytoplasmic;
- cells do not contain enzymes to replicate dsRNA, they are supplied by the virus;
- free dsRNA or free negative-strand ssRNA are never found in infected cells; in fact, dsRNA segments are formed within nascent subviral particles and once the negative strand is synthesized, it remains associated with the positive-strand;
- levels of intracellular calcium are crucial to allow virus assembly and integrity.

Based on all data so far collected, a general description of the replicative cycle can be provided (Fig. 8). After entry into the host cell the virion loses the outer layer to become a DLP. At this stage the viral RdRp, VP1, transcribes plus-strand RNAs, which are capped but not polyadenylated, and are extruded from the viral particle into the cytoplasm. This single plus-strand RNA functions as both:

- messenger RNA for the synthesis of viral proteins;
- template for the synthesis of the dsRNA genome segments ("replication").

Once critical amounts of viral proteins are synthesized, viral proteins accumulate in cytoplasmic inclusion bodies called "viroplasms", which appear early (2-3 hours) after infection and are considered to be sites of the synthesis of dsRNA and assembly of progeny DLPs. Subviral particles assembled in viroplasms bud through the membrane of the endoplasmic reticulum (ER) acquiring a transient envelope. Budding is mediated by the NSP4 molecules incorporated into the ER, which function as intracellular receptors for DLPs. The transient envelope is then lost and replaced by the

VP4-VP7 layer. TLPs are released either by cell lysis or by a non-classical, Golgi-independent, vesicular transport involving interaction with lipid "rafts" near the plasma membrane and not resulting in extensive cytopathic effect (91).

The details, the most plausible hypothesis and the controversial findings about the various phases of the replicative cycle are presented in the following paragraphs.

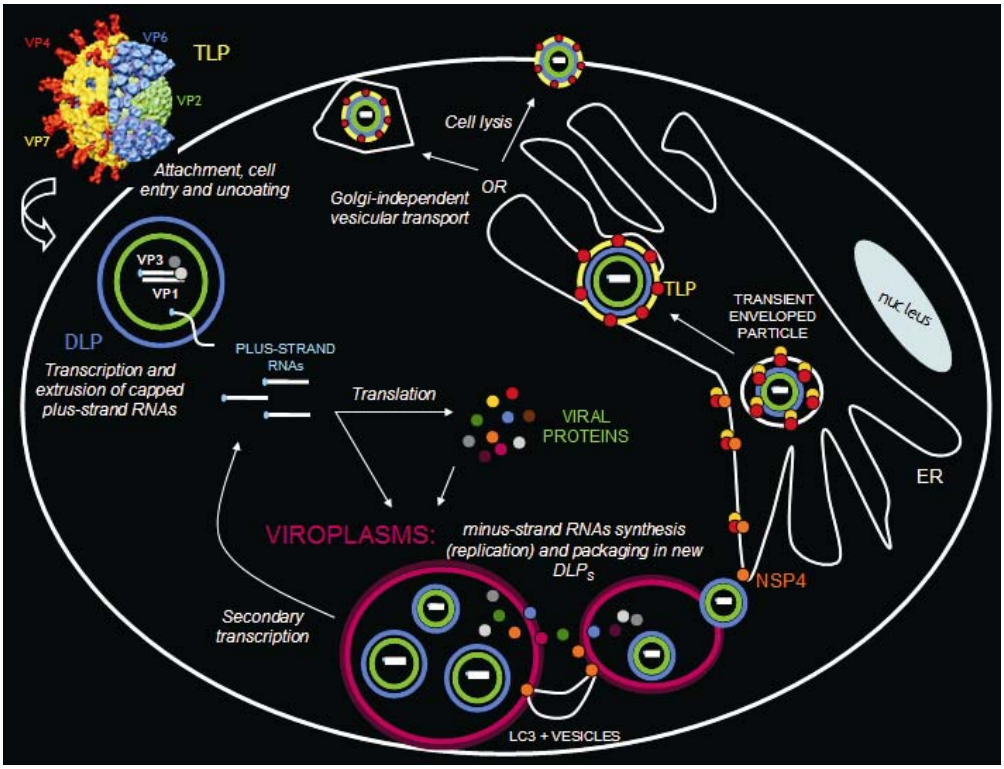

FIG. 8: Schematic representation of the major features of the rotavirus replicative cycle.

4.2. CELL ATTACHMENT AND ENTRY

Rotavirus attachment to target cells and the following entry are a complex and not yet entirely elucidated process involving sequential interactions of VP4 and VP7 with different cellular receptors.

Although VP7 has been shown to contribute to the attachment (102, 248, 306), VP4 plays a major role in this preliminary phase of cell entry (146, 167). The first event involving VP4 (88KDa) is its cleavage by intestinal trypsin into two fragments, VP5* (60KDa) and VP8* (28KDa), which remain associated in the virion (94, 98). However, this cleavage does not appear to be essential for cell binding (59, 144), rather, it has been associated with cell entry (see below). Sialic acid (SA) was the first rotavirus receptor identified as crucial for cell attachment based on hemagglutination of red blood cells induced by some rotavirus strains (17, 98). VP8* was recognized as the functional component of rotavirus hemagglutinin (98, 100). However, since many rotavirus strains, including all human rotaviruses, were shown to initiate infection independently of sialidase treatment of cultured cells and were not believed to bind to SA (58, 179), rotavirus strains were classified in two categories: SA-dependent and SA-independent. This distinction is now considered imprecise. In fact, there is increasing evidence that several sialidase-insensitive strains bind to sialic acids located internally within oligosaccharide structures, and thus not accessible to sialidases, or to sialic acids modified and thus resistant to sialidase treatment (71, 126, 127, 140). Therefore, a classification only based on the sensitivity of infectivity to sialidase treatment is preferable. This idea is also supported by x-ray crystallographic studies of complexes formed by sialic acid derivatives and purified VP8* derived from both sialidase-sensitive and sialidase-insensitive strains (28, 82).

A second receptor shown to be involved in rotavirus attachment, and possibly penetration (57), is $\alpha 2\beta 1$ integrin, which is bound by VP5* through the sequence DGE (120, 121, 304, 305).

Additional cellular receptors play an important role in virus entry in a post-attachment phase:

- the heat shock cognate protein 70 (Hsc70), whose binding with VP5* may modify the conformation of the virus particle to help entry (124, 216, 303); a recent report suggests also an involvement of VP6 in interaction with Hsc70 (123);
- $\alpha v\beta 3$ integrin and $\alpha x\beta 2$, which are bound by VP7 (120, 122, 125);
- $\alpha 4\beta 1$ and $\alpha 4\beta 7$ integrins: since neutralizing monoclonal antibodies against both VP5* and VP7 inihibit binding of rotavirus to these integrines, they may be bound by both VP5* (possibly through its YGL sequence) and VP7 (119).

The internalization process occurs through a not completely elucidated mechanism. It has been demonstrated that (91):

- it requires active cellular processes because it does not take place at 4°C;
- it does not depend on endosome acidification (as found for influenza viruses);
- it is enhanced by trypsin cleavage of VP4, as trypsinased particles enter cells more quickly than non-trypsinased (7, 94).

However, molecular details of cell entry remain unclear. Two pathways are proposed to be involved: direct penetration (144, 268) and a non-classical endocytosis. This latter would depend either on endocytic vesicles that maintain low Ca^{2+} levels (50) or on the presence of cholesterol on the cell membrane and on a functional dynamin, independently of both clathrin and caveolin (50, 251). Since the mechanisms of cell entry are not well defined, the role of trypsin cleavage also remains poorly understood. Trypsin has been found incorporated in TLPs in an inactive form and is activated in an environment containing low concentrations of Ca^{2+} (18), as might occur near the plasma membrane following cell binding. It has been proposed that trypsinization induces VP4 spikes to switch from a disordered to an ordered structure and that conformational changes of VP4 at a post-attachment stage allow sequential interactions with multiple receptors involved in penetration (64, 217). Moreover,

fragments deriving from trypsin cleavage of VP7 and VP4 were shown to be capable of disrupting membranes (47, 72, 245), allowing access of DLPs into the cytosol.
The loss of VP4 and VP7 (uncoating) resulting from the cell entry represents a key event, as it triggers the emergence of transcriptionally active DLPs (see below). Many reports agree on a correlation between the uncoating process and a lowering of Ca^{2+} concentration at the membrane proximity (50, 61, 172, 245, 247), even if the details and the sequential order of the events leading to the access of uncoated virions into the cytosol remain to be clarified.

4.3. TRANSCRIPTION

Synthesis of full-length positive-strands from the negative-strands of the dsRNA genome (transcription) occurs after cell entry (primary transcription) and also when new DLPs are formed within viroplasms (secondary transcription) (91, 166, 265). The process is considered to occur in three stages (157, 158):

- initiation, which consists in synthesis and capping of the nascent transcript (6-7 nucleotides);
- elongation, in which the transcript starts separating from the genomic template and nucleotidyl transfer proceeds;
- translocation, in which the growing transcript pass through type I channels, to be extruded from the DLP.

The transcriptase activity of the viral particle is activated *in vitro* by removal of VP4 and VP7 through chelating agents or heat shock treatment (61, 264). Therefore, the uncoating process seems to be the essential event triggering primary transcription. This hypothesis is strengthened by the fact that DLPs can generate a productive

infection when they are liposome-transfected into cells (16). It has to be noted that TLPs cannot be defined properly as transcriptionally incompetent, they rather contain a latent transcriptase activity: in fact, *in vitro* they can produce 5-7 nucleotide long capped mRNA fragments (157), suggesting that polymerase and capping enzyme are both functional in TLPs and that some structural properties related to the presence of the outer capsid interfere with elongation, and possibly translocation, of the transcripts. Many factors have been proposed to explain this inhibitory effect: conformational changes of VP6, induced *in vitro* by both VP7 and some anti-VP6 antibodies (97, 156); a steric hindrance blocking the exit of nascent mRNAs through type I channels, as shown for VP7 (159); structural constraints arising from the geometry imposed by proteins of both the external and the intermediate layers (162). However, the details remain to be elucidated.

Rotavirus contains all the necessary enzymatic machinery to synthesize complete capped mRNA transcripts within the core without the need for disassembly. Indeed, transcription occurs efficiently only when the transcriptionally competent particle is fully intact (158). This particle comprises VP1, the RdRp, VP3, which functions as a guanylyl-transferase and methylase, VP2 and VP6, whose mutual interactions maintain a spatial architecture needed for the transcriptase activity (48). The enzymatic activities of the transcriptionally competent particle have either been demonstrated biochemically or they are inferred because rotavirus transcripts made *in vitro* in the presence of S-adenosyl methionine (SAM) have a methylated 5'-terminal cap structure m^7GpppGm (52, 164, 225), and transcription is inhibited by pyrophosphate (264). Since the template is a dsRNA, a helicase activity has been thought to be required to unwind the template, but that enzymatic property has so far not been demonstrated for any of the viral structural proteins.

Cryoelectron microscopy studies indicated that transcription occurs near the 5-fold axes, where VP1 and VP3 are located, and that multiple newly transcribed RNAs pass through type I-channels and are released simultaneously from an actively transcribing particle (159, 234), confirming the fact that DLPs can transcribe concomitantly many different ssRNA molecules (264) and that the transcription process is continuous. However, the mechanisms driving the movement of the genome segments through the enzyme complex to allow repeated cycles of transcription remain unknown.

As already mentioned, plus-strand RNAs deriving from transcription are extruded from the DLP into the cytosol, where they can be used either for the synthesis of viral proteins or for the synthesis of new dsRNA genomes.

4.4. TRANSLATION

Rotavirus mRNA transcripts are capped and not polyadenylated. These are two important peculiarities to be considered to understand how rotavirus uses the cellular translation machinery. The cap structure can be recognized by the cellular cap binding protein eIF4E, which promotes the association with the 40S ribosomal subunit. The eIF4E protein belongs to a complex called eIF4F, in which two other proteins are found: a helicase, which unwinds RNA secondary structures, and the scaffolding protein eIF4G, which binds the poly(A)-binding protein (PABP), in turn bound to the poly(A) at the 3' end of eukaryotic mRNAs, thus approximating the two mRNA ends to ensure an efficient initiation of translation (237). This complex does not seem to be able to recruit PABP onto rotavirus mRNAs, not only because there is no poly(A) tail at the 3' end of viral mRNAs, but also because a rotavirus

nonstructural protein, NSP3, is able to compete with PABP for binding to eIF4G (223, 224). Since NSP3 recognizes also the consensus sequence 5'-UGACC-3' at the 3'UTR of viral mRNAs (74, 226, 227), this protein has been considered to be able to promote the circularization of rotaviral mRNAs, thus enhancing their translation (224). At the same time NSP3 hampers the translation of cellular mRNAs through its competion with PABP for binding to eIF4G (224) and concomitantly causes a translocation of the free PABP from the cytoplasm to the nucleus (192). NSP3 and eIF4G also interact with a cellular protein called RoXaN (Rotavirus X protein associated with NSP3) forming a ternary complex, whose role remains to be determined (292). However, despite a general agreement on the role of NSP3 in inhibiting translation of cellular proteins, its role in rotavirus mRNAs translation is still controversial: on one side it has been shown that NSP3 enhances translation of rotavirus-like mRNAs both *in vivo* and *in vitro* (289), on the other hand silencing of the expression of both NSP3 and eIF4G by siRNAs does not affect synthesis of viral proteins and may even increase the yield of viral progeny (191). The binding of NSP3 to viral plus-strand RNAs has been then proposed to protect viral mRNAs from degradation and/or to keep a pool of plus-strand RNAs in the cytoplasm available for translation (191).

Interestingly, three additional viral proteins have recently been shown to be involved in inhibition of cellular protein synthesis: VP2, NSP2 and NSP5. They seem to be involved in phosphorylation of the α subunit of the translation initiation factor eIF2, an event that inhibits the translation of cellular mRNAs (192). However, further investigations are needed to demonstrate the details of their involvement.

Most rotavirus proteins are synthesized on free ribosomes because of the absence of signal sequences for targeting to the ER. However, VP7 and NSP4 contain such signal sequences at their N-termini and are synthesized on ribosomes associated with

the membrane of the ER. The signal sequence of VP7 is cotranslationally cleaved, whereas that of NSP4 is not (91).

4.5. GENOME REPLICATION AND PACKAGING

Rotavirus RNA replication and packaging represent one of the most unexplored and intriguing aspects of the replicative cycle. Its understanding would help in constructing reassortant rotaviruses and rotaviruses by reverse genetics and also be helpful for the further development of safe vaccines.

As already mentioned, the newly synthesized viral plus-strand RNAs are used not only as transcripts for the synthesis of viral proteins, but also as templates for the synthesis of the complementary negative-sense strand RNA, leading to the emergence of dsRNA genome segments. This process is named "replication". After replication, dsRNAs remain associated with subviral particles (complexes separable by sedimentation through sucrose or CsCl gradients), suggesting that free dsRNA is not found in the cytoplasm of infected cells (91).

The proteins involved in replication have been studied by analysis of subviral particles capable of completing nascent negative-strand synthesis *in vitro* (Replication Intermediates or RI), by cell-free systems supporting the synthesis of viral RNAs from exogenous RNA templates and by the analysis of production of dsRNAs in infected cells transfected with small interfering RNAs (siRNAs) against specific viral RNA segments:

- Replication Intermediates (RI): VP1, VP2, VP3 and the nonstructural proteins NSP2, NSP3 and NSP5, together with attached RNAs, have been identified in the minimum particle purified from infected cells with replicase activity associated (104, 210). This suggests that all these proteins have a role in

replication. By immunoprecipitation from extracts of infected cells with a monoclonal anti-NSP2 antibody, an active replicase complex has been reported, which contained VP1, VP2, VP3 and VP6 but lacked NSP1, NSP3 and NSP5. This complex was able to complete the synthesis of nascent negative-strand RNAs, but not to use exogenous RNAs as templates (5).

- Template-dependent cell-free replication systems (55, 208): such systems containing only the structural proteins of the core, derived from either virions or baculovirus recombinants, showed that VP1 and VP2 are necessary and sufficient to provide replicase activity *in vitro* (212, 308). However, the levels of replicase activity were significantly higher in the presence of VP3 (212, 308). These observations supported the view that nonstructural proteins are not essentially required for replicase activity, but did not rule out that they can increase replication efficiency *in vivo* or may have a role in genome packaging.
- Experiments with siRNA and analysis of dsRNA production: such experiments confirmed the involvement of VP1, VP2, NSP5 and NSP2 in viral RNA replication (45, 166, 261, 262) and showed that silencing of NSP3 (191), NSP4 (262) and VP7 (261) does not reduce the amounts of replicated dsRNAs.

All viral proteins found in RI, with the exception of NSP3, were also found in perinuclear nonmembrane-bound electron-dense cytoplasmic inclusion bodies called viroplasms, where VP6 was detected in addition (219, 220, 241) (Fig. 9). These inclusion bodies, representing accumulations of viral proteins and RNA, appear early (2-3h) after infection and are considered sites of viral RNA replication and DLP assembly based on their protein composition and on electron microscopy analysis showing newly made core and DLPs assembled within them (4, 90, 220).

Viroplasms were also shown to be sites of transcription, possibly mediated by the newly assembled DLPs and therefore termed secondary transcription (261). Two nonstructural proteins, NSP5 and NSP2, are considered essential for the formation of these inclusion bodies: they were shown to be able to form VLS when coexpressed in uninfected cells (96) (Fig. 9) and suppression of their expression in infected cells abolished viroplasm formation, viral RNA replication and production of infectious viral progeny (45, 166, 261, 285).

Beyond the involvement of the indicated proteins in replication, the experiments with siRNAs revealed another important aspect of genome replication. Since the viral transcripts function both as messengers and as templates of genome synthesis, it was expected that siRNAs directed to transcripts encoding proteins not involved in replication, like VP4 and VP7, would impair the synthesis of both the protein and the corresponding dsRNA. However, it has been reported that siRNAs directed to VP4 and VP7 allowed the synthesis of regular amounts of all eleven genome segments, despite the synthesis of the target protein was almost completely ablated (67, 165, 261). This led to the idea of two separate pools of viral plus-strand RNAs, one used for translation and the other for replication. How this physical separation occurs and may be maintained is not clear. Viroplasms might create a protective environment for replicating plus-strand RNAs or the association with some viral RNA-binding proteins might make them inaccessible to the cytoplasmic RNA interference machinery. With this regard, it has been shown that a labelled rotavirus-like plus-strand RNA transfected in cells one or five hours after infection was not recruited into viroplasms, leading to the conclusion that pathways for delivering plus-strand RNAs from cytosol to viroplasms do not exist (261). According to these data, a model was suggested for which DLPs would function as nucleation sites for viroplasm formation following the accumulation of newly synthesized proteins. Once the levels of new transcripts made

in viroplasms exceeds the binding capacity of the RNA binding proteins, the transcripts would leave viroplasms and be used for a further synthesis of viral proteins (261). The suggested lack of pathways that transport plus-strand RNAs to viroplasms would explain the failure of numerous attempts to construct a recombinant rotavirus (91). Whilst the insertion of an exogenous viral RNA into the viral progeny has recently been achieved (see description of the system in chapter 5) (150), the very low efficiency of recovery of recombinant virus suggests that the accessibility of exogenous RNAs to viroplasms is limited.

Except for VP1, the functions of individual proteins involved in viral RNA replication remain controversial and obscure. Apart from functioning as a transcriptase, VP1 catalyzes the synthesis of viral minus-strand RNAs after specific recognition of the template at both the 5' and 3'UTRs (280, 281). More in detail, it has been shown that the 5' end contains a specific recognition signal associated with the G2 residue of the 5'-consensus sequence and that the 3' end contains signals in both the conserved and nonconserved regions (280, 281). The binding of VP1 to these sites is essential to promote replication, possibly stabilizing the putative cyclization of the template in a panhandle structure (281). On the other hand, in replication assays recombinant VP1 is not sufficient to promote minus-strand synthesis, unless VP2 is added (280).

VP2, which has a strong affinity for the single-strand template but less for the dsRNA (212), and binds RNA in a nonspecific manner (209), must have a role linked with binding to the template, to VP1 and possibly to VP3 (307). The fact that dsRNA synthesis in replication assays with recombinant VP1 and VP2 was maximal when the ratio between the two proteins was 1:10 indicated that replicase activity requires structures similar to those observed at the vertexes of the core, suggesting an important structural role for VP2 (280). However, the exact function of this protein in

this context remains still undefined. Assays performed with recombinant VP1 and VP2 also showed that the order of interaction of these proteins with the template affects the efficiency of formation of active replicase complexes, suggesting that their formation *in vivo* would start in an environment free of VP2 (291).

Without recognizing any specific signal in the template and through its affinity to VP1, VP2 and/or RNA, VP3 might have the role of increasing the rate at which replication complexes are assembled (in addition to its function of capping enzyme during viral transcription) (209, 212, 286).

As already mentioned, the nonstructural proteins NSP5 and NSP2 have an important role in forming viroplasms but do not seem to be essential for the replicase activity. However, they might increase or regulate the replication process or have a role in genome packaging.

Because of its ssRNA binding and helix destabilizing properties, the octamer NSP2 has been proposed as a platform that organizes replication complexes and unravels any secondary structure in positive-sense RNA templates in preparation for the dsRNA synthesis (272). How NSP2 distinguishes between viral and cellular RNAs is still an open question. RNA binding seems to induce a conformational change in NSP2 (139, 255), which might have a role in regulating interactions with other viral proteins, such as VP1 (145) or NSP5 (2, 96). Although the role of the enzymatic activities of NSP2 (NTPase, RTPase, NDP kinase; see chapter 3 for details) is still unclear, it has been proposed that NSP2 acts as a molecular motor providing the energy deriving from hydrolysis of NTPs for genome replication and/or packaging (138, 272) and maintaining a pool of nucleotides in viroplasms for RNA synthesis and for processes requiring ATP (i.e. transcription or RNA packaging) (151). Interestingly, an inhibitory role for NSP2 in the formation of the replication initiation complexes has been demonstrated in *in vitro* assays with recombinant VP1 and VP2.

In detail, NSP2 was shown to interfere not with the binding of VP1 to the template, but with the function of VP2, possibly as a result of competition for RNA binding (291).

The role of NSP5 in RNA replication and packaging is even more obscure than that of NSP2: it has recently been shown that a truncated form of NSP5 competes with RNA for binding to NSP2 (139), suggesting that NSP5 might have a regulatory role in the RNA binding activity of NSP2. Moreover, based on the description of an interaction between NSP5 and VP2 (23), it has been suggested that NSP5 may act as a physical adapter between NSP2 and VP2. However, a strong interaction between NSP5 and the polymerase VP1 has recently been observed [described in this thesis and (8)], indicating the need of further studies to investigate new possible functions of NSP5.

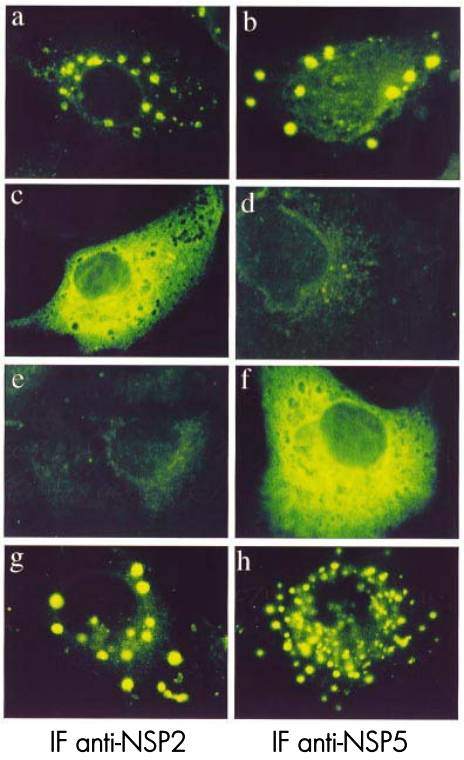

FIG. 9: Localization of rotavirus NSP2 and NSP5 in viroplasms and VLS. The two proteins were detected by immunofluorescence microscopy using antibodies specific for NSP2 or NSP5 as indicated, in cells infected with SA11 rotavirus (a, b), transfected with either NSP2 (c, d) or NSP5 (e, f), or cotransfected with NSP2 and NSP5 (g, h). From Fabbretti et al, 1999.

Genome packaging is a selective process capable to guarantee the presence of all eleven genome segments in equimolar amounts in every newly assembled viral particle. Signals and mechanisms driving the assortment of the genome segments are unknown. The requirements for packaging are rather complex, as indicated by *in vitro* replication assays: if VP1 and VP2 are sufficient to provide replicase activity, they are not to package the newly synthesized dsRNAs (212). Secondary structures of the eleven dsRNA segments and/or nonstructural proteins may be of importance for packaging.

Several models have been proposed for describing genome replication and packaging (213):

- precore precursor model: a precore consisting of viral RNA, VP1 and VP3 would function as a nucleation site for the binding of VP2 to form a core. This model is based on the isolation from infected cells of precores without replicase activity and containing RNA, VP1 and VP3 (104).
- empty capsid precursor model: empty cores (VP1, VP2, VP3) would be first made and would be filled with RNA through a "packaging motor" formed by nonstructural proteins (e.g. NSP2, see above). This model is based on the ability of capsid proteins to self-assemble into empty virus-like particles (VLPs) able to support RNA replication (308) and on data obtained with a bacterial dsRNA virus, the bacteriophage phi6.
- simultaneous encapsidation and capsid assembly model: each RNA-VP1-VP3 complex would associate with a specific RNA segment and attract VP2, which would form pentamer subunits; interactions between RNAs of the different pentameric units would then induce the formation of cores; structural changes of VP2 after pentamer-pentamer binding may activate replication. Structural studies of the rotavirus core supports this model, which differs from

the precore precursor model for the formation of functionally separate pentameric units before core formation (234).

Further studies are needed to clarify which model is correct and if and how they may need to be modified.

4.6. VIRUS MORPHOGENESIS

Initial assembly of viral progeny starts in viroplasms, where new DLPs are synthesized and viral genome segments are sorted and packaged through a still unknown mechanism. During the course of viral infection, viroplasms mature showing an increase in size and a decrease in number, suggesting a continued accumulation of proteins, RNA and newly formed viral particles and a fusion process among different viroplasms (85). It has been reported that silencing expression of the nonstructural protein NSP4 leads to a defect in viroplasm maturation, with a concomitant maldistribution of viroplasmic proteins, and to a decreased assembly of packaged particles (262). This suggested a role for the nonstructural protein NSP4 in linking the process of genome packaging and capsid morphogenesis. With this regard, it has been reported that part of NSP4 is distributed in vesicles throughout the cytoplasm, colocalizing with the autophagosomal marker LC3 and in association with viroplasms (21). Therefore, these vesicles have been proposed as a lipid membrane scaffold for the formation of large viroplasms by recruiting early viroplasms and also as regulators of genome packaging and transcription (through NSP4 association with VP6) (21). Furthermore, a role for NSP4 in facilitating the assembly of VP6 on the top of cores has been suggested by the fact that well-defined particles are apparent only at the periphery of viroplasms (181, 218, 230) and that purified DLPs aggregate and change their structure when incubated with soluble NSP4 (276).

However, silencing NSP4 expression still allows DLPs formation, even with a lower yield, and rather causes an accumulation of empty DLPs, confirming the hypothesis of a role of NSP4 in linking genome packaging and morphogenesis rather than in regulating the VP6 assembly on cores (165, 262).

Once newly packaged DLPs are formed, rotavirus morphogenesis proceeds through a complex process consisting of several steps:

- DLP budding into the ER;
- acquisition of a transient envelope;
- loss of the transient envelope and formation of the outer capsid layer;
- TLP release from the host cell.

The first step is mediated by the interaction of VP6 present on the surface of newly synthesized DLPs with NSP4 molecules localized in the ER membrane to act as intracellular receptors for DLPs (9, 19). The affinity between the cytosolic (C-terminal) tail of NSP4 and VP6 drives this interaction (180, 275-277). VP7 and VP4 do not seem to have a function in the transit of DLPs into the ER, because in their absence DLPs can still bud into the ER (67, 165). However, they oligomerize with NSP4 forming a heterotrimeric complex (170), which may play a role in the following step, when a transient envelope containing all three proteins is acquired (229). When VP4 is silenced, TLPs are still formed, although without spikes and less infectious, suggesting that VP4 does not have an essential role at this stage (67). By contrast, silencing the expression of VP7 impairs TLP formation (261) and leads to the accumulation of enveloped particles, indicating a role for VP7 in the removal of the lipid membrane from particles maturating in the ER (165, 261). NSP4 glycosylation was also proposed to be critical at this stage (69, 218). However, the mechanisms underlying the loss of the envelope and the following correct assembly of capsid proteins are not yet understood. By contrast, it is well known that rotavirus maturation

in the ER is a calcium-dependent process. In fact, experimental disruption of calcium gradients, in particular inhibition of the endoplasmic reticulum calcium pump (SERCA pump), decreases the production of infectious particles significantly with the concomitant accumulation of enveloped particles (181, 230, 258, 259); on the other hand, inhibition of the SERCA pump at late infection times induces the disassembly of already matured particles within the ER (246). During rotavirus infection the plasma membrane permeability to calcium increases and consequently cytosolic calcium concentration and calcium sequestering into the ER rise (181). siRNA experiments have shown that changes in calcium homeostasis are mediated mainly by NSP4 and to a lesser extent by VP7 (302). This is consistent with the evidence of higher cytosolic calcium levels in uninfected cells expressing recombinant NSP4 (22, 77, 278) and with the inhibition of the calcium permeability of the plasma membrane by the use of tunicamycin, an inhibitor of the ER N-linked glycosylation involving both rotavirus glycoproteins NSP4 and VP7. However, VP7 glycosylation does not seem to be essential, as rotavirus strains with a non-glycosylated VP7 exist which are capable to produce fully infectious particles (91). How NSP4 alters the calcium homeostasis is currently unknown: it might destabilize the plasma membrane directly, act as a viroporin or interact with cellular proteins to exert its permeabilizing activity. The exact role of an environment rich in calcium for virus morphogenesis is not known: it has been proposed that it triggers the lateral interaction of VP7 molecules forming a tighter layer able to interact with VP6 and concomitantly remove lipids and NSP4 (165). In fact, among the consequences of an experimental calcium depletion in the ER, there are the alteration of VP4-VP7-NSP4 heterotrimers (230) and a block of VP7 trimerization (80). In addition to calcium concentrations, other factors are essential for a proper virus assembly in the ER: the ATP concentration (185) and the presence of some chaperones, among them

PDI (protein disulfide isomerase), grp78, calnexin and reticulin, which have been shown to be essential for the correct folding of NSP4 and VP7 (173, 184, 186).

A controversial issue is how and when VP4 is inserted into newly formed viral particles. VP4 assembly was initially thought to occur concomitantly with VP7 in an NSP4-dependent process within the ER (170). However, in infected Caco-2 cells VP4 was not found to colocalize with ER-markers (69), and was detected in association with raft-type membrane microdomains (RTM), which are absent in the ER and were shown to be involved in targeting rotavirus particles to the cell surface (66, 252). Moreover, treatment of infected Caco-2 cells with tunicamycin, a drug blocking enveloped particles in the ER, did not show any effect on VP4 localization, trafficking and association with rafts (69). Therefore, it has been proposed that VP4 is added to particles in a an extra-reticular compartment after removal of the transient envelope (69). In addition, it has been reported that VP4 can reach the plasma membrane through the microtubule network independently of the presence of other viral proteins (196). However, in MA104 cells both siRNAs against VP4 or NSP4 and tunicamycin treatment significantly reduce the targeting of VP4 to rafts suggesting that association of VP4 with viral particles may occur in the ER (65). Moreover, the *in vitro* recoating of DLPs requires that VP4 is added before VP7 to obtain infectious TLPs (283), which suggests the need in the ER of VP4 or of DLPs previously coated by VP4 for a correct assembly. It has then been proposed that two pools of VP4 exist, one associated with particles in the ER and the other independently localized at the plasma membrane (65). Interestingly, it has been shown that there are significant differences in raft composition and in VP4 association to rafts in Caco-2 and MA104 cells, which might in turn imply differences in virus assembly and release in the two cell types (68). These date indicate the importance of using a model that is as similar as possible to the natural target of rotavirus (the polarized small intestinal enterocytes).

In conclusion, further studies are needed to elucidate location and timing of VP4 assembly into newly formed viral particles.

4.7. VIRUS RELEASE

Another still unclear issue is the pathway used by rotavirus to leave the host cell: using MA104 cells, rotavirus was initially believed to exit by cell lysis (4, 195); afterwards, studies in polarized Caco-2 cells showed that rotavirus is released almost exclusively at the apical pole through a non-conventional vesicular transport that bypasses the Golgi apparatus and lysosomes (142). This process occurs in the absence of cell lysis, which fits the histopathological data found *in vivo* (142). Assuming that VP4 is assembled in the ER and that both VP4 and NSP4 have a role in virus release, the demonstrated associations of these proteins with rafts, actin and/or microtubules might be critical at this stage. More in detail, VP4 association with rafts (66, 252) might be mediated by the N-terminal galectin-like domain of VP4 that would confer the same capacity of galectin-4 of using the "nonclassical secretory pathway" (68, 198); furthermore, VP4 might account for the apical release of progeny virions through binding to actin bundles of the brush border of cells, which causes a dissolution of apical microvilli (105, 106). Another report suggests that NSP4 contributes to the polarized virus release by stiffening the basolateral actin network in a calcium-dependent manner, through decreased phosphorylation of the actin remodelling protein cofilin (20). However, the signals directing particles formed in the ER to the nonclassical secretory pathway are unknown. In the conventional secretion pathway the cargo proteins transit from the ER to the Golgi apparatus through a vesicle-mediated transport system that constitutes the so called ER-Golgi intermediate compartment (ERGIC) and can be visualized by two marker proteins

usually recycling among ER, ERGIC and Golgi: ERGIC-53 and β-COP (297). Increasing evidence suggest participation of the ERGIC in rotavirus maturation, because NSP4, VP4 and VP7 were all found in this compartment (65, 187, 297). In addition, the overexpression of NSP4 in transfected cells as well as natural rotavirus infection change the distribution of ERGIC-53 from a juxtanuclear vesicle-like pattern to a more dispersed one (65, 297). It has then been proposed that at some stages organelles containing ERGIC-53 and rotavirus proteins exit the traditional secretory pathway and do not reach the cis-Golgi (65). Furthermore, in transfected cells NSP4 was found to be responsible for blocking trafficking of transport vesicles from the ER to the Golgi apparatus through its association with microtubules (297). Since NSP4 localizes in lipid rafts (66, 252), can bypass the Golgi apparatus to reach the plasma membrane (21, 267) and binds to caveolin-1 (a protein component of the *caveolae*, a subset of lipid rafts functioning as vesicular carriers that mediate vesicle formation, docking and fusion) (182, 204, 267), it is possible that during rotavirus maturation a fusion event between vesicles containing NSP4 and raft vesicles containing VP4 occurs, as already proposed in a model by Delmas and colleagues (70). Indeed, a contribution of NSP4 in rotavirus raft association has been demonstrated by silencing NSP4 expression (65). However, to elucidate the molecular details of virus release, further studies are needed.

5. PATHOGENESIS, ILLNESS, IMMUNE RESPONSE AND VACCINES

Rotaviruses replicate in the non-dividing mature enterocytes in the middle and upper region of the small intestinal villi: virus infection causes mild lesions and mild inflammation, but the damage to the enterocytes results in villous atrophy, malabsorption, loss of digestive enzymes and increased osmotic pressure in the gut

lumen. This is the origin of the rotavirus-induced diarrhoea, whose severity depends also on the degree of Cl^- secretion of the crypt cells that lye in the proximity of the infected enterocytes. The enteric nervous system may be involved since drugs blocking its functionality attenuate the rotavirus-induced diarrhoea (168). Analysis of different virus reassortants identified several viral proteins as being involved in virulence, in particular NSP4, which acts as an enterotoxin (as already discussed in chapter 3), but also VP3, VP4, NSP1, VP6, VP7, NSP2 and NSP3 (41, 91). Recent studies reported antigenemia and viremia in children with acute rotavirus gastroenteritis (29). However, systemic disease is rare, suggesting that spread of rotavirus may depend on a concomitant disease of different origin (91).

After a short incubation of 1-2 days, clinical symptoms often start with vomiting followed by a watery diarrhoea lasting 4-7 days and rapid dehydration. Usually, only the first infection is symptomatic, afterwards the immune system provides protection against disease from re-infections. The primary infection usually elicits a predominantly homotypic humoral response, and subsequent infections elicit a broader heterotypic response. Humoral immunity, involving neutralizing antibodies against VP7, VP4 and antibodies against VP6, is believed to play an important role in protection, since a high level of serum IgA antibodies correlates with protection. A rotavirus-specific cytotoxic T cell response has also been detected, but its exact role in protection remains to be established (73, 91).

Rotaviruses are transmitted by the fecal-oral route. Their resistance to physical inactivation and their ability to survive on various surfaces under different conditions may account for their rapid spread and their efficient transmission. Improvements in water or hygiene conditions in developing countries are thus thought to have little effect on rotavirus transmission. Therefore, safe and effective vaccines represent an urgent need, and their development has been in progress since the early 1980s. In

August 1998, a rhesus rotavirus tetravalent vaccine (RotaShield®) was approved by the Food and Drug Administration (FDA): it contained a mixture of a rhesus monkey rotavirus of G3 serotype and three rhesus-human mono-reassortant strains carrying human G1, G2, and G4 genes and proteins. However, it was withdrawn in 1999 because of a number of intussusception cases, which were epidemiologically associated with vaccine doses, particularly the first one (194). Following re-analysis of these cases, it emerged that the age at the time of vaccination rather than the vaccine itself was responsible for intussusception, suggesting that RotaShield may still be a valid option. Currently, two vaccines are licensed in many different countries: a pentavalent human-bovine reassortant live-attenuated, oral vaccine (RotaTeq®, developed by Merck Research Co.) and a monovalent vaccine derived from an attenuated human rotavirus (Rotarix, developed by GlaxoSmithKleine). The first was licensed for use in the USA in 2006 and the second has been approved in 90 countries worldwide as of May 2007. Immunogenicity, safety and efficacy were demonstrated for both, but at present only based on vaccinations of children of industrialized and middle-income countries. Their efficacy in the poorest parts of the world still needs to be assessed, and relevant vaccine trials are ongoing. A lamb rotavirus strain, LLR, has been licensed in China as a live attenuated vaccine, but no clinical trial data are available at present. Although it is indisputable that an orally administrated rotavirus vaccine can protect against rotavirus diarrhoea, the risk of undesirable effects of live attenuated vaccines (clinical complications, revertance to virulence, genetic reassortment with co-circulating wild-type strains) remains a real possibility, underlining the importance of intensive post-marketing surveillance (73, 91). Another major issue is the delivery of vaccines to the developing countries at costs that those countries can bear. In this regard, the WHO intends to provide funding for the development of liquid or dry powder formulations of rotavirus vaccines

to facilitate their delivering. Finally, special efforts in prevention are required in India, China and Indonesia, where one third of all rotavirus-dependent deaths occurs, since these countries depends almost entirely on vaccines manufactured domestically.

6. INVESTIGATING INTERACTIONS AND FUNCTIONS OF ROTAVIRUS PROTEINS: THE CHALLENGE OF REVERSE GENETICS

As it has become clear from the previous chapters, the investigation of functions and interactions of rotavirus proteins is mainly based on the following systems:

- expression of recombinant proteins, individually or in combination, in insect cells using recombinant baculovirus or in transfected mammalian cells;
- infection with temperature-sensitive mutants;
- RNA interference;
- *in vitro* replication systems;
- yeast two-hybrid assays;

In addition, an intracellular antibody-capture technology has been employed to investigate the role of NSP5 in the viral replication cycle (285). However, the ideal methodology would consist in studying the effect of defined mutations intentionally introduced into the viral genome segments and incorporated into infectious viral particles (reverse genetics). The problem is that members of the family *Reoviridae* have been shown to be very refractory to this approach for many years, and it is only recently that some systems have being proposed as useful and relatively simple tools for studying *Reoviridae* protein functions. The first strategy was developed for orthoreoviruses and was based on a complicated and never reproduced approach that combined infection with a helper virus and transfection with viral dsRNAs, viral mRNA, a T7 transcript and *in vitro* translated viral proteins (242, 243). The first and

sole reverse genetics system reported for rotavirus is also based on the use of a helper virus: briefly, a modified VP4 gene was cloned under the control of the T7 promoter, and the resulting plasmid was transfected into cells previously infected with a recombinant vaccinia virus supplying the T7 RNA polymerase; one day after transfection, cells were infected with a helper virus of a strain different from that of the recombinant VP4; twenty-four hours later, cultures were harvested and the recovered viruses were amplified; selective pressure against the helper virus VP4 was provided by the use of two monoclonal antibodies that specifically neutralized the VP4 of the helper virus strain; recombinant viruses were then identified with a very low efficiency in the rescued viruses (150).

Both the system proposed for orthoreoviruses and for rotavirus are limited by the need of a helper virus and by the inability of introducing desired mutations in each viral genome segment. Recently, recombinant reoviruses have been constructed through an entirely plasmid-based approach driving the expression of all genome segments by the recombinant T7 vaccinia virus system and avoiding both helper viruses and coexpression of equivalent wild-type proteins (147). A step further was the very recent achievement of a recombinant bluetongue virus (BTV) following lipofection of a complete set of *in vitro* synthesized plasmid-derived RNA transcripts (34). The success of the last two reverse genetics approaches indicates that the mRNAs of the high-number segmented dsRNA viruses are infectious and that the establishment of a helper virus-independent reverse genetics system is theoretically achievable also for rotavirus. Therefore, efforts aimed at obtaining an easy and flexible method to introduce desired mutations into rotavirus genes are worthwhile and will benefit the understanding of regulatory sequence or protein functions, the comprehension of still obscure processes like genome segment reassortment and packaging and the design of new vaccines based on rationally attenuated recombinant viruses.

MATERIALS AND METHODS

CELL CULTURE

MA104 cells (embryonic African green monkey kidney cells) were grown as monolayers in Dulbecco's modified Eagle's medium (DMEM) containing 10% foetal calf serum (FCS) (Invitrogen), 2mM L-glutamine and 50µg/ml gentamicin (Invitrogen).
MA104 cells stably transfected with an NSP5-EGFP fusion gene were obtained by calcium phosphate procedure as described previously (3, 85) and cultured in DMEM complete medium supplemented with 500µg/ml geneticin (G-418, Invitrogen).

VIRUS PROPAGATION

The simian SA11 (G3, P6[1]), bovine RF (G6, P6[1]) and porcine OSU (G5, P9[7]) strains of rotavirus were propagated in MA104 cells as described previously (93, 118).
T7-recombinant vaccinia virus (strain vTF7.3) was propagated in HeLa cells as described by Fuerst et al. (101).
Viral titres were determined by plaque assay (118).

CONSTRUCTION OF PLASMIDS

pT_7v-NSP5 and pT_7v-NSP2 were obtained as previously described (96). The NSP5 gene was derived from the OSU rotavirus strain (Genbank accession number: D00474), the NSP2 gene from the SA11 strain (L04532). The VP1 and VP2 genes (X16830 and L33364, respectively) were cloned from extracts of SA11 rotavirus-

infected cells: viral RNA was extracted from 500µl of cell supernatant after complete cytopathic effect (CPE) had been reached. The cDNA was obtained by reverse transcription, using random hexamers (Sigma) and MuLV reverse transcriptase (Applied Biosystem) (136). Subsequently, the cDNA spanning the open reading frame (ORF) of VP1 was amplified in two portions by PCR with the couples of primers VP1/I for - VP1/I rev and VP1/II for - VP1/II rev, respectively (Table 2): the VP1/I amplicon reached from nucleotide 19 (first nt of the start codon of the coding region) to nucleotide 1322 and the VP1/II amplicon from nucleotide 1231 to nucleotide 3285 (last nt of the stop codon). Both amplicons were subcloned into pGEM-T Easy vectors (Promega) following the supplier's instructions and sequenced (MWG-Biotech, Ebersberg, Germany). The VP1/I amplicon was transferred into the pcDNA3 vector (Invitrogen) by cut with EcoRI restriction enzyme and insertion into the EcoRI-digested pcDNA3 vector. The correct orientation of the insert was checked by restriction analysis. Since in the overlapping region present in both VP1/I and VP1/II fragments (nt 1231-1322) there is a NsiI site, the VP1/II amplicon was cloned downstream the VP1/I fragment in the pcDNA3 vector using NsiI and XhoI restriction enzymes. In order to construct a histidine-tagged derivative of VP1/I and express the fusion protein in bacteria, the VP1/I amplicon was subcloned into the NcoI- and EcoRI-digested Pet23d vector (Novagen) containing a sequence encoding the histidine tag. The pcDNA3-SV5-VP1 plasmid was obtained by inserting the gene encoding the SV5 tag (12 amino acid long) (263) upstream the VP1 cDNA. The oligonucleotides SV5/VP1 A and SV5/VP1 B (Table 2) were annealed and inserted into the HindIII- and KpnI-digested pcDNA3-VP1 vector.

The cDNA spanning the ORF of VP2 was also amplified in two portions by PCR with the couples of primers VP2/I for - VP2/I rev and VP2/II for - VP2/II rev, respectively (Table 2). The VP2/I and VP2/II amplicons were cloned into pGEM-T Easy vectors

and sequenced. To obtain the complete VP2 cDNA, the VP2/II amplicon was cut with the HindIII and EcoRV restriction enzymes and inserted downstream of VP2/I in the pGEM-T Easy-VP2/I vector, previously cut with HindIII and EcoRI followed by end filling with the Klenow fragment of DNA polymerase. The complete VP2 cDNA was inserted into the pcDNA3 vector following the digestion with the KpnI and NotI restriction enzymes. The VP2/I amplicon (corresponding to the first 1078 nucleotides of the coding region of VP2) was transferred from the pGEM-T Easy-VP2(I) vector into a pGEX vector (GE Healthcare) to express in bacteria the first 357 amino acids of VP2 fused to GST. The pGEX-2T vector was preliminary modified with the insertion in the BamHI-EcoRI sites of an oligonucleotide derived from annealing of GEX-KpnI A and GEX-KpnI B oligonucleotides (listed in Table 2), in order to add the KpnI site and to insert VP2(I) in KpnI-EcoRI sites.

The constructs coding for the deletion mutants of NSP5 pT_7v-ΔN33 **[**termed Δ1**]**, pT_7v-Δd34-80 **[**Δ2**]**, pT_7v-Δd81-130 **[**Δ3**]**, pT_7v-Δd131-179 **[**Δ4**]**, pT_7v-ΔC18 **[**ΔT**]**, pT_7v-Δ4ΔT **[**Δ4ΔT**]**, pT_7v-ΔC48 **[**ΔC48**]**, and the pT_7v-(dom1EGFP4T) **[**1E4T**]**, pT_7v-(EGFP-4T) **[**E4T**]**, pT_7v-(dom1EGFP) **[**1E**]** and pNSP5-EGFP vectors have been either reported or obtained as described previously (2, 86, 87, 96). The constructs coding for the phosphorylation mutants of NSP5 pT_7v-NSP5/S67A and pT_7v-NSP5a were obtained as described by Eichwald et al. (84).

The pT_7v-VP6 vector was obtained by cloning the VP6 gene (L33365) from SA11 rotavirus-infected cells: the cDNA was obtained as described for VP1 and VP2 and the region spanning the open reading frame (ORF) of VP6 was amplified with primers VP6-for and VP6-rev listed in Table 2. The VP6 amplicon was cloned into the pGEM-T Easy vector, sequenced and cut with KpnI and EcoRV. It was then inserted into pT_7v-Δd81-130 **[**Δ3**]** vector previously digested with the same restriction enzymes in order to remove the insert Δ3 and allow the insertion of the VP6 amplicon.

The siRNA against the cellular kinase CK1α was as previously described by Campagna et al. (43).

The vector pcDNA3-HA-PP2A/Cα encoding the 35KDa catalytic subunit of PP2A was constructed by cloning an N-terminally HA-tagged cDNA encoding PP2A/Cα into plasmid pcDNA3, and was the kind gift of David Pim (221).

NAME	SEQUENCE
VP1/I for	5'-tagggtaccATGGGGAAGTACAATCTAATC-3' (NcoI)
VP1/I rev	5'-atggaattcggCGTGTATCTTTCGTTAGC-3' (EcoRI)
VP1/II for	5'-tagggtaccTCAAGGCAGCTAAAGTTTGG-3'
VP1/II rev	5'-ccgctcgagCTAATCTTGAAAGAAGTTCGC-3' (XhoI)
VP2/I for	5'-tatcaggtaccATGGCGTATCGAAAACGTGGA-3' (KpnI)
VP2/I rev	5'-ttgtcaaagcttCCAATTGCAAATCTTG-3' (HindIII)
VP2/II for	5'-aattggaagcttTGACAATACAATCAGAGA-3' (HindIII)
VP2/II rev	5'-taataagatatcTTACAGTTCGTTCATGAT-3' (EcoRV)
SV5/VP1 A	5'-agcttgtaccATGGGCAAACCAATCCCA AACCCACTGCTGGGTCTGGATGGTAC-3' (HindIII, KpnI)
SV5/VP1 B	5'-CATCCAGACCCAGCAGTGGGTTT GGGATTGGTTTGCCcatggtaca-3' (KpnI, HindIII)
GEX-KpnI A	5'-gatccggtaccggtgctggacccgggg-3' (BamHI, KpnI, EcoRI)
GEX-KpnI B	5'-aattcccgggtccagcaccggtaccg-3' (EcoRI, KpnI, BamHI)
VP6-for	5'-tatcaggtaccATGGATGTCCTATACT-3' (KpnI)
VP6-rev	5'-taataagatatcTCATTTAATGAGCATGCTT-3' (EcoRV)

TAB. 2: Oligonucleotides used in cloning procedures. The portions of sequence corresponding to coding sequences are indicated in capital letters. The portions of sequence indicated in green and orange correspond to sites or to sticky ends of sites of the restriction enzymes used (indicated in brackets). Start codons and stop anticodons are underlined. The SV5 peptide coding sequence is indicated in violet.

PRODUCTION OF ANTIBODIES

Anti-NSP5 and anti-NSP2 sera were produced by immunization of guinea pigs and mice and anti-VP7 serum by immunization of rabbits as described previously (2, 8, 112). Serum anti-VP1 was produced by immunization of guinea pigs with the histidine tagged VP1/I protein fragment (amino acids 1-435). The protein was produced in the E. coli BL21 strain (GE Healthcare). Cultures were induced with 3mM isopropyl-beta-D-thiogalactopyranoside (IPTG) for 3-4 hours at 37°C. Bacteria were centrifuged, and the pellet was washed with ice-cold PBS and resuspended in 1.5% laurylsarcosin-PBS supplemented with 0.1µg/µl lysozyme, 1X CLAP cocktail (chymostatin, leupeptin, aprotinin, and pepstatin; 10µg/ml each, Sigma), and 5mM dithiothreitol (DTT) for sonication (6 times, 10 seconds, using the Soniprep 150 instrument with the 9,5mm probe tuned at 23KHz). The supernatant was supplemented with 1% Triton X-100 in PBS (pH 7.2) and with Ni-NTA His-Bind resin (Novagen) equilibrated in 20mM imidazole in PBS. After rolling for 1 hour at 4°C, the sample was centrifuged at 1,000g for 5 minutes at 4°C, and the resin was washed with 10 volumes of 35mM imidazole in PBS. Elution was performed with two volumes of 250mM imidazole. The purified protein was quantified by staining with Coomassie brilliant blue after separation by PAGE and using Low Range MW (Bio-Rad) as standards. Guinea pigs were injected intraperitoneally (i.p.) with 100µg of protein and boosted 3 times (100µg every 15 days i.p.) in the presence of Incomplete Freund Adjuvant. Sera of the immunized guinea pigs were tested by Western blot on extracts of rotavirus-infected and uninfected cells.

Anti-serum to VP2 was produced by immunization of guinea pigs and mice with the GST-tagged VP2/I protein fragment (amino acids 1-357). The protein was produced in the E. coli BL21 strain with a procedure similar to that used for histidine tagged VP1/I but with the following modifications: cultures were induced with 1mM IPTG

for 4 hours at 25°C; the bacterial pellet was washed with ice-cold STE (10mM TrisHCl pH8, 100mM NaCl, 1mM EDTA pH8) and resuspended in STE supplemented with 0.1µg/µl lysozyme, 1X CLAP cocktail, 0.3-0.5% laurilsarcosine, and 2mM DTT for sonication; after addition of 1% Triton X-100 in STE, GST-VP2(I) was purified from bacterial lysates by affinity chromatography using GSTrap™ HP columns prepacked with Glutathione Sepharose™ High Performance medium (GE Healthcare) and was eluted under mild, nondenaturing conditions using reduced glutathione, following manufacturer's instructions. Guinea pigs and mice were injected subcutaneously with 125µg and 40µg of protein, respectively, and boosted 3 times every 15 days (with 50µg and 40µg of protein, respectively). Sera of the immunized guinea pigs and mice were tested by Western blot on extracts of rotavirus-infected and uninfected cells.

TRANSIENT TRANSFECTION AND LABELLING WITH [^{35}S]-METHIONINE OF MA104 CELLS

T7 RNA polymerase expressed from a vaccinia virus recombinant (101) is used to increase the expression level of proteins encoded by the transfected genes engineered downstream the T7 promoter. Since the vaccinia virus replication cycle is cytoplasmatic, exogenous gene transcription and translation are coupled in the cytoplasm of the transfected cells. For transfection experiments confluent monolayers of MA104 cells in 6-well plates (Falcon) were infected with T7-recombinant vaccinia virus [strain vTF7.3 (101)] at a multiplicity of infection (MOI) of 20 and 1 hour later transfected with a maximum total of 3µg/well of plasmid DNA (1µg of each plasmid in cotransfections) using 5µl of Lipofectamine 2000 (Invitrogen)/well and following the manufacturer's instructions. Transfected cells were harvested at 18 hours post-transfection (p.t.). For transfection of siRNAs, approximately 1.5 x 10^5 cells were

transfected with 2µg of siRNAs in 1ml of serum free medium containing 5µl Transfectam reagent (Promega). After 6 hours at 37°C, cells were washed twice with serum free medium, incubated for additional 32-35 hours in medium supplemented with 10% foetal bovine serum (Invitrogen) and then infected with vaccinia virus and transfected as described above.

For labelling with ^{35}S-methionine, at 18 hours p.t. cells were starved with DMEM lacking methionine for 30min and were then labelled with 30µl (11.1MBq) of ^{35}S-methionine (ProMIX [^{35}S] cell labelling mix, specific activity: >1000Ci (37,000GBq)mM^{-1}, GE Healthcare). Subsequently, cells were washed with PBS and harvested. Labelled proteins were detected by autoradiography at -70°C using X ray films (Hyperfilm; Amersham Biosciences) enhanced by fluorography using Amplify (Amersham Biosciences).

CELLULAR LYSIS

Lysates (corresponding to about 5x10^5 cells) were prepared in 100µl of TNN lysis buffer (100mM Tris-HCl pH8.0, 250mM NaCl, 0.5%NP40) at 4°C and were subsequently centrifuged at 2000g for 5 minutes at 4°C. Usually 10µl of supernatants were used in PAGE and Western immunoblot analyses, and 40-80µl were used for immunoprecipitation experiments. The pellets were washed 3 times with PBS (170mM NaCl, 10mM phosphate, 3mM KCl, pH 7.4) and resuspended in 20µl of loading buffer for PAGE and Western blot analyses.

CHEMICAL DSP CROSS-LINKING AND UV TREATMENT OF CELLS

Dithiobis(succinimidylpropionate) (DSP) was purchased from Pierce. Monolayers of transfected cells were washed twice with PBS, overlaid with 1.5ml PBS containing

600µM DSP and incubated at 4°C for 30 minutes. After removing the reactant solution, the reaction was quenched twice with 2ml Tris Buffered Saline (TBS; 40mM TrisHCl pH8, 150mM NaCl) for 3 minutes at 4°C. Cellular extracts were prepared in 100µl TNN buffer as described above.

For UV treatment, cells were washed twice with PBS and overlaid with 1ml TBS, kept on ice and exposed for 3 minutes to 486mJ of UV light of 254nm wavelenght by UV Stratalinker 1800 (Stratagene). Cellular extracts were then prepared as described above.

IMMUNOPRECIPITATION, PAGE AND WESTERN IMMUNOBLOT ANALYSIS

Cellular extracts (usually 4/5 of the total extract, i.e. approx. 80µl) were immunoprecipitated for 2 hours at 4°C after addition of 1µl of undiluted antibody, 1µl of 100mM PMSF, 50µl of 50% protein A-Sepharose CL-4B beads (Amersham Biosciences) in TNN buffer, and 20µl of TNN buffer. Beads were then washed four times with TNN buffer, once with PBS and resuspended in 20µl of loading buffer. Sample components were separated by SDS-PAGE (154) (using the Precision Plus Protein Standards molecular markers, Bio-Rad) and after electrophoresis transferred to polyvinylidene difluoride membranes (Millipore) (282). The membranes were incubated with the antibodies listed in Table 3. Signals were detected by using the enhanced chemiluminescence (ECL) system (Pierce).

PRIMARY ANTIBODIES				HRP-CONJUGATED SECONDARY ANTIBODIES			
Anti:	Animal species:	Dilution used:	Source:	Anti:	Animal species:	Dilution used:	Source:
NSP5	guinea pig	1:8,000	O. Burrone	guinea pig IgG	goat	1:10,000	Jackson Immuno Research
NSP2	guinea pig	1:2,500	O. Burrone				
VP1	guinea pig	1:1,000	O. Burrone				
VP7	rabbit	1:1,000	O. Burrone	mouse IgG	goat	1:5,000	KPL
VP2	guinea pig	1:2,000	J. Patton (for the experiment shown in Fig. 26)				
VP2	guinea pig	1:5,000	O.Burrone				
VP2	mouse	1:2,000	O. Burrone				
SV5	mouse	1:10,000	O. Burrone				
Actin	rabbit	1:500	Sigma	rabbit IgG	goat	1:5,000	Thermo Scientific Pierce
GFP	rabbit	1:1,000	Santa Cruz Biotechnology				
CK1α	rabbit	1:2,000	Santa Cruz Biotechnology				

TAB. 3: Antibodies used for Western blot.

RNase TREATMENT OF PROTEIN COMPLEXES

For RNase treatment, cellular extracts were prepared by applying a lysis buffer consisting of PBS diluted 1:10 (to reduce salt concentration) and containing NP40 (0.5%). Subsequently, 70µl of these extracts were treated with 10 units of RNase One (Promega) in 8µl of reaction buffer (provided by Promega) for 10 minutes at 37°C. Afterwards, 1µl undiluted antibody, 50µl of 50% protein A-Sepharose CL-4B beads in TNN buffer, 1µl of 100mM phenylmethylsulfonyl fluoride (PMSF) and TNN buffer were added to obtain a final volume of 500µl for immunoprecipitation.

λ-PHOSPHATASE TREATMENT OF IMMUNOPRECIPITATES

70µl out of 100µl of a cellular extract obtained from transfection/infection of about $5x10^5$ cells were immunoprecipitated over night with anti-NSP5 serum and then divided in two aliquots to be incubated with or without 2µl of λ-phosphatase (400U/µl, BioLabs) in buffer for λ-phosphatase treatment (50mM Tris-HCl pH 7.5, 100mM NaCl, 0.1mM EGTA, 2mM DTT, 0.01% Brij 35) (BioLabs) supplemented by 2mM $MnCl_2$. The reaction was incubated for 2 hours at 30°C and was stopped with 10µl of PAGE loading buffer (40% glycerol, 6% SDS, 125mM Tris-HCl pH 6.8, 0.04% bromo phenol blue, 5% β-mercaptoethanol).

INDIRECT IMMUNOFLUORESCENCE MICROSCOPY

For indirect immunofluorescence microscopy, cells were fixed in 3,7% paraformaldehyde in PBS for 10 minutes at room temperature. Cover slips were washed in PBS and blocked with 1% BSA in PBS for 30 minutes and incubated with primary antibody at room temperature. After three washing in PBS, slides were incubated either with another primary antibody for double staining or directly for 45 minutes with RITC- or FITC-conjugated secondary antibodies. After three washings, nuclei were stained with Hoechst dye 2µg/ml for 10 min, washed and mounted with ProLong mounting medium (Molecular Probes). Samples were analysed by confocal microscopy (Axiovert; Carl Zeiss). The antibodies used in immunofluorescence are listed in Table 4.

PRIMARY ANTIBODIES				SECONDARY ANTIBODIES				
Anti:	Animal Species:	Dilution used:	Source:	Anti:	Conjugated with:	Animal species:	Dilution used:	Source:
NSP5	guinea pig	1:1,000 for transfected cells; 1:3,000 for infected cells	O. Burrone	guinea pig	RITC	goat	1:200	KPL
NSP2	guinea pig	1:200	O. Burrone					
SV5	mouse (monoclonal)	1:300	O. Burrone	mouse	FITC	goat	1:200	Jackson Immuno Research
VP2	mouse	1:200	O. Burrone	mouse	RITC	goat	1:200	KPL
VP2	guinea pig	1:200	O. Burrone					
VP6	mouse (RV138, monoclonal)	1:50	D. Poncet					
HA	rat (monoclonal)	1:100	Roche	rat	FITC	goat	1:200	KPL

TAB. 4: Antibodies used for immunofluorescence.

PURIFICATION OF VIRAL PARTICLES OBTAINED FROM CELLS EXPRESSING SV5-TAGGED VP1

Confluent monolayers of MA104 cells in six 6-well plates were infected with T7-recombinant vaccinia virus (strain vTF7.3) at a MOI of 20 and 1 hour later transfected with pcDNA3-SV5-VP1 (2µg of DNA per well), using Lipofectamine 2000 (Invitrogen, 5µl per well). Six hours p.t. cells were washed with serum free medium and infected with the bovine RF rotavirus strain at a MOI of 3. Viral particles were purified from cell cultures after harvest at about 20 hours p.i. when almost complete

CPE had been reached. Virus was pelleted by ultracentrifugation, the pellets extracted with Freon (trichloro-trifluoro-ethane, Sigma) and banded by equilibrium ultracentrifugation in CsCl gradient, essentially as described by Patton et al. (205). This allowed to obtain three well separated gradient bands containing empty particles (EPs), TLPs and DLPs. Empty particle, TLP and DLP suspensions were diluted in 20mM PIPES buffer pH6.6 containing 10mM $CaCl_2$ and pelleted by ultracentrifugation at 110,000g for 1 hour in a Beckman ultracentrifuge using an SW55 rotor. The pellets containing the different viral particles were resuspended in 35µl of water and used in SDS-PAGE and Western immunoblot analyses.

EDTA TREATMENT OF PURIFIED TLPs

Pellets derived from ultracentrifugation of CsCl purified TLP suspensions were resuspended in 60µl of PIPES buffer pH6.6 containing 0.5mM $CaCl_2$ and treated with 5mM EDTA in PBS for 30 minutes at 37°C in modification of the procedure by Estes et al. (95). The resulting particles were pelleted by ultracentrifugation and analyzed by SDS-PAGE and Western blot.

RESULTS

The molecular events that take place during rotavirus replication are not yet completely elucidated. In particular, the intermediate structures formed during the sequential phases of genome replication and packaging, and the role of the different viral proteins in this process are not entirely clear. Although the involvement of the nonstructural proteins NSP2 and NSP5 in the replicative cycle is unquestioned, since in their absence viroplasms are not formed, genome viral replication does not occur and no infectious progeny virus is made, their precise functions also remain to be clarified. So far, a crucial structural role for NSP5 in the assembly of viroplasms, most likely through its interaction with NSP2, has been proposed. The data presented here suggest additional functions for NSP5 in the context of genome replication, being related to the interaction with the two structural proteins shown to be essentially involved in viral RNA replication: the polymerase VP1 and the scaffold protein VP2. In the first part [Results (1)], a characterization of the interaction between NSP5 and VP1 is presented and in the second part [Results (2)], a relevant effect of the scaffold protein VP2 on NSP5 cellular distribution and its hyperphosphorylation is described. In both parts of the Results section, the involvement of other viral proteins is examined with the aim to elucidate the temporal and spatial organization of the events leading to the viroplasm assembly and to the synthesis of dsRNA viral genome.

RESULTS (1)

VP1 coimmunoprecipitates with NSP5

Previous experiments of our laboratory showed that a complex containing VP1, NSP2 and NSP5 was immunoprecipitated by anti-NSP5 antibody from extracts of rotavirus-infected cells, as long as cells were cross-linked *in vivo* with DSP (2). DSP is a reagent with two reactive groups separated by a spacer of 12Å length, able to permeate cell membranes and to cross-link proteins interacting inside the cell through their amino groups. In addition, a disulfide bridge within this spacer allows the separation of the components of the cross-linked complex under reducing conditions. Since VP1 was not coimmunoprecipitated by anti-NSP5 antibody without DSP cross-linking and, differently from NSP2, not even after UV treatment (2), and based on the evidence of an interaction between NSP2 and VP1 (145), we were initially considering that an interaction between NSP2 and VP1 may be stronger than between NSP5 and VP1. With the aim of investigating the requirement of either of the two nonstructural proteins, and in particular of NSP5, in the interaction with VP1, we carried out experiments of transient expression of the single proteins. First, we found an interaction between NSP5 and VP1 in the absence of other viral proteins by coimmunoprecipitation with anti-NSP5 antibody from extracts of cells transiently transfected, labelled with ^{35}S-methionine and *in vivo* cross-linked with DSP (Fig. 1A, lane 3). Coimmunoprecipitation of NSP2 with NSP5, which are well known to interact (2), served as an internal control (Fig. 1A, lane 2). A similar result was obtained with MA104 cells transfected with plasmids expressing the NSP5 and VP1 genes, immunoprecipitated with anti-NSP5 antibody, and tested by Western blot with an anti-VP1 serum (Fig. 1B). The lower expression level observed for NSP5 when

coexpressed with other viral proteins rather than alone (compare lanes 2-3 with lane 1 of Fig.1A) was observed in several independent experiments (see also Figs. 9B, 12, 27), although not in all of them (see Figs. 19A, 22A, 26, 28). This effect was shown to be non-specific by cotransfection of an irrelevant gene (EGFP) with genes expressing VP1 or VP2 in the presence of an internal control of transfection: since the levels of EGFP expression were lower than in the control of EGFP expressed alone (data not shown), it is probable that the plasmids or the mRNAs encoding VP1 and VP2 are favoured compared to those encoding NSP5 or EGFP in the competition for transcripition or translation factors.

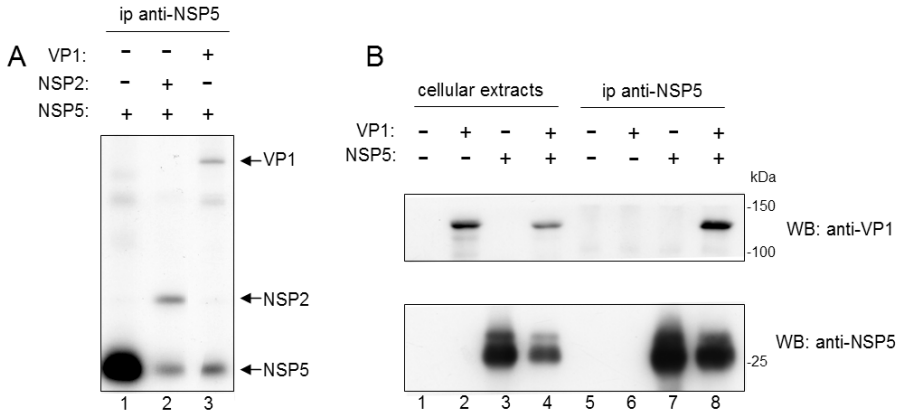

FIG. 1: Coimmunoprecipitation of VP1 and NSP5. A) Immunoprecipitation (ip) with anti-NSP5 serum of DSP cross-linked extracts of ^{35}S-methionine labelled cells transiently transfected with the indicated genes. B) Western blot analysis of DSP cross-linked cellular extracts (lanes 1-4) and immunoprecipitates (lanes 5-8) derived from cells cotransfected with VP1 and NSP5. After separation by PAGE and Western blotting, the upper and lower parts of the blot were reacted with specific anti-VP1 and anti-NSP5 antibodies, respectively.

In order to further investigate the interaction between NSP5 and VP1, and because the anti-VP1 antibody did not react in immunoprecipitations nor in immunofluorescence, we used a VP1 derivative (tag-VP1) containing at its N-terminus the 12 amino acid long SV5 tag derived from a small epitope present on the P and V proteins of simian virus 5 (263) and for which a potent monoclonal antibody (anti-

tag) was available. The amino acid sequence of this tag and a scheme of the gene encoding tag-VP1 are indicated in Fig. 2A. Extracts from cells cotransfected with NSP5 and tag-VP1 vectors (pT7v-NSP5 and pcDNA3-SV5VP1, respectively) were immunoprecipitated with either anti-NSP5 or the anti-tag antibody, and the immunoprecipitates were analyzed by Western blot with both antibodies. It was found that NSP5 and tag-VP1 coimmunoprecipitated in both cases (Fig. 2B). The ratio between the two proteins observed in the cellular extracts (Fig. 2B, lane 1) was found to be conserved in both coimmunoprecipitation approaches (Fig. 2B, lanes 6, 10), suggesting a strong interaction between the two proteins. The comparison between assays using cross-linked or non-cross-linked cellular extracts revealed that DSP cross-linking was needed only for immunoprecipitations with anti-NSP5 antibody (Fig. 2C, compare lanes 3 and 6), but not with the anti-tag antibody (Fig. 2C, compare lanes 9 and 12), suggesting that the high-affinity hyperimmune polyclonal anti-NSP5 antibody might have dissociating activity. To test whether cellular RNA mediates interaction between NSP5 and VP1, cellular extracts from non-cross-linked cells were treated or not treated with the ribonuclease RNase One before immunoprecipitation and Western blot analysis. This ribonuclease has been chosen, because it cleaves the phosphodiester bond between any two ribonucleotides and allows the degradation of both single-strand and double-strand RNA. Since this ribonuclease is inhibited by high concentrations of sodium chloride and potassium phosphate, cellular extracts were prepared by applying a lysis buffer consisting of PBS diluted 1:10 (to reduce salt concentration) and containing NP40 (0.5%). Figure 2D shows that RNase treatment did not change the ability of anti-tag antibody to coimmunoprecipitate NSP5, indicating that cellular RNA does not mediate interaction between NSP5 and VP1.

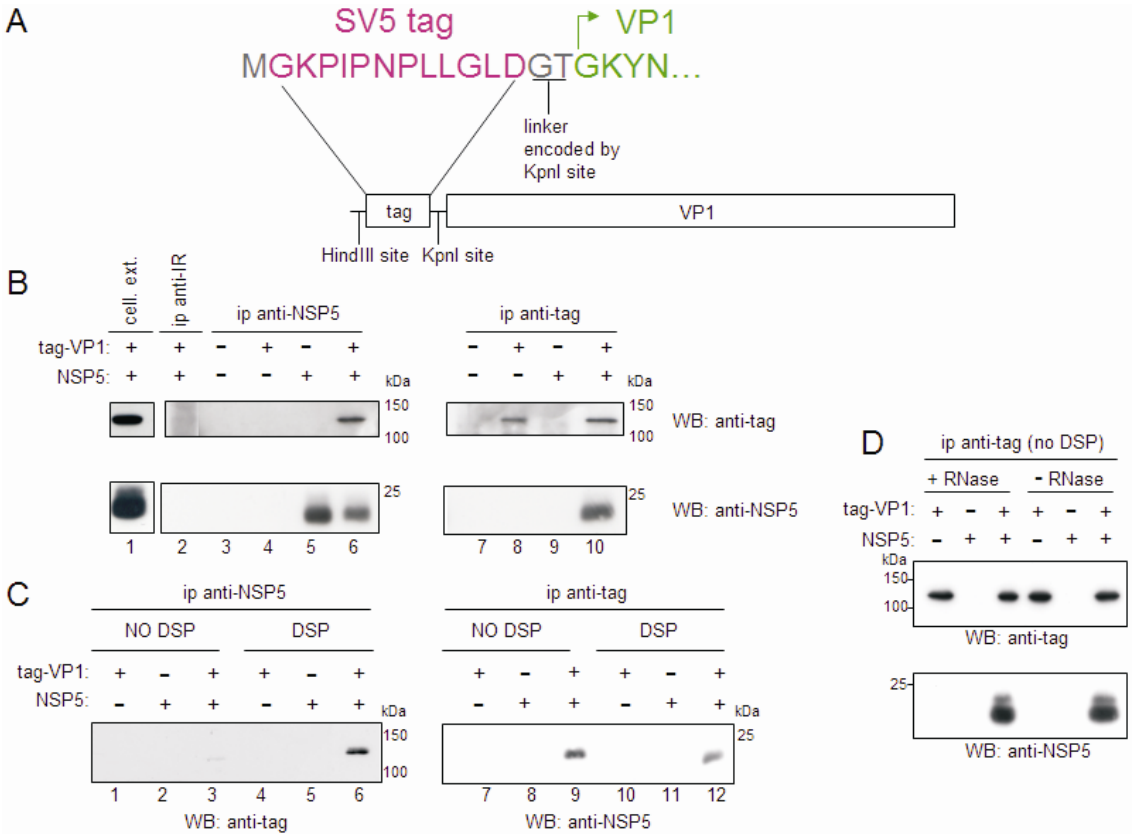

FIG. 2: Coimmunoprecipitation of NSP5 and tagged VP1. A) Amino acid sequence of SV5 tag, indicated in colour purple, and diagram of tag-VP1 gene. B) Western blot of immunoprecipitates of DSP cross-linked extracts from MA104 cells cotransfected with NSP5 and tag-VP1 genes. Immunoprecipitates were obtained with an anti-NSP5 serum (anti-NSP5) or the anti-SV5 monoclonal antibody (anti-tag) and upper and lower parts of the blots developed with either of them, as indicated. C) Western blot of immunoprecipitates obtained with anti-NSP5 or anti-tag from extracts of both non-cross-linked or DSP cross-linked cells, and developed with the indicated antibodies. D) Western blot of immunoprecipitates obtained with anti-tag antibody from extracts of non-DSP cross-linked cells, treated or non-treated with RNase.

We also examined UV treatment of cells as an alternative method to cross-link nucleic acids to proteins. It has been previously observed that UV treatment of rotavirus-infected cells allowed stabilization of NSP5-NSP2 complexes, which could be immunoprecipitated by anti-NSP5 antibodies. Under these conditions, coimmunoprecipitation of VP1 did not take place and required cross-linking with DSP (2). In agreement with this finding and with the lack of an effect of RNase digestion, UV treatment of cells coexpressing tag-VP1 and NSP5 did not result in coimmunoprecipitation of tag-VP1 with anti-NSP5 antibody (Fig. 3).

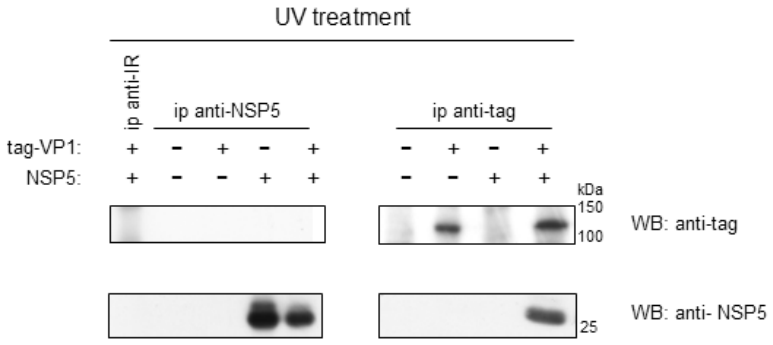

FIG. 3: Western blot of immunoprecipitates of extracts from MA104 cells cotransfected with NSP5 and tag-VP1 and exposed to UV treatment. Immunoprecipitates were obtained with anti-NSP5 or anti-tag antibodies and upper and lower parts of the blots developed with either of them, as indicated.

Tag-VP1 can act as a structural replacement of VP1

To ensure the validity of using tag-VP1 instead of VP1, the behaviour of the tagged protein in the course of viral infection was investigated. We tested whether the transfected tag-VP1 was incorporated into particles of viral progeny in MA104 cells expressing tag-VP1 and infected with rotavirus. To allow this, cells were first infected with vTF7.3 recombinant vaccinia virus, which increases the expression level of proteins encoded by genes positioned under the control of the T7 promoter. One hour later cells were transfected with a plasmid encoding tag-VP1, and six hours later

superinfected with the rotavirus RF strain. Twenty hours after rotavirus infection, viral progeny particles were concentrated by sedimentation and purified by CsCl gradient ultracentrifugation. Fractions of gradients containing the visible bands of empty particles (EPs; density 1.30g/ml), TLPs (1.36g/ml) and DLPs (1.38g/ml) (92) were analyzed by Western blot with anti-tag and anti-VP1 antibodies. Since VP7 is present only in TLPs, Western blot analysis with anti-VP7 antibodies was also performed as a control. Cellular extracts of transfected cells in the presence or in the absence of vaccinia virus and/or rotavirus were tested in the same way. The whole procedure is illustrated in the scheme of Fig. 4A. Tag-VP1 was found to be incorporated into viral particles in a reproducible fashion in several experiments (Fig. 4). These experiments showed some variability in the relative amounts of tag-VP1 found in TLPs, DLPs and EPs. In some experiments tag-VP1 was incorporated mostly into TLPs, and only faint tag-VP1 bands were observed in DLPs and EPs (Fig. 4B); in others, tag-VP1 was preferentially present in DLPs (Fig. 4D). To rule out non-specific trapping of tag-VP1 in the outer shell of TLPs, we treated purified TLPs with EDTA to remove the outer layer (95). The treatment did not release tag-VP1 (Fig. 4D), indicating that tag-VP1 was genuinely incorporated into DLPs. This conclusion was strengthened by comparison of the relative amounts of VP1 (anti-VP1) and tag-VP1 (anti-tag) in lanes 10, 13 and 14, which showed similar ratios. The difference in PAGE mobility between tag-VP1 and wild-type VP1 (Fig. 4C) was due to the two different parental strains (tag-VP1, SA11 strain; wild-type VP1, RF strain).

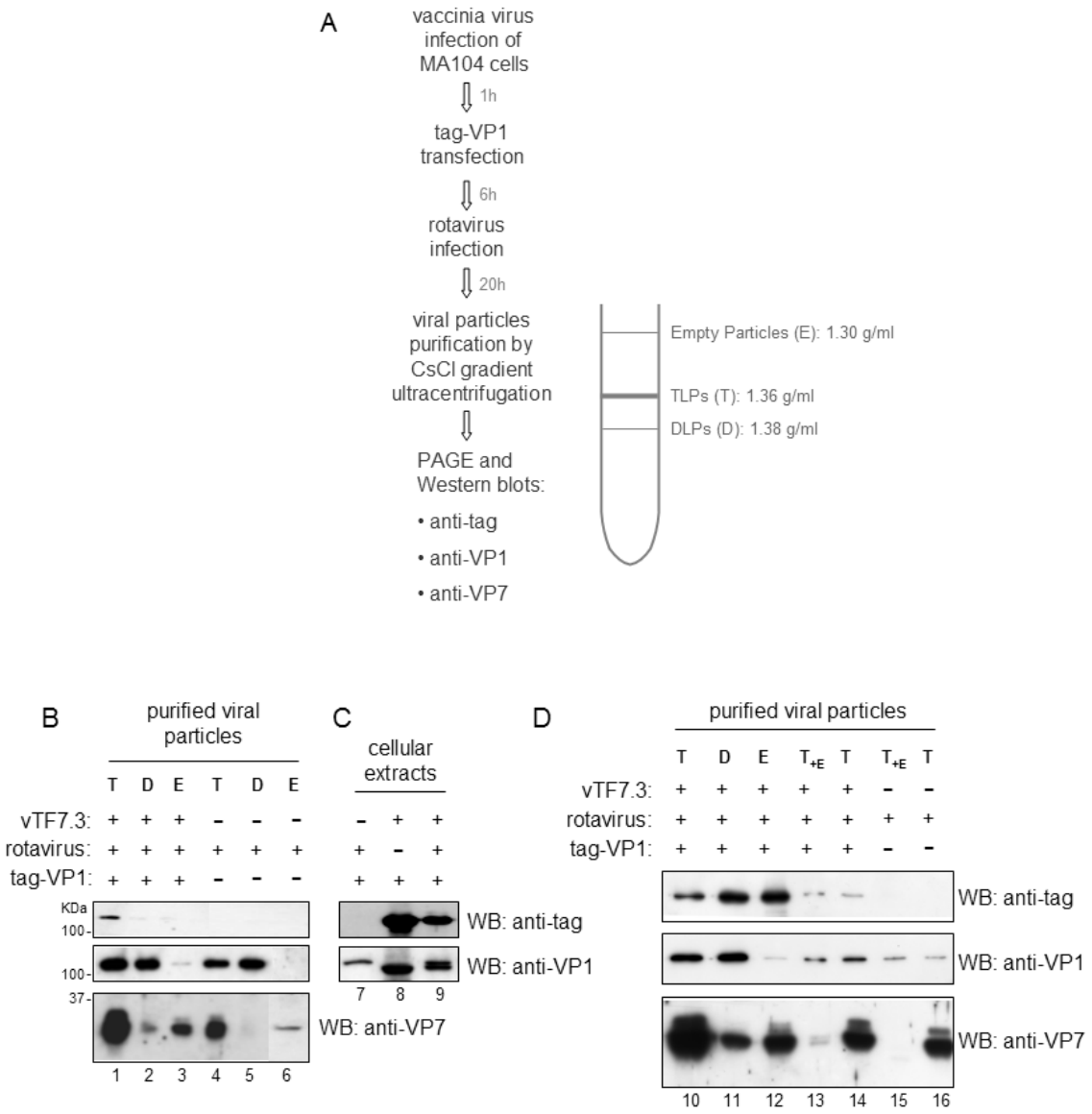

FIG. 4: Packaging of tag-VP1. A) Scheme of the technical procedure. B) Rotavirus particles (T=TLPs; D=DLPs; E=EPs) obtained from cells transfected with tag-VP1 (lanes 1-3) or non-transfected (lanes 4-6) were analyzed by Western blot as indicated. C) Western blot of total cellular extracts. Lane 9 corresponds to the conditions under which viral particles shown in lanes 1-3 were obtained. Of note, tag-VP1 (SA11 strain, lane 8) migrated faster than the untagged VP1 (RF strain, lane 7). D) Western blot with anti-tag, anti-VP1 and anti-VP7 antibodies of TLPs, DLPs and EPs (lane 10-12, respectively). Tag-VP1 TLPs and control TLPs were treated with EDTA as described (T_{+E}, lanes 13 and 15, respectively) or mock-treated (lanes 14 and 16, respectively). Traces of VP7 in the DLP preparations (lanes 2, 11) are due to contamination with small amounts of TLPs.

Tag-VP1 colocalizes with NSP5 in viroplasms and in VLS

In virus-infected cells, NSP5 and VP1, as well as NSP2, colocalize in the cytoplasmic viroplasms. In addition, we found that tag-VP1 also localizes in viroplasms. As shown in Fig. 5, confocal microscopy with different fluorescence labels for the NSP5 and the tag-VP1 signals revealed that part of tag-VP1 colocalized with NSP5 in the viroplasms of rotavirus-infected cells. When tag-VP1 was coexpressed in uninfected cells, either with NSP5 or with NSP2 in the absence of any other rotavirus protein, a diffuse cytoplasmic distribution for each individual protein was observed (Fig. 6A, horizontal rows 2 to 3). By contrast, when NSP5 and NSP2 were both present, a substantial part of tag-VP1 was found to localize in the characteristic viroplasm-like structures (VLS), which are formed by the two nonstructural proteins (96) (Fig. 6A, row 4, and Fig. 6B). This was further confirmed by cotransfecting NSP2 with a mutant of NSP5 lacking the 18 amino acid C-terminal tail region (ΔT), which had previously been demonstrated to be unable to form VLS (96). As expected, all three proteins showed a diffuse distribution (Fig. 6A, row 5). While VLS of cells containing tag-VP1 appear to be smaller and less numerous than VLS formed only by NSP5 and NSP2, they still retain the typical ring appearance (Fig. 6A, row 4).

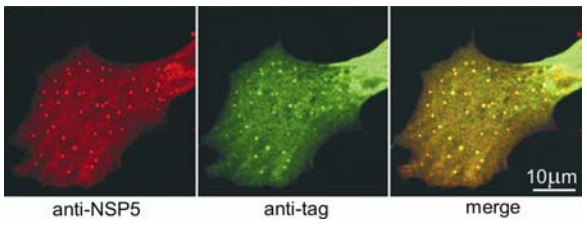

FIG. 5: Colocalization of tag-VP1 in viroplasms. Confocal immunofluorescence of tag-VP1 (green) and NSP5 (red) in MA104 cells, transfected with the tag-VP1 expressing plasmid and infected with SA-11 rotavirus. The individual and the merged patterns are shown.

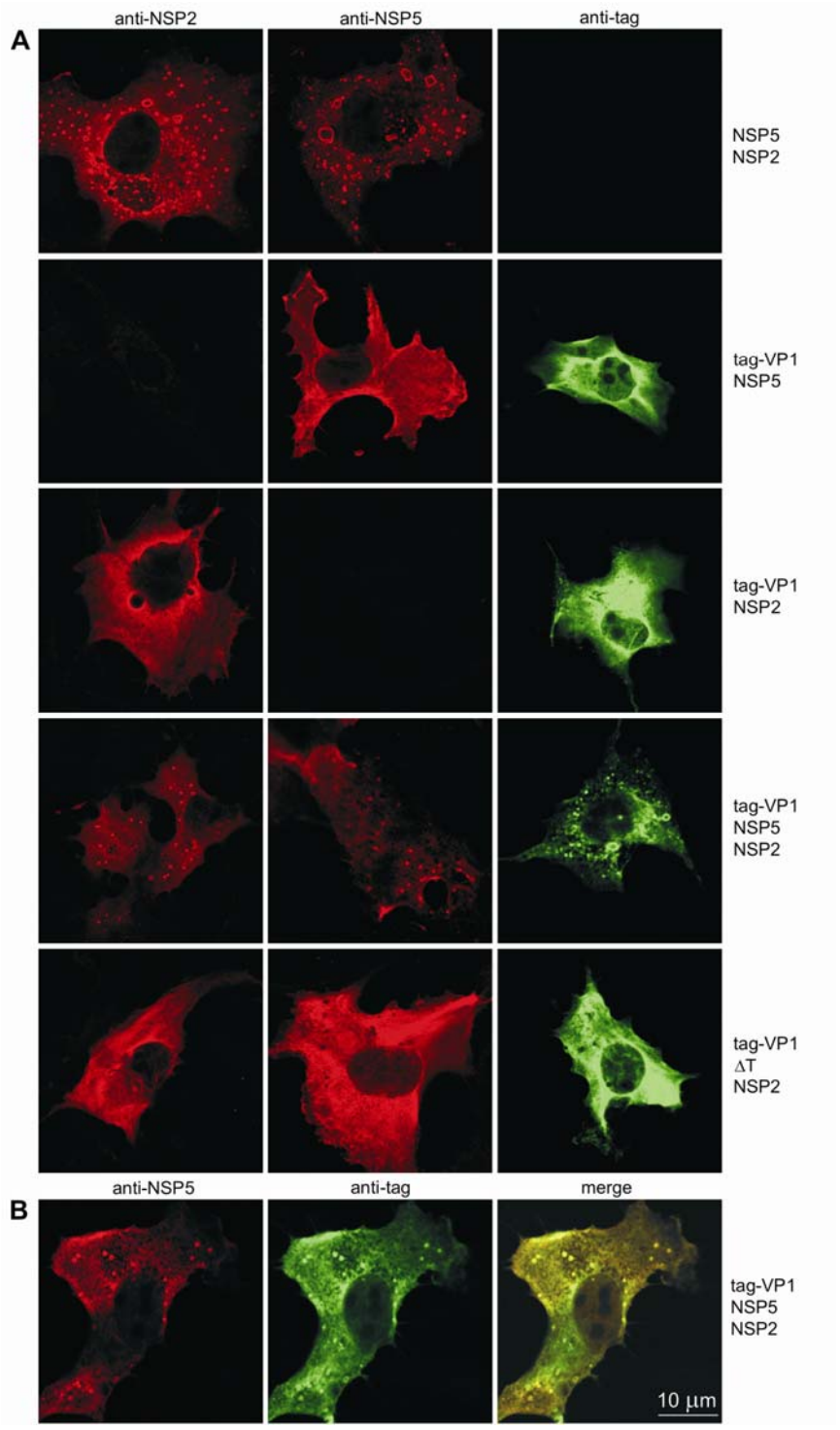

FIG. 6: Localization of tag-VP1 in viroplasm-like structures (VLS). A) Immunofluorescence of tag-VP1 (green), NSP2 (red) and NSP5 (red) in cells cotransfected with the indicated genes. B) Colocalization of tag-VP1 and NSP5 in VLS formed in cells coexpressing NSP5, NSP2 and tag-VP1, as shown by confocal microscopy with anti-NSP5 (red) and anti-tag (green).

VP1 interacts more strongly with NSP5 than with NSP2

As previously mentioned, NSP5, NSP2 and VP1 can be coimmunoprecipitated from virus-infected cells (1). Similarly, all three proteins were coimmunoprecipitated by anti-NSP5 antibody from DSP cross-linked extracts of cells coexpressing them in the absence of other viral proteins (Fig. 7A, lane 6). As previously reported, anti-NSP2 antibody did not pull down NSP5 (2) nor tag-VP1 (data not shown).

We investigated the ability of VP1 to interact with either of the two nonstructural proteins by comparing the ability of anti-tag antibody to coimmunoprecipitate NSP5 and/or NSP2 from extracts of DSP cross-linked and, more importantly, non-cross-linked cells. Anti-tag antibody was able to coimmunoprecipitate NSP5 and NSP2 when tag-VP1 was coexpressed with either of them (Fig. 7B, lanes 7, 8 and 10, 11) or with both (Fig. 7B, lanes 9, 12). However, coimmunoprecipitation of NSP5 is much more efficient than coimmunoprecipitation of NSP2. In fact, although the input of cellular extracts used for immunoprecipitations represented four times as much as used for the analysis of cellular extracts (Fig. 7B, lanes 1 to 6), only a small fraction of NSP2 was recovered from the immunoprecipitates (about one fifth to one tenth: compare lanes 8, 9, 11, 12 with lanes 2, 3, 5, 6 of Fig. 7B), whereas the amount of NSP5 recovered was significantly larger (about five to ten times: compare lanes 7, 9, 10, 12 with lanes 1, 3, 4, 6 of Fig. 7B). In several experiments we observed that the amount of NSP2 coimmunoprecipitated from DSP cross-linked extracts with VP1 was larger when NSP5 was present (Fig. 7B, compare lanes 11 and 12). Altogether these data indicate that in the presence of NSP2 the interaction of VP1 with NSP5 is stronger than the interaction between VP1 and NSP2.

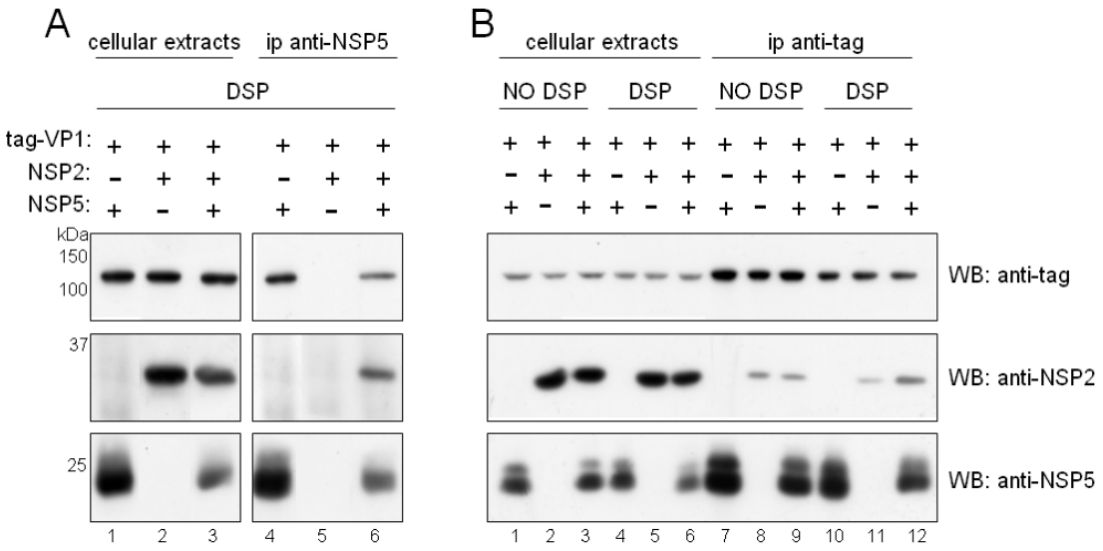

FIG. 7: Coimmunoprecipitation of NSP2, NSP5 and tag-VP1. A) Western blot of cellular extracts (lanes 1-3) or anti-NSP5 immunoprecipitates (lanes 4-6) derived from cells transfected with NSP2, NSP5 and tag-VP1 and DSP cross-linked. B) Western blot of cellular extracts (lanes 1-6) or anti-tag immunoprecipitates (lanes 7-12) derived from cells transfected with NSP2, NSP5 and tag-VP1, DSP cross-linked (lanes 4-6, 10-12) or non-cross-linked (lanes 1-3, 7-9). Upper, middle and lower parts of the blots were cut and reacted with anti-tag, anti-NSP2 and anti-NSP5 antibodies, respectively.

Since NSP5 becomes hyperphosphorylated in the presence of NSP2 (2), we expected to find the hyperphosphorylated forms of NSP5 in the immunoprecipitates. However, after DSP cross-linking, these forms were only found in the insoluble fraction, which contains approximately 50% of the total amount of NSP5 (Fig. 8A, lane 4), and were surprisingly absent when tag-VP1 and NSP2 were present (Fig. 8A, lane 6). Furthermore, even in extracts not cross-linked with DSP, the relative hyperphosphorylation of NSP5 in cells coexpressing tag-VP1 and NSP2 was clearly impaired. In fact, the ratio between bands at 28 and 26KDa was about 1:10 (Fig. 8B, lane 3), like for NSP5 expressed alone, while it is about 1:1 to 1:2 when NSP5 is expressed with NSP2 only (Fig. 8B, lane 1). This suggests that VP1 somehow inhibits the up-regulation of NSP2-mediated NSP5 hyperphosphorylation.

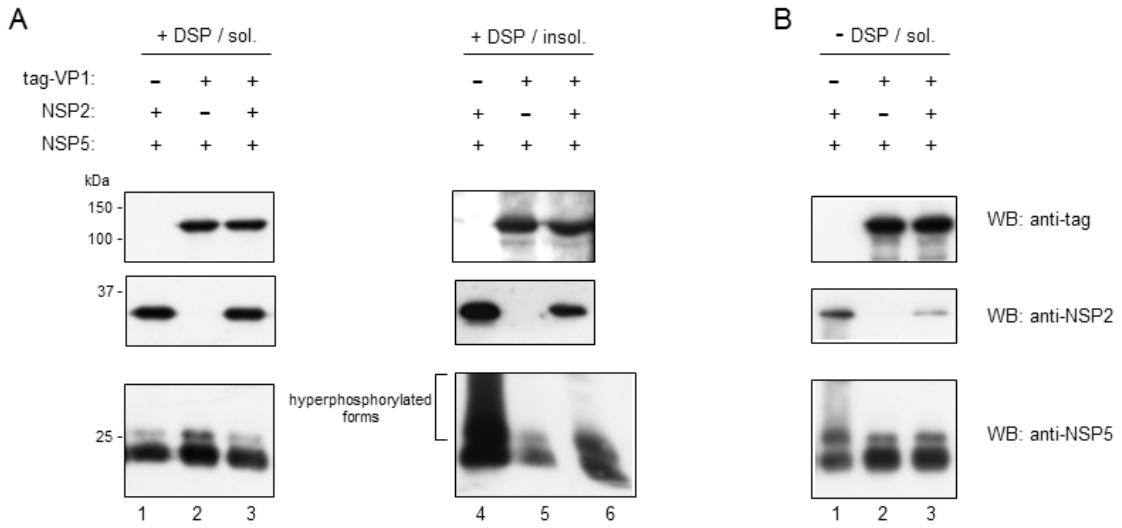

FIG. 8: Effect of DSP cross-linking and tag-VP1 on NSP5 hyperphosphorylation. A) Western blot analysis of soluble (left panel, lanes 1-3) and insoluble (right panel, lanes 4-6) fractions derived from extracts of DSP cross-linked cells transfected with the indicated genes. B) Western blot of the soluble fractions of non-cross-linked cells. Upper, middle and lower parts of the blots were cut and reacted with anti-tag, anti-NSP2 and anti-NSP5 antibodies, respectively.

The C-terminal 48 amino acids of NSP5 are essential for interaction with VP1

To map the region of NSP5 essential for the interaction with VP1, we first performed coimmunoprecipitation assays using DSP cross-linked extracts of cells cotransfected with plasmids encoding tag-VP1 and the deletion mutants of NSP5 illustrated in Fig. 9A. Only traces of mutants Δ2 and Δ4 (lacking amino acids 34-80 and 131-179, respectively) were detectable in both the extracts and the anti-NSP5 immunoprecipitates in several experiments (Fig. 9B, lanes 5, 7, 13, 15, 21, 23). However, tag-VP1 was surprisingly coimmunoprecipitated with all NSP5 mutants using anti-NSP5 antibodies, and consistently, all NSP5 mutants were coimmunoprecipitated by anti-tag antibody (Fig. 9B, lanes 11-16, 20-24) (with the exception of Δ4, whose expression was compromised for unknown reasons, as shown in Fig. 9B, lane 23). The comparison of the ratios between tag-VP1 and the coexpressed NSP5 mutants in the cellular extracts and in the immunoprecipitates

revealed a good interaction between tag-VP1 and Δ1 (lacking the first 33 N-terminal amino acids) (Fig. 9B, lanes 4, 12, 20) and a weak interaction between NSP5 and ΔT (lacking the 18 amino acid long C-terminal tail). In fact, lane 16 of Fig. 9B shows a small fraction of NSP5 coimmunoprecipitated from the total amount present in the extract (visualized in lane 8) and, consistently, lane 24 shows a small fraction of coimmunoprecipitated tag-VP1. Therefore, we proceeded with coimmunoprecipitation assays of DSP cross-linked extracts of cells cotransfected with wild-type VP1 and Δ1 or wild-type VP1 and ΔT. As confirmed in Fig. 9C, anti-NSP5 coimmunoprecipitated VP1 when coexpressed with Δ1, whereas only a small amount of VP1 was obtained when VP1 was coexpressed with ΔT. In conclusion, these data indicate that the interaction with VP1 did not involve the N-terminal region of NSP5 and was substantially reduced by the removal of the last 18 amino acids from the C-terminus.

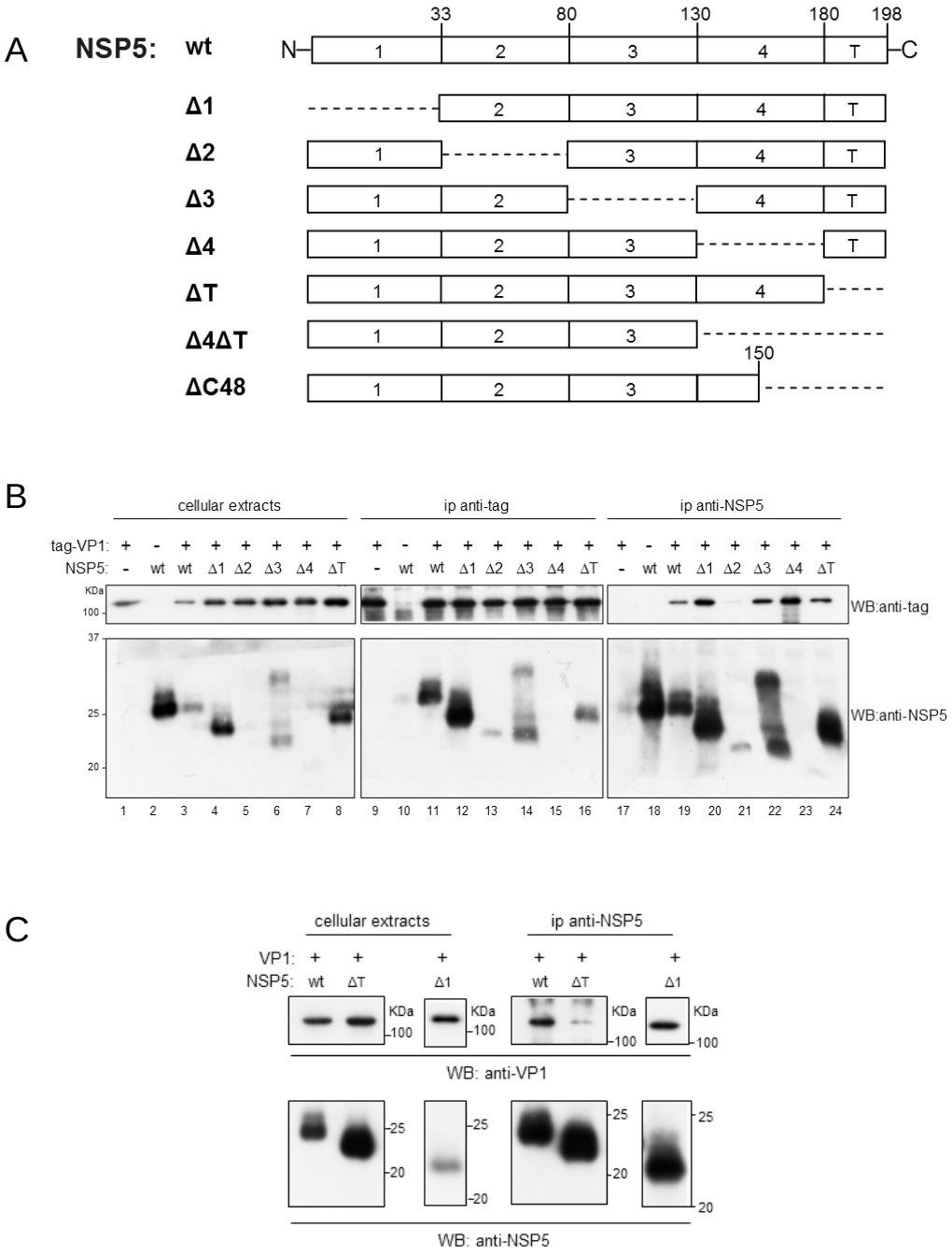

FIG. 9: Interaction of VP1 with NSP5 mutants. A) Diagram of NSP5 mutant constructs used. B) Western blots of DSP cross-linked cellular extracts and immunoprecipitates of cells cotransfected with tag-VP1 and NSP5 or NSP5 mutants, as indicated. C) Western blots of DSP cross-linked cellular extracts and immunoprecipitates of cells cotransfected with wild-type VP1 and NSP5 or NSP5 mutants, as indicated.

For further confirmation, we used other constructs, in which enhanced green fluorescent protein (EGFP) was fused to different regions of NSP5 (see diagrams in Fig. 10A). Cells were cotransfected with tag-VP1 and the different EGFP constructs and DSP cross-linked, and lysates were immunoprecipitated with anti-tag antibody. While the EGFP protein fused with only region 1 was not coimmunoprecipitated with anti-tag antibody, the fusion proteins containing regions 4 and T (amino acids 130 to 198), with or without region 1, were pulled down (Fig. 10B), confirming that the N-terminus does not bind to VP1 and, more importantly, that the last 68 amino acids (4T) were sufficient for the interaction. Furthermore, coimmunoprecipitation of tag-VP1 with EGFP-4T was also obtained with anti-NSP5 (Fig. 10B).

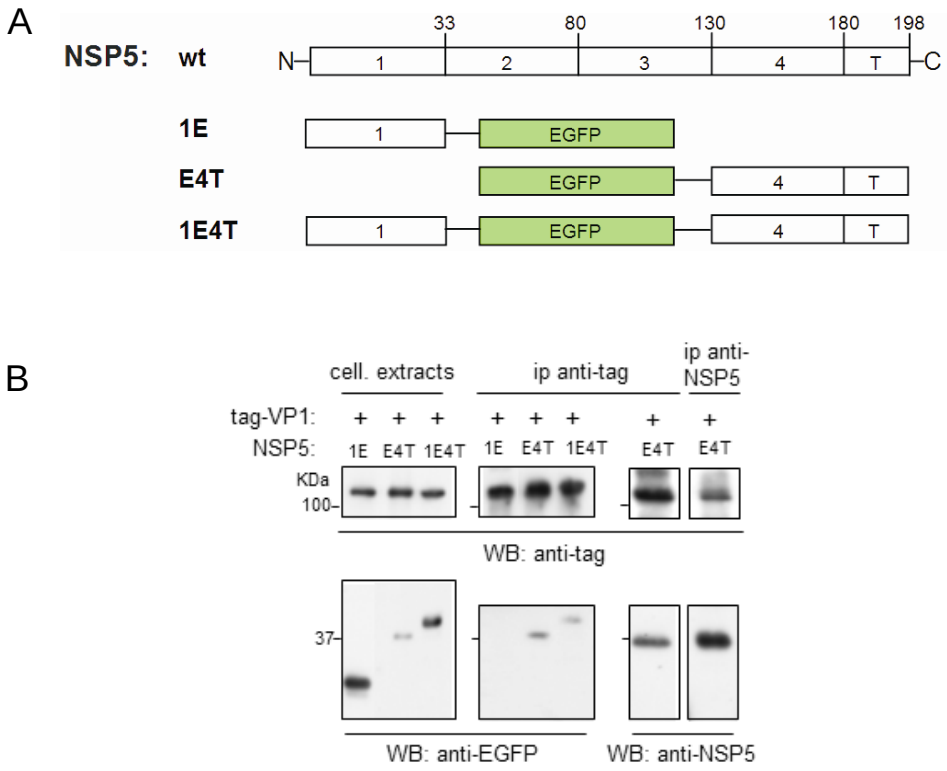

FIG. 10: Interaction of VP1 with NSP5 mutants. A) Diagram of NSP5 constructs used. B) Western blots of cellular extracts and immunoprecipitates of DSP cross-linked cells cotransfected with tag-VP1 and different NSP5-EGFP fusion constructs, as indicated.

In order to better define the region involved in the interaction with VP1, we analyzed another deletion mutant of NSP5, lacking the last 48 amino acids (ΔC48) (see diagram in Fig. 11A). In parallel, we tested mutants ΔT and Δ4ΔT as controls. After cotransfection with tag-VP1, the anti-tag antibody did not coimmunoprecipitate ΔC48, nor did anti-NSP5 tag-VP1 (Fig. 11B). Moreover, when supernatants of samples already immunoprecipitated with anti-tag were subsequently immunoprecipitated with anti-NSP5, the non-interacting mutants (ΔT, Δ4ΔT and ΔC48) were detected, while the interacting wild-type NSP5 was not (Fig. 11C).

To rule out the possibility that the lack of interaction of mutant ΔC48 with tag-VP1 was the consequence of the removal of a series of basic residues (two arginines and seven lysines, see Fig. 11A) that could have been involved in the cross-linking with DSP, we carried out immunoprecipitations with anti-tag, which does not require cross-linking and efficiently coimmunoprecipitates wild-type NSP5. As shown in Fig. 11D, anti-tag was completely unable to coimmunoprecipitate ΔC48. Taken together, the results presented in figures 9 to 11 indicate that the 48 amino acids of the C-terminal region of NSP5 are essential for interaction with VP1.

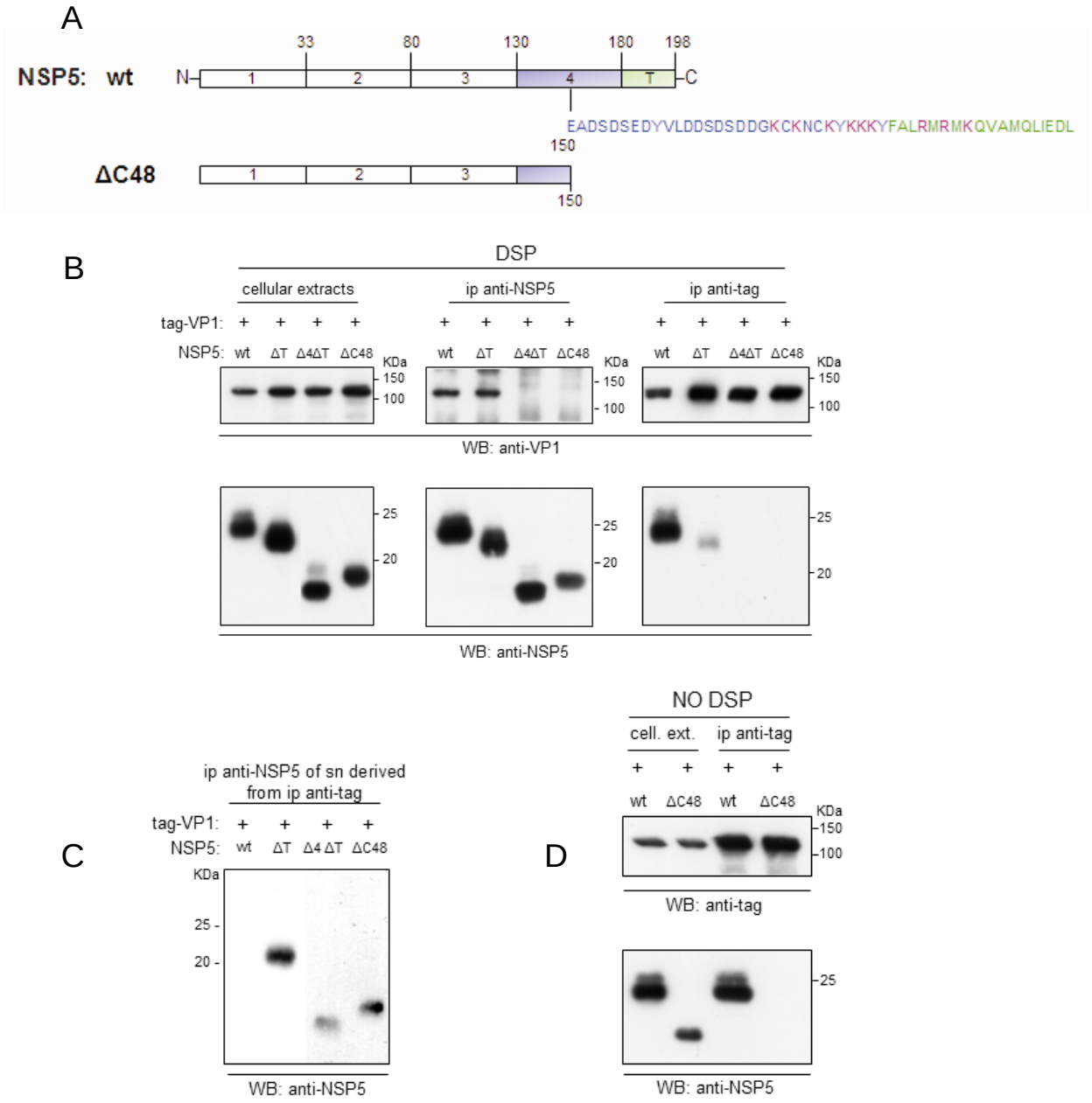

FIG. 11: Interaction of VP1 with NSP5 mutants. A) Diagram of ΔC48 mutant in comparison with wt NSP5 and amino acid sequence of the region deleted in ΔC48. B) Western blots of cellular extracts and immunoprecipitates of cells cotransfected with tag-VP1 and NSP5 deletion mutants, and DSP cross-linked, as indicated. C) Western blots of supernatants (sn) derived from anti-tag immunoprecipitates of Fig. B and immunoprecipitated with anti-NSP5. D) Western blot of extracts and immunoprecipitates derived from cells cotransfected with tag-VP1 and either wt NSP5 or ΔC48 mutant, and non-cross-linked.

The VP1 C-terminal 15 amino acids seem to be involved in interaction with NSP5

The following experiment was based on a personal communication by Dr. John Patton (National Institute of Allergy and Infectious Diseases, NIH), who has crystallized and determined the structure of VP1 (not yet published). They found that the fifteen C-terminal residues of VP1 form an α-helical plug, which reduces for almost half the diameter of the (-)ssRNA/dsRNA exit channel. We hypothesized an interaction between this region of VP1 with NSP5, which might move the plug affecting production of (-)ssRNA/dsRNA. We constructed a tagged deletion mutant of VP1 lacking the last fifteen amino acids (tag-VP1ΔC15). Preliminary data of coimmunoprecipitation of NSP5 with tag-VP1ΔC15 suggest the involvement of the VP1 C-terminus in the interaction with NSP5. Extracts of cells coexpressing NSP5 and either wild-type VP1 or tag-VP1ΔC15, treated or not treated with DSP, were immunoprecipitated with anti-NSP5 and anti-tag antibodies, respectively. Analysis of the immunoprecipitates showed that NSP5 was not coimmunoprecipitated with tag-VP1ΔC15 by anti-tag antibody from non-DSP cross-linked extracts, while it was with wild-type tag-VP1 (Fig. 12, compare lanes 3, 8 and lanes 5, 10). On the other hand, very small amounts of tag-VP1ΔC15 were coimmunoprecipitated with NSP5 by anti-NSP5 antibodies from DSP cross-linked extracts (Fig. 12, compare lanes 13, 18 and lanes 15, 20). Taken together, these preliminary data suggest an involvement of the C-terminus of VP1 in the interaction with NSP5.

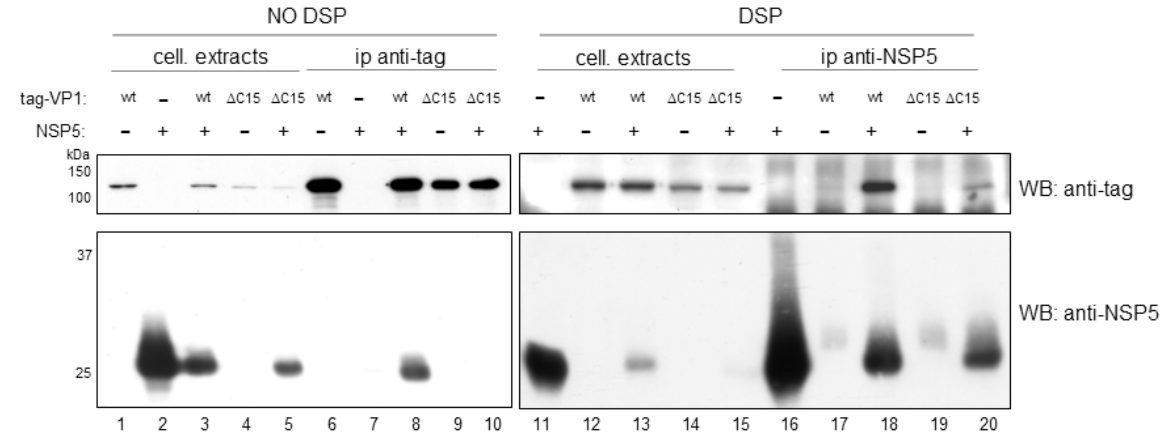

FIG. 12: Interaction of NSP5 with tag-VP1ΔC15. Western blot analysis of DSP cross-linked or non-cross-linked extracts of cells cotransfected with NSP5 and tag-VP1 or tag-VP1ΔC15, and of the corresponding immunoprecipitates obtained with anti-NSP5 or anti-tag, as indicated.

RESULTS (2)

Like VP1, the scaffold protein of the core, VP2, has been shown to be critically involved in viral RNA replication and to localize in viroplasms. Furthermore, an interaction with NSP5 has been described (23), although in our laboratory we never succeeded in coimmunoprecipitating VP2 with NSP5 from rotavirus-infected cells, even after cross-linking with DSP. In the following Results (2) section, we investigated the behaviour of VP2 after coexpression with NSP5 in uninfected cells. Furthermore (as we have done when investigating the interaction between VP1 and NSP5), we coexpressed other viroplasmic proteins together with VP2 and NSP5 and tested their interactions by confocal immunofluorescence and coimmunoprecipitation experiments. Studying the interactions and the relative localization of the single viroplasmic components is aimed at understanding the still undefined process of viroplasm assembly, which is critical for viral RNA replication and packaging as well as for viral particle formation.

VP2 induces NSP5 to form VLS

Following coexpression of NSP5 and VP2 in uninfected cells, immunofluorescence experiments with anti-NSP5 antibodies revealed the formation of structures similar to those formed by NSP5 and NSP2, but less numerous and less uniformly distributed (Fig. 13). Based on the morphological similarity with VLS formed by NSP5 and NSP2, we named these structures VLS as well and in order to distinguish between VLS induced by NSP2 from those induced by VP2, we named them VLS(NSP2i) and VLS(VP2i), respectively.

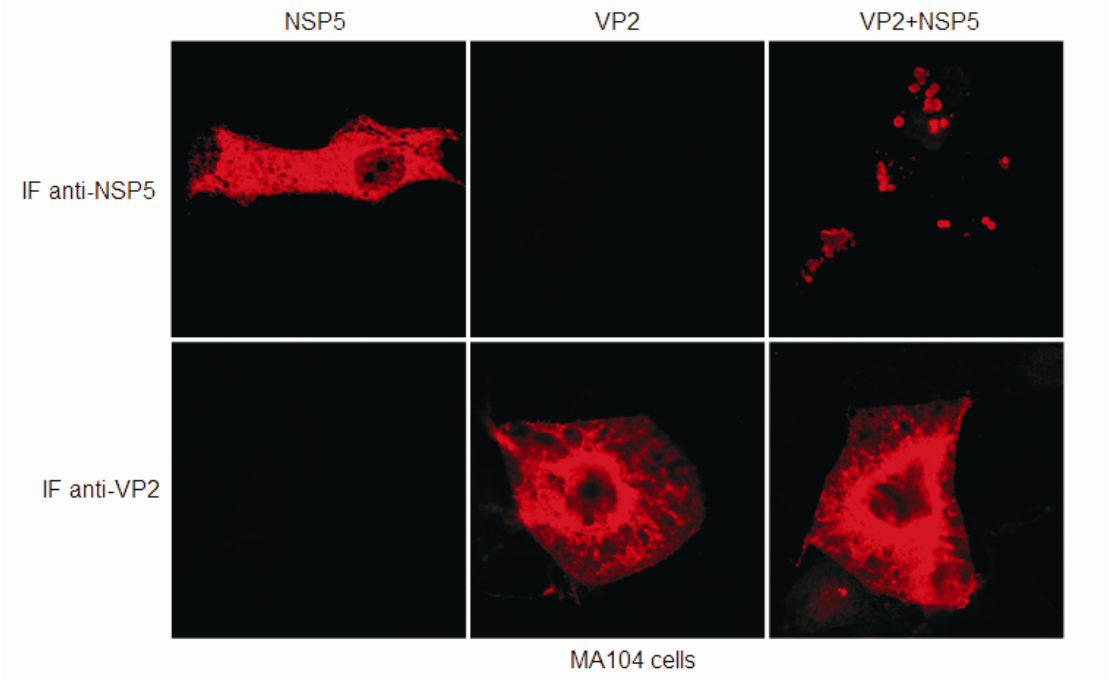

FIG. 13: VLS(VP2i). Immunofluorescence of NSP5 and VP2 in cells cotransfected with 1µg of both NSP5 and VP2 plasmids or with either of them, as indicated.

By immunofluorescence with anti-VP2 antibodies, a diffuse distribution of VP2 was frequently observed when 1µg of both plasmids was transfected (Fig. 13). However, a clear recruitment of VP2 into VLS(VP2i) was easily detectable, when the amount of the plasmid encoding VP2 was reduced to 0.1µg or 0.01µg (Fig. 14).

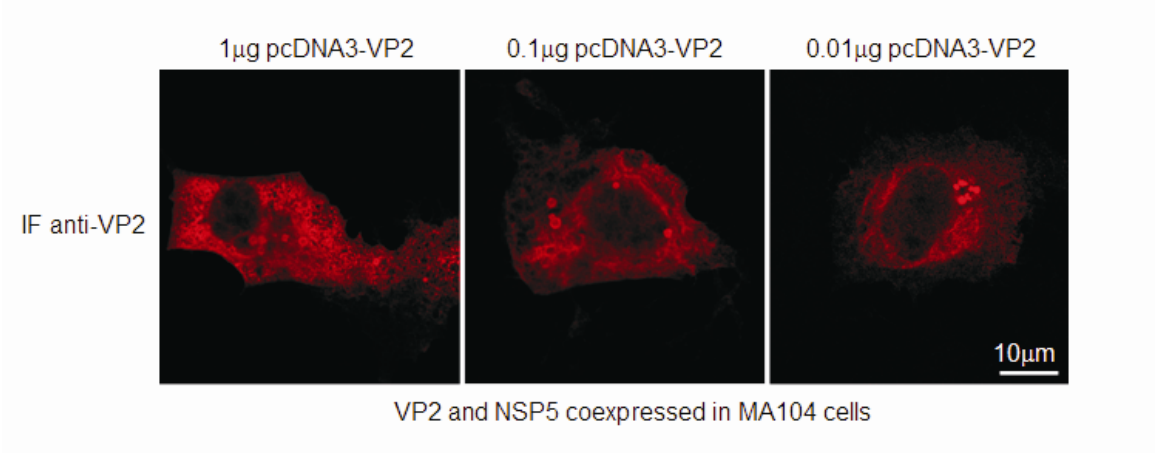

FIG. 14: VP2 recruitment into VLS(VP2i). Immunofluorescence of VP2 in cells cotransfected with different amounts of VP2 plasmid, as indicated, and a fixed amount of NSP5 plasmid (1µg).

Recruitment of VP2 into VLS(VP2i) was further confirmed using a stable cell line expressing the fusion protein NSP5-EGFP. The fluorescence of NSP5-EGFP in these cells can be visualized, when the fusion protein is concentrated in viroplasms following rotavirus infection (Fig. 15). Transfection of VP2 plasmid in this cell line led to the formation of visible VLS(VP2i). This was observed either by the autofluorescence of NSP5-EGFP or by immunofluorescence with anti-NSP5 antibodies (Fig. 16A). VP2 was found colocalized with NSP5-EGFP in these structures as long as the plasmid encoding wild-type NSP5 was also cotransfected (compare bottom row of Fig. 16A with Fig. 16B). The need of wild-type NSP5 was observed even when NSP2 plasmid was transfected in this cell line, with the interesting difference that the wild-type NSP5 coexpression was required not only for the recruitment of NSP2 into VLS, but also for VLS(NSP2i) formation (Fig. 16C,D).

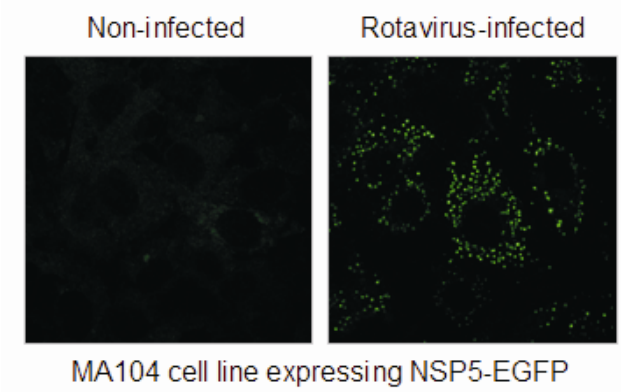

FIG. 15: Fluorescence of NSP5-EGFP in non-infected and rotavirus-infected MA104 NSP5-EGFP cells.

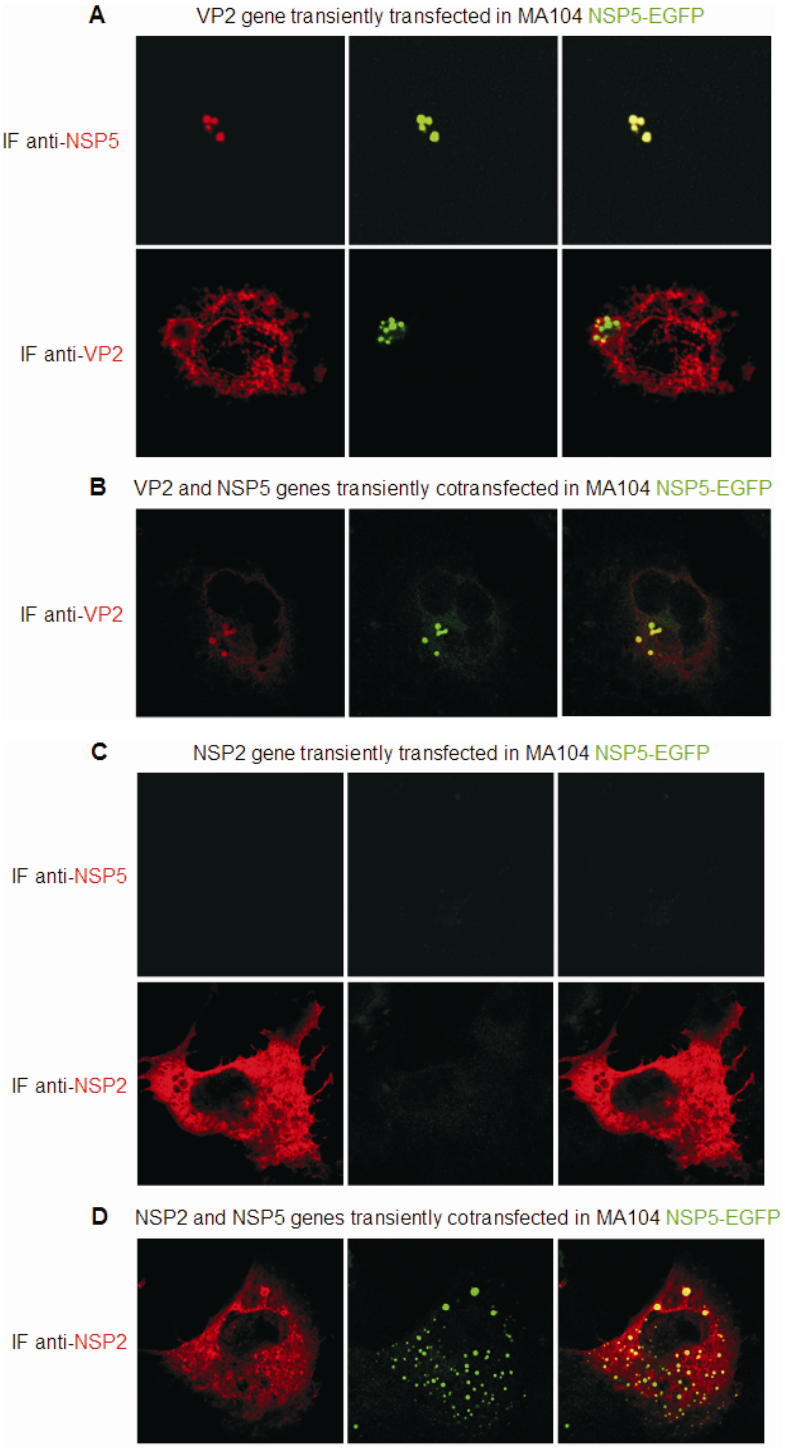

FIG. 16: VLS formation in transfected MA104 NSP5-EGFP stable cell line. A-B) Fluorescence of NSP5-EGFP (green) and immunofluorescence of NSP5 or VP2 (red) in MA104 NSP5-EGFP cells transiently transfected with VP2 (A) or cotransfected with VP2 and NSP5 plasmids (B). C-D) Fluorescence of NSP5-EGFP (green) and immunofluorescence of NSP5 or NSP2 (red) in MA104 NSP5-EGFP cells transiently transfected with NSP2 (C) or cotransfected with NSP2 and NSP5 plasmids (D).

Cotransfection of the NSP5-EGFP cell line with both VLS-inducers VP2 and NSP2 led to the formation of VLS, where neither VP2 nor NSP2 were recruited, and with the typical distribution of VLS(VP2i) (Fig. 17A). However, when wild-type NSP5 was also cotransfected, VLS containing all three components were observed in numbers and distribution typical of VLS(NSP2i) (Fig. 17B).

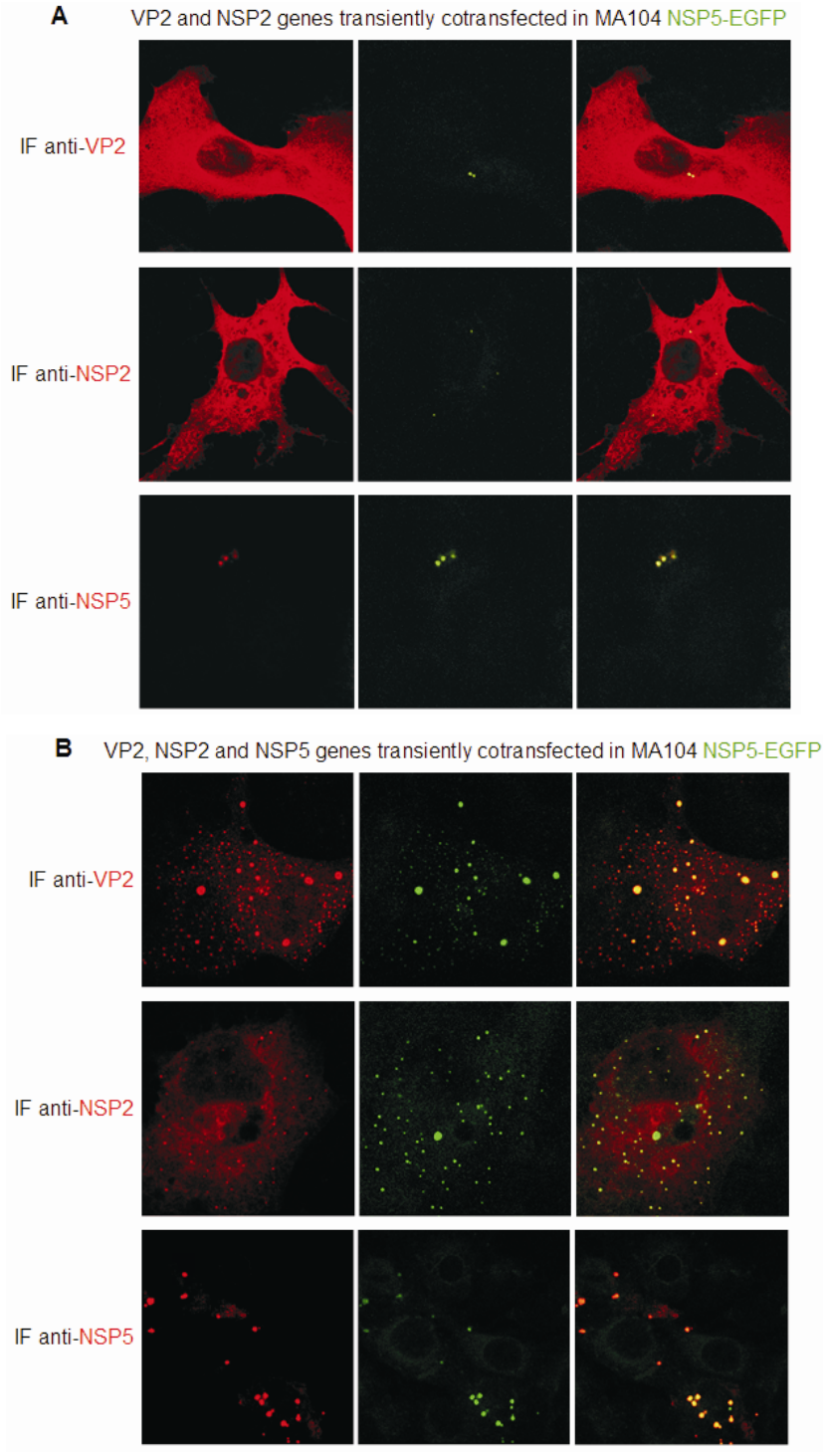

FIG. 17: VLS formation in transfected MA104 NSP5-EGFP stable cell line. Fluorescence of NSP5-EGFP (green) and immunofluorescence of VP2 (red), NSP2 (red) or NSP5 (red) in MA104 NSP5-EGFP cells transiently cotransfected with VP2 and NSP2 plasmids with (B) or without (A) concomitant cotransfection of NSP5 plasmid, as indicated.

The need of wild-type NSP5 could be explained either by an inadequate ratio between VP2 or NSP2 and NSP5-EGFP in the stable cell line or by the requirement of a free C-terminus in at least a fraction of NSP5 molecules. In order to discriminate between these two interpretations, wild-type MA104 cells were transiently cotransfected with 1µg of NSP5-EGFP plasmid and 0.1µg of VP2 plasmid. As shown in Fig. 18, VLS(VP2i) formed exclusively by NSP5-EGFP were able to recruit VP2, suggesting that the ratio between NSP5 and VP2 proteins was the critical variable affecting VLS formation.

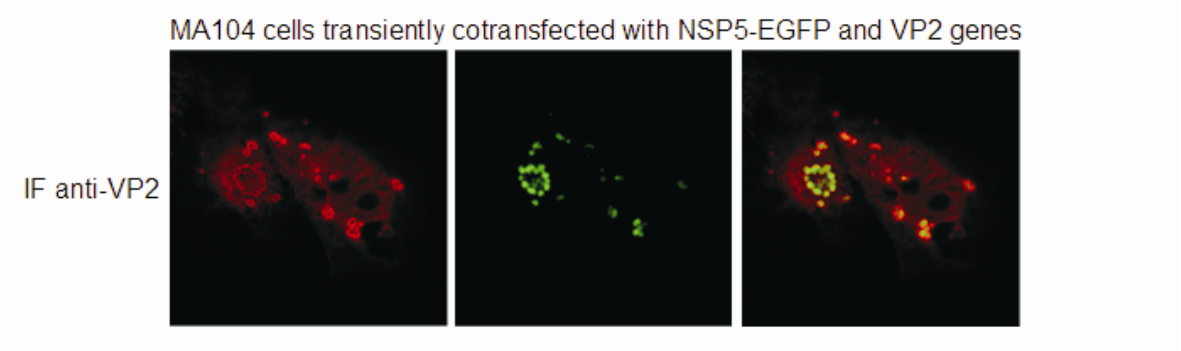

FIG. 18: VLS(VP2i) formation in wild-type MA104 cells transiently cotransfected with 1µg of NSP5-EGFP plasmid and 0.1µg of VP2 plasmid, as indicated by fluorescence of NSP5-EGFP (green) and immunofluorescence of VP2 (red).

All these data suggest that cotransfection of plasmids encoding viroplasmic proteins can be considered a valid strategy towards the understanding of the assembly of viroplasms. The data also show how critical the relative amounts of the different viroplasmic components are in determining the formation of these structures.

VP2 increases NSP5 hyperphosphorylation

Western blot experiments on extracts of uninfected cells cotransfected with VP2 and NSP5 genes showed a remarkable increase of NSP5 hyperphosphorylation (Fig.

19A, lane 5). When NSP5 is expressed alone, one main band is visible at 26KDa and a much weaker band of phosphorylated NSP5 at 28KDa (Fig. 19A, lane 4). By contrast, in extracts of infected cells the band at 28KDa is much more abundant and a series of higher bands is visible, whose apparent molecular weights span from 30 to 34KDa (Fig. 19A, lane 2). As mentioned in the Introduction, all bands different from 26KDa have previously been shown to correspond to many different phosphorylated isoforms of NSP5 (3, 26, 112, 228). We found that the pattern of bands of NSP5 coexpressed with VP2 in uninfected cells was similar although not identical to that observed for NSP5 from infected cells (compare lanes 2 and 5 of Fig. 19A). We verified that the effect of VP2 on NSP5 was actually an increased hyperphosphorylation by treatment with lambda-phosphatase. Following immunoprecipitation with anti-NSP5 antibodies of NSP5 coexpressed with VP2, immunoprecipitates treated with lambda-phosphatase showed a single band at 26KDa (Fig. 19B, lanes 3, 4). In addition, we performed *in vivo* experiments coexpressing NSP5, VP2 and the catalytic subunit of the cellular phosphatase PP2A, which is an ubiquitous and conserved serine/threonine phosphatase with broad substrate specificity (298). As shown in Fig. 19C, the presence of the catalytic subunit of PP2A led to a significant reduction of the NSP5 bands at higher molecular weight and to an inversion of the relative intensity of the bands at 26KDa and 28KDa (Fig. 19C, lanes 3, 6). All these data confirm that the presence of VP2 increases NSP5 hyperphosphorylation. The mechanisms and the enzymes involved in this process remain obscure. Attempts of coimmunoprecipitation of NSP5 and/or VP2 with the catalytic and regulative subunits of PP2A were performed, but neither NSP5 nor VP2 were found coimmunoprecipitated with PP2A (data not shown). Moreover, by experiments of RNA interference against kinase CK1α, which was recently shown to be involved in NSP5 phosphorylation in infected cells (43), we observed that

CK1α does not contribute significantly to the effect of VP2. Lane 2 of figure 20 shows a very slight conversion of the band at 28KDa to the band at 26KDa and the pattern of all bands resembles that of NSP5 coexpressed with VP2 and an irrelevant siRNA (even though the absolute amount of NSP5 is lower and the intensity of all bands is reduced) (compare lane 1 and 2). Beyond questioning the involvement of this kinase in the VP2-mediated NSP5 hyperphosphorylation, these data suggest that the concurrence of different kinases and phosphatases takes place in the context of viral infection to determine the phosphorylation status of NSP5.

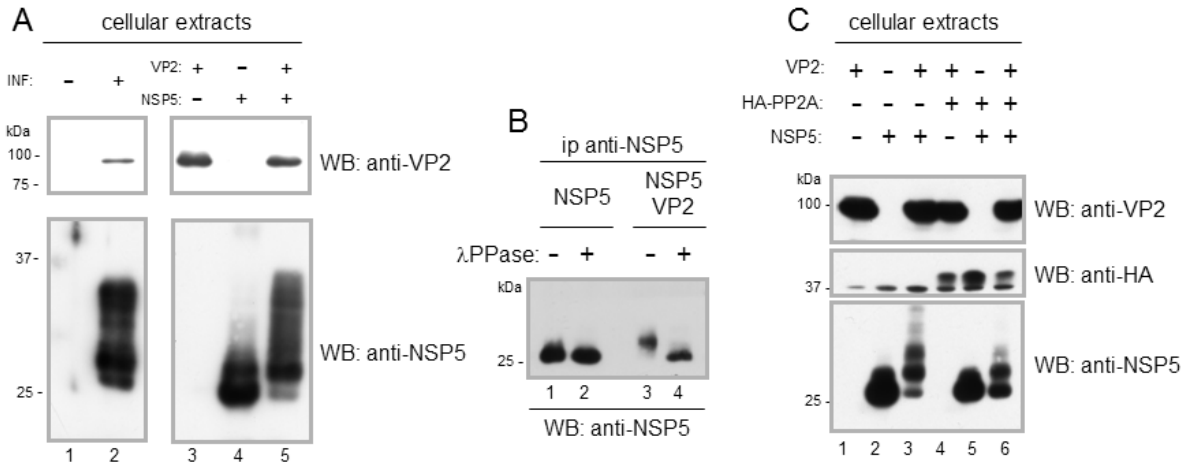

FIG. 19: NSP5 hyperphosphorylation induced by VP2. A) Western blot analysis of extracts of rotavirus-infected MA104 cells and cells cotransfected with NSP5 and VP2 plasmids. B) Western blot of immunoprecipitates, treated or mock-treated with lambda-phosphatase, from extracts of cells cotransfected with the indicated genes. C) Western blot analysis of extracts of cells coexpressing the indicated combinations of VP2, NSP5 and the catalytic subunit of phosphatase PP2A tagged with hemagglutinin (HA).

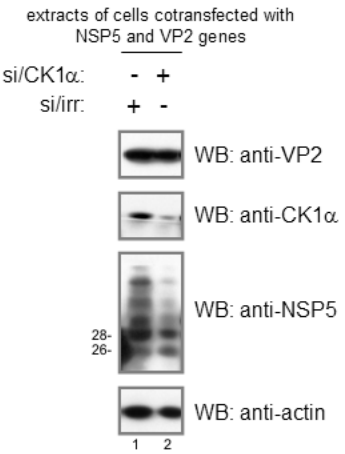

FIG. 20: Involvement of kinase CK1α in NSP5 hyperphosphorylation induced by VP2. Western blot of extracts of cells transiently cotransfected with NSP5 and VP2 plasmids and treated with si/CK1α or an irrelevant si/RNA, as indicated.

VLS formation and VP2-induced NSP5 hyperphosphorylation

Since VP2 induces both VLS formation and NSP5 hyperphosphorylation, we investigated whether there was a correlation between the two events. By immunofluorescence, we tested the formation of VLS in four different conditions, in which inhibition of VP2-induced NSP5 hyperphosphorylation was observed:

- coexpression of the catalytic subunit of phosphatase PP2A: although PP2A induces a decrease of NSP5 hyperphosphorylation induced by VP2 (Fig. 19C), the formation of VLS(VP2i) was not impaired and the cytoplasmic distribution of VLS(VP2i) in these conditions was similar to that of VLS(NSP2i) (Fig. 21A, picture C and 21B, picture E). Interestingly, the pattern of bands of NSP5 coexpressed either with VP2 and PP2A or with NSP2 is very similar (compare lane 6 of Fig. 19C with lane 1 of Fig. 8B).

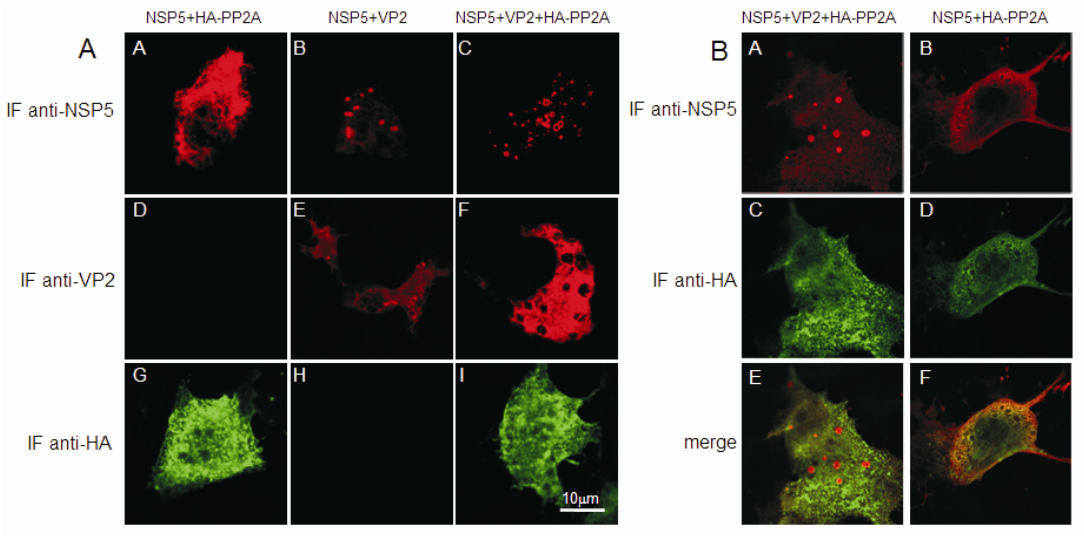

FIG. 21: VLS formation in MA104 cells coexpressing NSP5, VP2 and the catalytic subunit of phosphatase PP2A. A) Single immunofluorescence of HA-PP2A (green), NSP5 (red) and VP2 (red) in cells cotransfected with the indicated genes. B) Confocal microscopy showing the relative localization in the same cell of NSP5 (red) and HA-PP2A (green) upon cotransfection with the indicated genes.

- coexpression of tag-VP1: surprisingly, coexpression of tag-VP1 with VP2 and NSP5 in uninfected cells hampered the effect of VP2 on NSP5 hyperphosphorylation (Fig. 22A, see also Fig. 27, lanes 4, 12), which is consistent with the evidence of an inhibitory activity of tag-VP1 on the NSP2-mediated NSP5 hyperphosphorylation (Fig. 8B). It remains to be investigated whether this is due to a depletion of substrate by tag-VP1 because of its strong interaction with NSP5 or to other mechanisms. Apart from that, when NSP5 is coexpressed with tag-VP1 and VP2 and its hyperphosphorylation decreases, VLS(VP2i) are still formed (Fig. 22B) and, interestingly, tag-VP1 is recruited into them colocalizing with both NSP5 (Fig. 22B, upper row) and VP2 (Fig. 22B, bottom row).

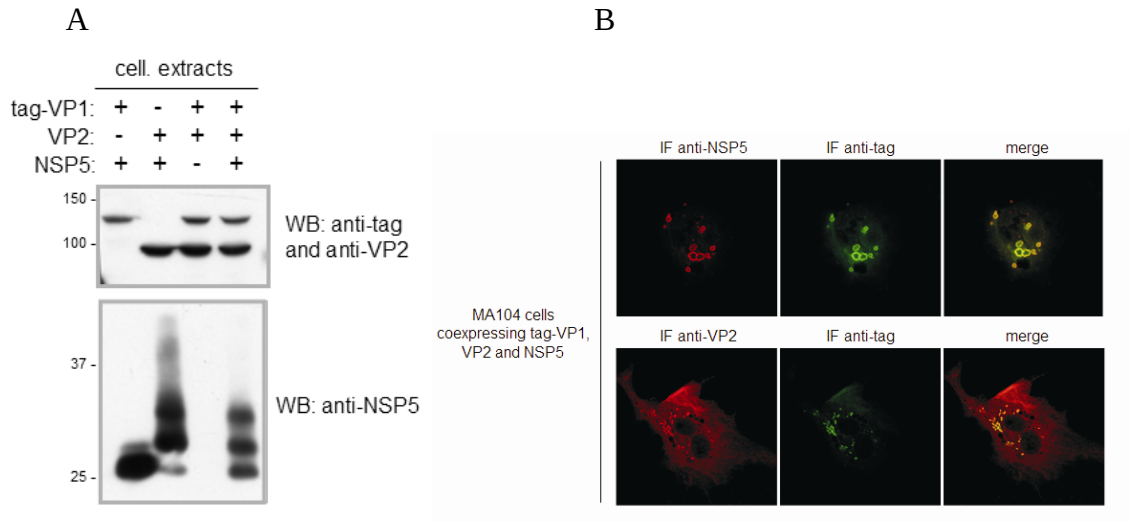

FIG. 22: Coexpression of tag-VP1, VP2 and NSP5 in MA104 cells. A) Western blot analysis of extracts of cells cotransfected with the indicated combinations of tag-VP1, VP2 and NSP5 plasmids. B) Colocalization of tag-VP1 and NSP5 or tag-VP1 and VP2 in VLS formed in cells coexpressing NSP5, VP2 and tag-VP1, as shown by confocal microscopy with anti-NSP5 (red) and anti-tag (green) or with anti-VP2 (red) and anti-tag (green) antibodies.

- coexpression of NSP5 phosphorylation mutants: as explained in the Introduction, NSP5 phosphorylation has been described as a hierarchical process starting from phosphorylation of a serine residue in position 67 (87). We coexpressed VP2 with either a point mutant of NSP5 containing an alanine in position 67 (S67A) or a mutant called NSP5a, where serines in positions 63, 65 and 67 were all substituted with alanines, in order to remove all phosphorylation sites from the entire serine-rich motif (Fig. 23A). The effect of VP2 on hyperphosphorylation and cellular distribution of the NSP5 point mutants were analyzed by Western blotting and immunofluorescence. As shown in Fig. 23B, VP2 increases the hyperphosphorylation of both mutants only slightly and does not induce the inversion of the ratio 26/28KDa typically observed in wild-type NSP5 coexpressed with VP2 (Fig. 23B, compare lane 2 with lanes 4 and 6). This

suggests the involvement of additional phosphorylation sites on NSP5 sequence. Importantly, despite being only slightly hyperphosphorylated in the presence of VP2, these mutants still form VLS, as shown by immunofluorescence in Fig. 23C.

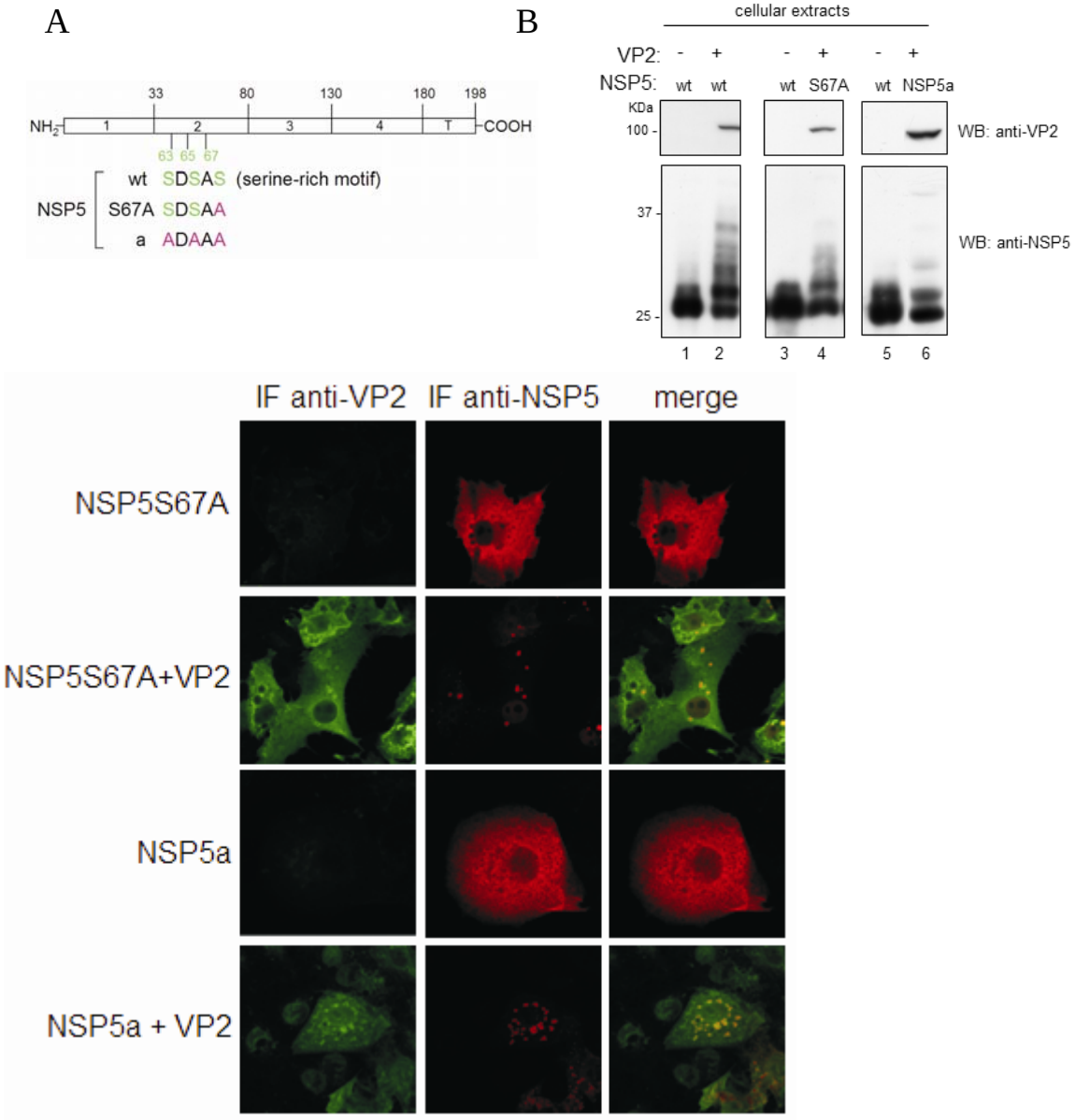

FIG. 23: Coexpression of VP2 with NSP5 phosphorylation mutants. A) Scheme of the mutated residues in NSP5 phosphorylation mutants. B) Western blot analysis of extracts of cells cotransfected with genes encoding VP2 and wild-type NSP5 or NSP5 phosphorylation mutants, as indicated. C) Localization of VP2 and wild-type NSP5 or NSP5 phosphorylation mutants in VLS formed in cotransfected MA104 cells, as shown by confocal microscopy with anti-NSP5 (red) and anti-VP2 (green) antibodies.

- coexpression of VP2 with low increase of NSP5 phosphorylation: when the relative amounts of plasmids encoding VP2 and NSP5 were varied, we found that a ratio corresponding to 1:10 (precisely 0.1µg pcDNA3-VP2 and 1µg pT7v-NSP5) does not lead to the typical increase of the band at 28KDa and the corresponding decrease of the band at 26KDa (Fig. 24A, lane 2). Under these conditions, most of NSP5 shows a pattern similar to NSP5 expressed alone, with the band at 26KDa mainly represented (Fig. 24A, lane 1). However, it still forms VLS, as assessed by immunofluorescence (Fig. 24B).

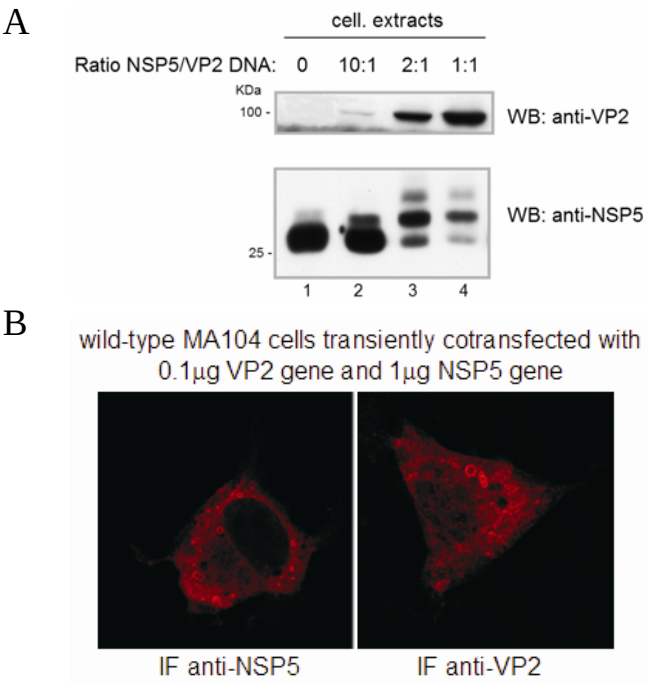

FIG. 24: Cotransfection of 1µg of NSP5 plasmid and 0.1µg of VP2 plasmid in MA104 cells. A) Western blot of extracts of MA104 cells cotransfected with different ratios between NSP5 and VP2 plasmids, as indicated. B) Localization of NSP5 and VP2 in VLS(VP2i) in MA104 cells transiently cotransfected with 1µg pT7v-NSP5 and 0.1µg pcDNA3-VP2, as shown by single immunofluorescence with anti-NSP5 (red) or anti-VP2 antibodies (red).

In summary, in all four conditions examined, NSP5 hyperphosphorylation induced by VP2 was significantly reduced, and yet VLS formation was not altered. Therefore, it is reasonable to conclude that the strong VP2-mediated NSP5 hyperphosphorylation does not correlate with VLS formation. However, stating that the two processes are totally unrelated would be imprecise, because in all the examples reported inhibition of the effect of VP2 on NSP5 hyperphosphorylation was never complete, and it could be argued that the residual fully hyperphosphorylated molecules suffice to drive VLS formation.

From VLS to viroplasms

Despite viroplasms being well defined morphological entities in rotavirus-infected cells, their detailed assembly has not been elucidated yet. It is known that they contain structural (VP1, VP2, VP3, VP6) and nonstructural proteins (NSP5, NSP2), but the recruitment of these proteins and their activities inside viroplasms remain unknown. Based on the morphological similarity with viroplasms, VLS might represent "incomplete viroplasms" and we are trying to coexpress all viroplasmic proteins in different combinations in order to understand the mechanisms of viroplasm assembly. Furthermore, these efforts require also to take into consideration recruitment into VLS of "viral" RNAs.

Until now, we have found that:

- VP2 and NSP2 are both VLS-inducers [(96); Fig. 6A, row 1; Fig. 13]
- VP1 is recruited into both VLS(NSP2i) and VLS(VP2i) (Fig. 6A, row 4; Fig. 22B);
- when coexpressed together, NSP5, NSP2 and VP2 are all recruited into VLS (Fig. 17B).

Like VP1, when the middle layer protein VP6 is coexpressed with NSP5, it does not induce VLS formation (Fig. 25, upper row) and forms tubular structures, as it does when expressed alone (data not shown). However, following coexpression of VP6 with NSP5 and VP2, we observed total recruitment of VP6 into VLS(VP2i) (Fig. 25, middle row), while coexpression with only VP2 in the NSP5-EGFP cell line led to a much less evident recruitment, despite the fact that VLS(VP2i) were clearly visible and VP6 tubules absent (Fig. 25, compare middle row with bottom row). Again, as in the previous experiments, the results obtained so far probably depend on the relative amounts of the coexpressed proteins.

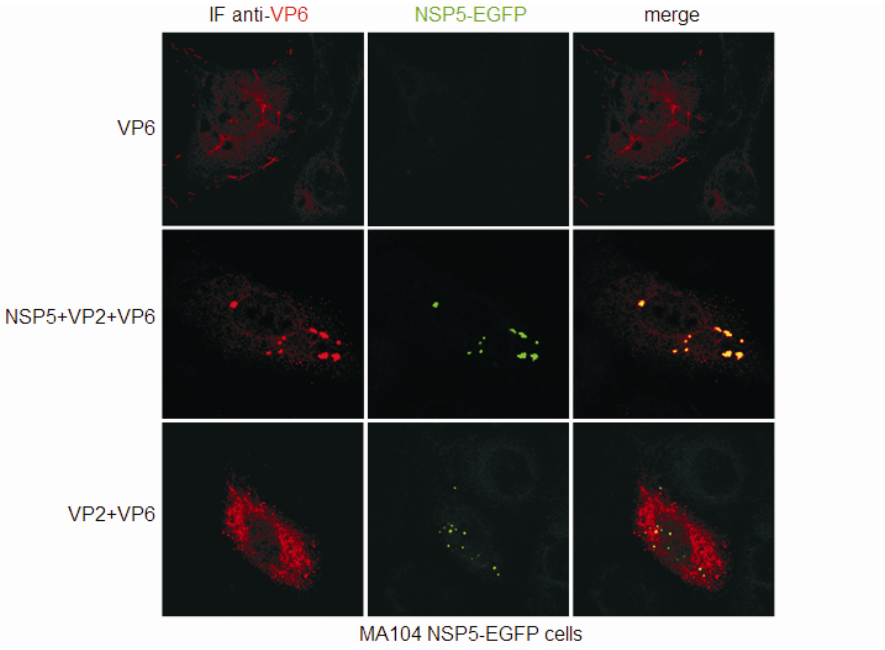

FIG. 25: Recruitment of VP6 into VLS formed in MA104 NSP5-EGFP cells transiently transfected with the indicated genes, as shown by confocal microscopy with the fluorescence of NSP5-EGFP (green) and with anti-VP6 antibodies (red).

The only viroplasmic protein, whose recruitment into VLS was not investigated, is VP3, because of the lack of a suitable antibody.

In conclusion, the data we have so far collected suggest a crucial role for NSP5 as an organizer of viroplasms, because it is the only protein essential for the formation of VLS induced in different ways and able to recruit other viroplasm components (NSP2, VP2, VP1, VP6).

Since all the immunofluorescence experiments indicated an association among the different viroplasmic proteins in structures similar to viroplasms, we attempted to verify these associations by coimmunoprecipitation experiments [as it has already been shown for NSP5, NSP2 and tag-VP1 in Results(1)]. First, we tried to coimmunoprecipitate VP2 and NSP5 from extracts of cells cotransfected with NSP5 and VP2 genes, without success. While both NSP5 and VP2 were well expressed, VP2 was not coimmunoprecipitated from cellular extracts with anti-NSP5 (Fig. 26, lanes 13, 16), regardless of whether cells had previously been treated or not treated with DSP. Similarly, anti-VP2 antibodies did not coimmunoprecipitate NSP5 (Fig. 26, lane 20). In addition, coimmunoprecipitation of VP2 with anti-NSP5 from extracts of infected cells was not observed either (Fig. 26, lane 10), in agreement with previous reports (1).

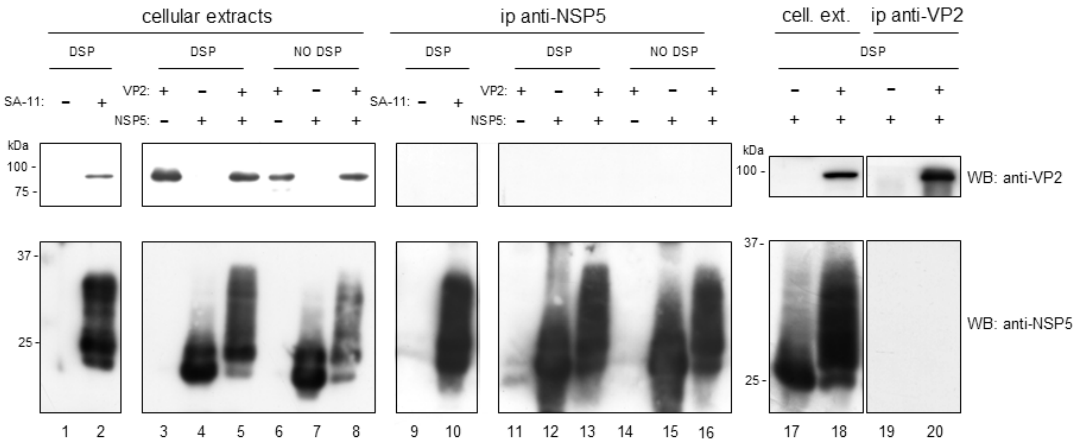

FIG. 26: Analysis of coimmunoprecipitation of VP2 and NSP5. Western blot analysis of cellular extracts (lanes 1-8, DSP cross-linked in lanes 1-5 and 17-18, and non-cross-linked in lanes 6-8) and immunoprecipitates with anti-NSP5 (lanes 9-16, DSP cross-linked in lanes 9-13 and non-cross-linked in lanes 14-16) or anti-VP2 (lanes 19-20, DSP cross-linked) derived from cells infected with rotavirus (lanes 1-2, 9-10) or cotransfected with VP2, NSP5 or both (lanes 3-8, 11-16, 17-20).

Since tag-VP1 was found in VLS(VP2i) (Fig. 22B), we performed coimmunoprecipitation assays from extracts of DSP cross-linked cells coexpressing tag-VP1, VP2 and NSP5. We observed that anti-NSP5 and anti-tag antibodies were still able to coimmunoprecipitate tag-VP1 and NSP5, respectively, while VP2 was not coimmunoprecipitated (Fig. 27, lanes 8, 12). In contrast, a faint band of coimmunoprecipitated VP2 was detected for extracts containing only NSP5 and VP2 (Fig. 27, lane 6, band indicated by a star). However, this band represented a very tiny amount compared to that in the extract, whereas the quantities of coimmunoprecipitated tag-VP1 and NSP5 were usually of the same order. The anti-VP2 serum was not very efficient in immunoprecipitating significant amounts of VP2 and, not surprisingly, did not coimmunoprecipitate any of the two other proteins (Fig. 27, lanes 13-16). It has to be noted that the anti-VP2 antibody used in this experiment and the anti-VP2 used in experiment of Fig. 26 were obtained from different sources. This may explain the different ability to immunoprecipitate VP2.

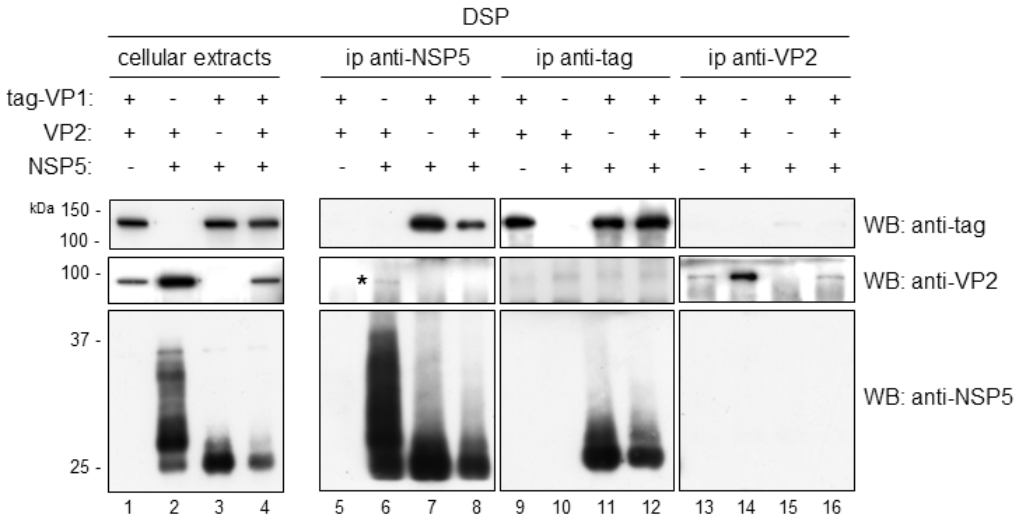

FIG. 27: Analysis of coimmunoprecipitation of NSP5, tag-VP1 and VP2. Western blot analysis of extracts (lanes 1-4) and immunoprecipitates with anti-NSP5 (lanes 5-8) or anti-tag (lanes 9-12) or anti-VP2 (lanes 13-16) derived from cells cotransfected with various combinations of NSP5, tag-VP1 and VP2 plasmids and DSP cross-linked, as indicated.

Finally, since we found that NSP5, NSP2 and VP2 were all present in VLS (Fig. 17B), we attempted to coimmunoprecipitate them with anti-NSP5 antibody from extracts of cells coexpressing all three proteins and DSP cross-linked. We observed that VP2 was not coimmunoprecipitated and, surprisingly, NSP2 was not either (Fig. 28, lane 8), or it was in amounts much smaller than in the absence of VP2 (Fig. 28, compare lane 6 with lane 8). More in detail, while in the absence of VP2 the ratio between NSP5 and NSP2 was maintained unaltered after coimmunoprecipitation (compare lane 2 with lane 6), in its presence it was not and only a faint band of coimmunoprecipitated NSP2 was visible (compare lane 4 with lane 8). Tiny amounts of coimmunoprecipitated VP2 were observed (lanes 7, 8). The decreased amount of coimmunoprecipitated NSP2 in the presence of VP2 might be due either to a reduced affinity between NSP5 and NSP2 or, alternatively, to a diminished cross-linking ability of DSP in the presence of VP2. Under those circumstances, the use of DSP would not be helpful, but, on the contrary, be disadvantageous, because DSP usually decreases the solubility of NSP5 (see Fig. 8). Therefore, it might cause the loss in the insoluble fraction of complexes formed by NSP5, NSP2 and VP2. Experiments of comparison between the relative amounts of the coexpressed proteins in the soluble and insoluble fractions are under way to evaluate potential artefacts produced by DSP.

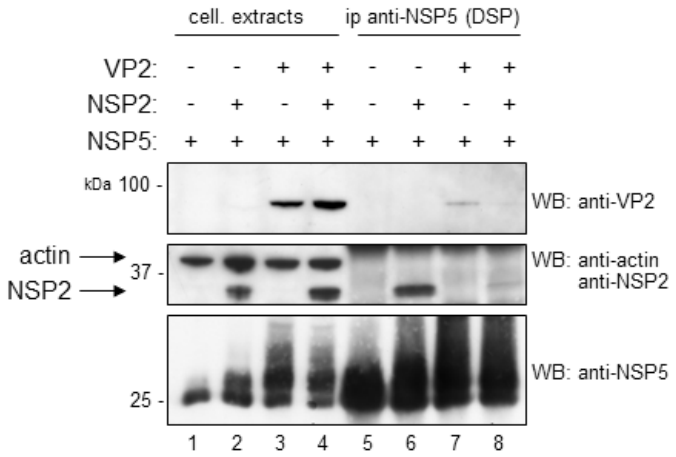

FIG. 28: Analysis of coimmunoprecipitation of NSP5, NSP2 and VP2. Western blot analysis of extracts (lanes 1-4) and immunoprecipitates with anti-NSP5 (lanes 5-8) derived from cells cotransfected with various combinations of NSP5, NSP2 and VP2 plasmids and DSP cross-linked, as indicated.

The failure of our attempts of coimmunoprecipitating all viroplasmic components might be simply due to methodological limitations (such as conditions of lysis, extraction, solubilisation, immunoprecipitation, etc.). However, the results obtained with our cotransfection experiments are strengthened by the fact that they are consistent with the data published for infected cells: NSP5, NSP2, VP1 and VP2 localize in viroplasms (220); NSP2 and VP1, but not VP2, coimmunoprecipitate with NSP5 from extracts of DSP cross-linked cells (2, 8).

DISCUSSION

Rotavirus RNA replication takes place in viroplasms and is mediated by several viral proteins, of which the polymerase VP1 and the core protein VP2 are sufficient to provide replicase activity *in vitro* (212, 308). *In vivo*, however, not well defined viral replication complexes are associated with the viroplasm-localised nonstructural proteins NSP2 and NSP5. Although the involvement of these two nonstructural proteins in the replicative cycle is unquestioned, since silencing their expression compromises viroplasm formation, viral genome synthesis and viral progeny production, their precise functions remain to be clarified. In this work we aimed at clarifying the interactions between NSP5 and the two structural proteins essentially required for viral RNA replication, VP1 and VP2. The involvement and the influence of other viral proteins in these interactions have also been examined with the aim to elucidate the temporal and spatial organization of the events leading to viroplasm assembly and synthesis of dsRNA viral genome.

In the first part of the work, the interaction between NSP5 and the polymerase VP1 was studied by coimmunoprecipitation and immunofluorescence experiments in both virus-infected and cotransfected cells. The capacity of NSP5 to interact with VP1 in virus-infected cells had already been observed in coimmunoprecipitation assays from DSP cross-linked extracts (2). The same experiments also showed an interaction between NSP5 and NSP2, which was subsequently confirmed by other works (85, 96, 139, 228) and, together with experiments of RNA interference (6, 45, 261) and intrabody-mediated silencing (285), led to identify an active role for NSP2 and NSP5 in the replication of viral genomic RNA. Because of its enzymatic activities (NTPase, RTPase, NDP kinase) and its ssRNA binding and helix destabilizing

properties, NSP2 has been suggested to work as a molecular motor that recruits and relaxes ssRNA templates and regulates the homeostasis of the nucleotide pools in viroplasms (151, 255, 270, 287). Proposing a role for NSP5, for which an ATPase activity was recently reported as its single recognized enzymatic activity (13), is more difficult. A structural role in viroplasm formation has been assigned to both nonstructural proteins, since in their absence viroplasms are not formed (45, 166, 261) and their coexpression in uninfected cells leads to the formation of viroplasm-like structures (VLS) (96). Here we provide a more detailed description of the nature of the interaction of VP1 with NSP5, with NSP2 or with both in the absence of other viral proteins or "true" viral RNA [the viral proteins are translated from transcripts of plasmids containing only cDNA comprising the coding regions and lacking the 5' and 3' UTRs (91)] (8). Using extracts of cotransfected MA104 cells, we show by coimmunoprecipitation assays that NSP5 has a strong interaction with VP1, which is not altered by the presence of NSP2. On the other hand, the interaction of NSP2 with VP1 appears to be much weaker and possibly stabilized by NSP5 (observed in DSP cross-linked extracts). Although it was not formally proven, the formation of a ternary complex of VP1, NSP5 and NSP2 is a possibility as tag-VP1 was found in the VLS formed as a consequence of the interaction of the two others (Fig. 6). An interaction between NSP2 and VP1 in rotavirus-infected cells has been previously reported (145). When VP1 was coexpressed with each of the nonstructural proteins individually, it became apparent that NSP5 interacted more strongly with VP1 than NSP2. However, when the three proteins were coexpressed, NSP5 seemed to enhance the interaction of VP1 with NSP2, a conclusion delineated from data using DSP cross-linked extracts. Interestingly, several attempted pull down experiments with anti-NSP2 serum did not coimmunoprecipitate NSP5 [as already published, (2)], nor

VP1. Thus, it is likely that most of the NSP2 molecules are buried within the cross-linked complex and therefore not accessible to the precipitating antibody.

In vivo cross-linking with DSP to stabilise complexes of interacting proteins was needed in experiments of coimmunoprecipitation with the anti-NSP5 antiserum, possibly because the high affinity hyper-immune polyclonal antibody has a dissociating activity. However, DSP must be used carefully, as it increases the insolubility of the hyperphosphorylated forms of NSP5 (Fig. 8) and may cause the loss of interacting complexes in the insoluble fraction. Differently from the anti-NSP5 serum, the anti-tag monoclonal antibody, which binds to the N-terminus of tag-VP1, allowed efficient coimmunoprecipitation of NSP5 or NSP2 or both from extracts that have not been cross-linked (Fig. 7).

Using NSP5 deletion mutants, we found that deletion of the N-terminal 33 amino acid region from NSP5 did not affect binding to VP1 while deletion of the last 18 amino acids from the C-terminus substantially reduced the interaction (Fig. 9) and deletion of the last 48 amino acids completely abolished it (Fig. 11). Also, results with single domain EGFP fusion chimeras allowed us to identify the 48 amino acids at the C-terminus as those involved in the interaction with VP1 (Fig. 10). As the last 18 C-terminal amino acids of NSP5 have previously been found to be involved in dimerisation (279), our data suggest that dimeric NSP5 is better suited for interaction, and that the binding region is located just upstream of the C-terminal tail. The region of VP1 interacting with NSP5 remains to be defined, but we found that the removal of the C-terminal 15 amino acids from tag-VP1 weakens the interaction with NSP5 (Fig. 12), suggesting an involvement of the C-terminus of VP1. Since the C-terminal 15 amino acids in the VP1 structure form an α-helical plug that reduces the diameter of the (-)ssRNA/dsRNA exit channel by almost half (Dr. John Patton, personal

communication), NSP5 might have a role in moving the plug affecting the production of viral genome segments.

Some of the results of this work were obtained by using a VP1 derivative in which the 12 amino acid long SV5 tag was fused to the N-terminus of VP1. The presence of the terminal tag allowed to recognize VP1 by immunoprecipitation or immunofluorescence assays. It also allowed us to overcome the problem of only having a poorly reactive antibody against the wild-type protein. The polyclonal antiserum against VP1 did not react in immunoprecipitation nor in immunofluorescence experiments, but only in Western blots. It is possible that the antibody, which was made against the N-terminal 435 amino acids, did not recognize the folded full-length VP1 protein while it was able to react with the denatured protein in Western blots. By contrast, the availability of a potent anti-tag monoclonal antibody allowed to study the interaction of VP1 with NSP5 and NSP2. In doing so, it had to be considered that fusing tags to a protein may modify its structural and functional properties and may lead to artefacts and misinterpretations (44). Therefore, in order to ensure the validity of using a tagged version of VP1, we analyzed the behaviour of such a protein in the context of viral infection by immunofluorescence and analysis of purified viral particles. We found that tag-VP1 was localized in viroplasms and VLS (Figs. 5, 6) and also packaged into viral progeny (Fig. 4). The incorporation efficiency was not high, but unequivocal and reproducible. Thus, only a few among the 12 molecules of the VP1 polymerase per viral particle (234) would be represented by the tagged VP1. The degree of tag-VP1 packaging was variable, possibly depending on the relative ratios of infectious units of vaccinia virus (used to express the T7 RNA polymerase that in turn transcribes transfected genes cloned under the control of the T7 promoter) and rotavirus, as well as on differences in the maturation of DLPs into TLPs. Non-specific attachment of tag-

VP1 to TLPs was ruled out by EDTA treatment of TLPs, which did not remove tag-VP1 (Fig. 4), and also by mixing TLPs with extracts containing an excess of tag-VP1, not leading to an association of these two components (results not shown). Succeeding in packaging tag-VP1 strengthens the results obtained in this work and represents a technical novelty. The system mainly used so far to study interactions among the structural proteins and their role in rotavirus morphogenesis (49, 63, 153, 249) is based on the coexpression of various combinations of structural proteins or derivatives thereof from baculovirus vectors in insect cells to form so-called virus-like particles (VLPs). Although VLPs have the structural characteristics and some of the functional properties of rotavirus particles (308), their assembly occurs outside the context of natural infection. The data provided here demonstrate that the incorporation of the exogenous protein into viral particles can take place during natural infection, indicating new possibilities for studying viral morphogenesis. While the improvement of an already developed reverse genetics system (149, 150) and the development of new ones are under investigation, inserting recombinant proteins into progeny particles during natural viral infection could help to further define the roles of viral proteins.

It has been reported that NSP5 interacts with VP2 based on two observations: (i) the coimmunoprecipitation of VP2 with an anti-NSP5 monoclonal antibody from extracts of either virus-infected MA104 cells or insect cells expressing recombinant NSP5 and VP2 from baculovirus recombinants; (ii) the pull down of either rotavirus cores or purified VLPs containing VP2 using a recombinant GST tagged derivative of NSP5 expressed in bacteria, purified and bound to glutathione-agarose beads (23). However, we found that NSP5 and VP2 were unable to coimmunoprecipitate either from infected cells or when coexpressed in uninfected cells, using extracts which had been cross-linked or not cross-linked with DSP (Fig. 26). In spite of these results, NSP5

hyperphosphorylation was considerably increased following coexpression with VP2 in uninfected cells (Figs. 19, 20, 23, 26, 27, 28). We proved that the migration of NSP5 bands with apparent higher molecular weight (28-34KDa) was due to the addition of phosphates: both *in vitro* treatment of anti-NSP5 immunoprecipitates with lambda-phosphatase and *in vivo* coexpression of NSP5 and VP2 with the catalitic subunit of the cellular phosphatase PP2A (Fig. 19) supported this conclusion, as in both cases a disappearance (with λ-phosphatase) or a strong reduction (with PP2A) of the NSP5 forms larger than 26KDa were observed. The increase of NSP5 hyperphosphorylation by VP2 represents a novel finding, which requires further analysis. At present, we have only ruled out an exclusive involvement of kinase CK1α by using an siRNA directed to this kinase in cells cotransfected with NSP5 and VP2 genes (Fig. 20). Since CK1α was recently shown to be involved in NSP5 phosphorylation in infected cells (43), our data confirm that different kinases and phosphatases participate in determining the phosphorylation status of NSP5 in the context of viral infection.

Following coexpression of VP1 either with NSP5 and NSP2 or with NSP5 and VP2 in uninfected cells, we observed a clear reduction in hyperphosphorylation of NSP5 (Figs. 8, 22), although the interactions between NSP5 and NSP2 or NSP5 and VP1 were not altered (Figs. 7, 27). Coimmunoprecipitation experiments from extracts of virus-infected cells indicated that both NSP5-NSP2 and NSP5-VP1 interactions occur, even when NSP5 hyperphosphorylation is inhibited by RNA interference against CK1α (43). While all these data clearly suggest that NSP5 phosphorylation is not required for interactions with VP1 and NSP2, at present there are insufficient results for a comprehensive interpretation of whether and how NSP5 hyperphosphorylation is linked to replication and packaging. With this regard, one open and controversial question is whether NSP5 hyperphosphorylation has a link with viroplasm/VLS

formation. Since (i) the two events have been found to be correlated during the course of viral infection (228), (ii) NSP2 behaves as an inducer of both NSP5 hyperphosphorylation and VLS formation (2, 96), (iii) expression of N-terminally tagged derivatives of NSP5 in the absence of any other viral protein results in both VLS formation (190) and hyperphosphorylation (44), a cause-effect relationship between the two events may be hypothesized. However, several lines of evidence suggest that NSP5 hyperphosphorylation cannot trigger viroplasm/VLS formation: (i) treatment of cells expressing NSP5 from a transfected gene with inhibitors of cellular phosphatases leads to NSP5 hyperphosphorylation, but not to VLS formation (27); (ii) NSP5 deletion mutants that are not phosphorylated are recruited into viroplasms of infected cells (87); silencing CK1α expression in infected cells blocks NSP5-hyperphosphorylation, but does not impair the formation of viroplasms, although it interferes with their maturation (43). Here we presented data showing that, like NSP2, VP2 also behaves as an inducer of both NSP5 hyperphosphorylation and VLS formation. As already observed in insect cells (23), coexpression of NSP5 and VP2 in mammalian cells results in the formation of a small number of spherical structures concentrated in a perinuclear area (Figs. 13, 14, 16B, 17A, 18). Based on the morphological similarity with VLS formed by NSP5 and NSP2, we named these structures VLS as well and in order to distinguish the two kinds of VLS, we chose the names VLS(NSP2i) and VLS(VP2i), in which "i" stands for "induced". While the correlation between the NSP5 hyperphosphorylation induced by VP2 and VLS(VP2i) formation would suggest once again a direct link between the two events, we found further evidence doubting this hypothesis. In fact, four conditions in which the VP2-mediated NSP5 hyperphosphorylation was inhibited resulted in a normal VLS(VP2i) formation: (i) coexpression of NSP5 and VP2 with the catalytic subunit of PP2A (Fig. 21); (ii) coexpression of NSP5 and VP2 with tag-VP1 (Fig. 22); (iii) coexpression of

VP2 with NSP5 point mutants that cannot undergo hyperphosphorylation (Fig. 23); (iv) coexpression of VP2 and NSP5 at the ratio 1:10, which does not lead to NSP5 hyperphosphorylation (Fig. 24). Therefore, NSP5 hyperphosphorylation is unlikely to be the event triggering VLS formation. The C-terminus of NSP5, in particular the last 18 amino acids, were shown to be required for VLS formation and recruitment of NSP5 deletion mutants into viroplasms (85, 87) and for initiating the cascade of hyperphosphorylation (84). Since the C-terminal 10 amino acids were shown to mediate NSP5 multimerization (279), it might be hypothesized that NSP5 needs to multimerize either to form VLS/viroplasms or to be hyperphosphorylated. Both NSP2 and VP2 might promote the multimerization of NSP5 possibly by inducing a conformational change that renders the C-terminus capable of interacting with other NSP5 molecules. This multimerization might involve the association of already formed dimers of NSP5, as a deletion mutant of NSP5 lacking the C-terminal 10 amino acids, and thus the multimerizing region, has been shown to be capable to form dimers bound to NSP2 (139) and has been reported to be unable to form VLS(NSP2i) (13). According to the proposed model, NSP5 hyperphosphorylation and VLS/viroplasm formation would be two concomitant events because of the dependence on a common cause, but independent from one another and requiring further distinct factors: a serine in position 67 that can be phosphorylated (84) and something modifying the NSP5 N-terminus [like a tag (190) or NSP2 (85)]. Such a model can explain the often found concurrence of NSP5 hyperphosphorylation and VLS/viroplasm formation. In addition, the fact that VP1 induces neither NSP5 hyperphosphorylation nor VLS formation may be due to its interaction with the C-terminus of NSP5, which might prevent the NSP5 multimerization. Experiments of coexpression of NSP5 and VP1 either with NSP2 or with VP2 revealed that the interaction between NSP5 and VP1 is strong and unaltered by coexpression of NSP2

or VP2 (Figs. 7, 27). A favored interaction between NSP5 and VP1 that detracts substrate from NSP2 and VP2 might be responsible for the reduced hyperphosphorylation of NSP5 in spite of the presence of NSP2 and VP2. However, it remains difficult to predict how VP1 is recruited into VLS(NSP2i) (Figs. 5, 6) and VLS(VP2i) (Fig. 22) according to the proposed model. While for understanding the localization of VP1 in VLS(VP2i) further data are needed, structural studies on the NSP2 octamer allow to propose an explanation for the recruitment into VLS(NSP2i). Since NSP2 was shown to be able to bind four dimers of NSP5 (139), it can be hypothesized that some sites of the NSP2 octamer bind NSP5-VP1 complexes, whilst other sites may bind free NSP5 molecules. These latter ones would have a C-terminus available for multimerization with other free NSP5 molecules bound in turn to other NSP2 octamers and would allow the formation of VLS(NSP2i) containing VP1. A delicate equilibrium between the amounts of NSP5, VP1 and NSP2 molecules appears to be required for VLS formation. In this regard, the experiments of coexpression of NSP5 with either NSP2 or VP2 in different relative amounts suggested that the ratio between the coexpressed proteins is critical for both VLS formation and recruitment into VLS: (i) a better recruitment of VP2 into VLS(VP2i) has been observed when NSP5 and VP2 plasmids were cotransfected in a ratio 1:10 or 1:100 (in terms of µg) (Fig. 14); (ii) the fusion protein NSP5-EGFP stably expressed in an MA104 stable cell line, which was transiently transfected with a NSP2 expressing plasmid, required a supplement of NSP5 transiently expressed to form VLS(NSP2i) and to recruit NSP2 into them (Fig. 16C-D); (iii) when the same cell line was transiently transfected with the VP2 gene, a supplement of NSP5 was not required for VLS(VP2i) formation but for recruitment of VP2 into VLS (Fig. 16A-B). The possibility that tagging NSP5 at the C-terminus interfered with VLS formation, as proposed in previous studies (190), has been ruled out by the detection of VLS following transient

cotransfection of NSP5-EGFP and VP2 plasmids (Fig. 18). The EGFP autofluorescence of the fusion protein as a tracer of VLS was validated by immunofluorescence assays with anti-NSP5 antibodies on MA104 NSP5-EGFP cells cotransfected with wild-type NSP5 and NSP2 or VP2 expressing plasmids, which showed a perfect colocalization of NSP5-EGFP and wild-type NSP5 (Figs. 16, 17).

Among the data presented, some are quite difficult to interpret and require further investigations: the difference in number and distribution between VLS(VP2i) and VLS(NSP2i); the fact that NSP5 partially dephosphorylated by the catalytic subunit of PP2A forms VLS(VP2i) similar in number and distribution to VLS(NSP2i); and above all the lack of coimmunoprecipitation of NSP5 and VP2, although both colocalize in VLS and although different conditions of cell lysis and immunoprecipitation have been tried. In order to widen the information about the interaction between NSP5 and VP2, experiments with different kinase inhibitors in infected and cotransfected cells will be performed. In addition, a tagged derivative of VP2 fused to a peptide that is *in vivo* biotinylated (236) will be expressed in uninfected cells, with or without concomitant expression of NSP5; VP2 will then be purified together with possibly interacting cellular partners by streptavidin magnetic beads and the purified material will be analyzed by mass spectrometry.

Coexpression of NSP5 with both VLS-inducers, NSP2 and VP2, provided the following evidence: (i) VLS were formed in number and distribution typical of VLS(NSP2i) and able to recruit both NSP2 and VP2 (Fig. 17B); (ii) the pattern of NSP5 phosphorylation bands was the same as observed in assays of coexpression of only NSP5 and VP2 (Fig. 28); (iii) the amount of NSP2 coimmunoprecipitated with anti-NSP5 antibodies from DSP cross-linked extracts was reduced compared to the amount coimmunoprecipitated in the absence of VP2 (Fig. 28). Several hypotheses can be proposed for the latter observation. VP2 might produce conformational

changes in NSP5 and/or NSP2 or modify their relative positions, compromising the capability of DSP to cross-link them. Alternatively, NSP5 molecules which have already interacted with VP2 may have a reduced affinity for NSP2. Finally, VP2 might dislodge NSP5 from NSP2 or *vice versa*. Finally, since all three proteins were found in VLS, it cannot be ruled out that DSP decreases the solubility of ternary complexes, which may get lost from the analysis by transfer into the insoluble fraction during preparation of cellular extracts. In order to explore this further, experiments of comparison of the relative amounts of the coexpressed proteins in the soluble and insoluble fractions are under way. Moreover, an interaction between VP2 and NSP2, which has never been described before, may be involved and thus it is worth investigating.

From all coexpression experiments presented, NSP5 appears to be the key protein for formation of different types of VLS and for recruitment of other viroplasmic proteins. Besides NSP2, VP2 and VP1, VP6 has also been found localized in VLS(VP2i) (Fig. 25). At present, there is no evidence of an interaction between VP6 and NSP5. In fact, NSP5 has been reported to dislodge VP6 from VLPs formed in insect cells (23). Experiments with siRNAs silencing NSP5 expression in infected cells showed an altered distribution of the viroplasmic proteins VP2, NSP2 and VP6, suggesting a role for NSP5 in the recruitment of viral proteins into viroplasms (166), in agreement with our data. In addition, silencing of NSP4 expression was also shown to cause a delocalization of VP6 concomitantly with a decreased expression of NSP5 and NSP2 (165). Therefore, it has been proposed that the distribution of VP6 is sensitive to the concentration of proteins that accumulate in viroplasms (166). Once again, the ratio between viroplasmic proteins appears to play a crucial role in determining their cellular distribution.

In conclusion, coexpression of different combinations of viroplasmic proteins can be considered a valid strategy to investigate their interactions and be of help towards a better understanding of viroplasm assembly. In order to "re-make" viroplasms by transfection experiments, the recruitment into VLS of transfected viral RNAs needs to be addressed. However, it has been shown that labelled exogenous viral mRNAs transfected into rotavirus infected cells do not localize in viroplasms suggesting the lack of pathways trafficking plus-strand RNAs from cytosol to viroplasms (261). This may represent a limit in "re-making" viroplasms by transfection experiments. However, it is encouraging that recombinant viruses of the family *Reoviridae* have been obtained starting from an exclusively plasmid-based system in the case of reoviruses (147) or from transfection of a complete set of viral mRNAs *in vitro* transcribed either by viral cores (34) or by the T7 *in vitro* transcription system (33) in the case of Bluetongue Virus.

In the process of viroplasm assembly also cellular proteins might be involved. It has been reported that a functional microtubule network is needed for viroplasm growth, presumably through an association of both NSP5 and NSP2 with tubulin (42). However, we could never reproduce the interaction with tubulin of the two nonstructural rotavirus proteins (Campagna and Burrone, unpublished results). In addition, an association between viroplasms and some components of cellular lipid storage organelles has recently been found and is under further investigation (Dr. Ulrich Desselberger, University of Cambridge, personal communication). The discovery of cellular factors interacting with viroplasmic proteins, in conjunction with the characterization of the dynamic interactions between the viral proteins found in viroplasms, could contribute to clarifying the mechanisms driving the viroplasm assembly.

Finally, we propose a model for the first phases of viroplasm formation and genome RNA synthesis, where NSP5 would play a key role in forming viroplasms and recruiting all the other viroplasmic components (see scheme below). Following viral protein translation, NSP5 may be distributed into three pools:

1. bound to replicase-incompetent precore replication intermediates (RI) (VP1-VP3-RNA) through interaction of its C-terminus with VP1; this pool would be hypophosphorylated and unable to be recruited into viroplasms;
2. forming "viroplasm precursors" [possibly around DLPs of the incoming infection (261)] because of interactions with the newly synthesized VP2 and/or NSP2; this pool would be hyperphosphorylated and able to recruit the other viroplasmic proteins;
3. free in cytosol; this pool would be hypophosphorylated.

Through its multiple binding sites the NSP2 octamer might hook up:

1. NSP5 bound to precore RI; this association might prevent VP2 binding impeding replication to start, as previously proposed (291);
2. free NSP5; this interaction would trigger the NSP5 multimerization resulting in viroplasm formation and recruitment of NSP2 itself and precore RI, as already proposed above.

Once located in viroplasms, NSP2-NSP5-precore RI complexes would lie in a VP2-rich environment. VP2 might determine a detachment of NSP2 and interact with precore RI, which would become consequently replicase-competent RI. Considering that NSP5 and RNA were shown to compete for the same binding sites on NSP2 (139), an impaired NSP5-NSP2 binding because of VP2 might advantage RNA, thus allowing NSP2 to exert its enzymatic activities. The hyperphosphorylation of NSP5 might influence the activity of the polymerase, as it has been shown for

phosphoproteins forming the regulatory subunits of polymerases of negative-strand RNA viruses (133, 254).

This model is consistent with the purification of replicase-incompetent precore RI from extracts of infected cells (104) and with the coimmunoprecipitation of VP1-NSP5-NSP2 complexes not containing VP2 (2). Future experiments will test the validity of such a model, in which NSP5 would have the dual function of directing the architectural assembly of viroplasms and recruiting the other viroplasmic proteins as well as the RNA templates via its interaction with VP1 and NSP2.

Model proposed for the first phases of viroplasm formation

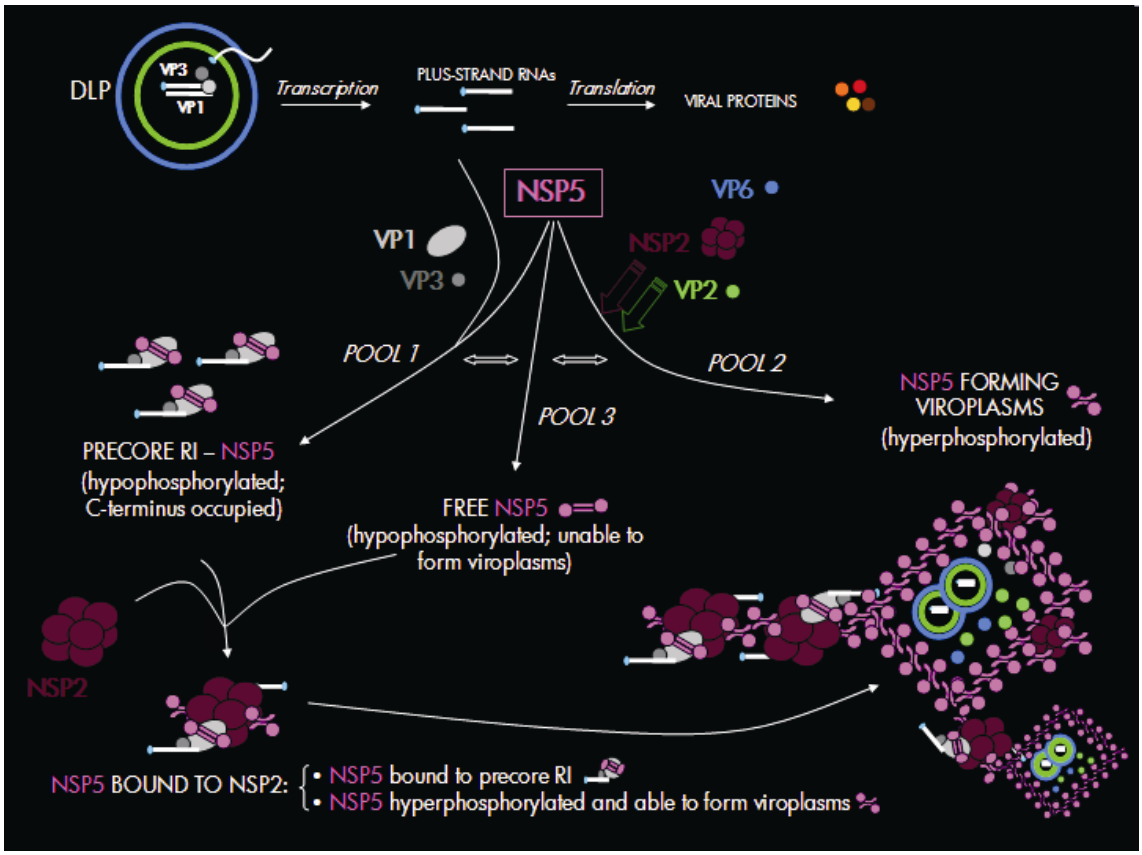

REFERENCES

1. Affranchino, J. L., and S. A. Gonzalez. 1997. Deletion mapping of functional domains in the rotavirus capsid protein VP6. J Gen Virol 78 (Pt 8):1949-55.
2. Afrikanova, I., E. Fabbretti, M. C. Miozzo, and O. R. Burrone. 1998. Rotavirus NSP5 phosphorylation is up-regulated by interaction with NSP2. J Gen Virol 79 (Pt 11):2679-86.
3. Afrikanova, I., M. C. Miozzo, S. Giambiagi, and O. Burrone. 1996. Phosphorylation generates different forms of rotavirus NSP5. J Gen Virol 77 (Pt 9):2059-65.
4. Altenburg, B. C., D. Y. Graham, and M. K. Estes. 1980. Ultrastructural study of rotavirus replication in cultured cells. J Gen Virol 46:75-85.
5. Aponte, C., D. Poncet, and J. Cohen. 1996. Recovery and characterization of a replicase complex in rotavirus-infected cells by using a monoclonal antibody against NSP2. J Virol 70:985-91.
6. Arias, C. F., M. A. Dector, L. Segovia, T. Lopez, M. Camacho, P. Isa, R. Espinosa, and S. Lopez. 2004. RNA silencing of rotavirus gene expression. Virus Res 102:43-51.
7. Arias, C. F., P. Romero, V. Alvarez, and S. Lopez. 1996. Trypsin activation pathway of rotavirus infectivity. J Virol 70:5832-9.
8. Arnoldi, F., M. Campagna, C. Eichwald, U. Desselberger, and O. R. Burrone. 2007. Interaction of rotavirus polymerase VP1 with nonstructural protein NSP5 is stronger than that with NSP2. J Virol 81:2128-37.
9. Au, K. S., W. K. Chan, J. W. Burns, and M. K. Estes. 1989. Receptor activity of rotavirus nonstructural glycoprotein NS28. J Virol 63:4553-62.
10. Au, K. S., N. M. Mattion, and M. K. Estes. 1993. A subviral particle binding domain on the rotavirus nonstructural glycoprotein NS28. Virology 194:665-73.
11. Au, W. C., P. A. Moore, D. W. LaFleur, B. Tombal, and P. M. Pitha. 1998. Characterization of the interferon regulatory factor-7 and its potential role in the transcription activation of interferon A genes. J Biol Chem 273:29210-7.
12. Ball, J. M., P. Tian, C. Q. Zeng, A. P. Morris, and M. K. Estes. 1996. Age-dependent diarrhea induced by a rotaviral nonstructural glycoprotein. Science 272:101-4.
13. Bar-Magen, T., E. Spencer, and J. T. Patton. 2007. An ATPase activity associated with the rotavirus phosphoprotein NSP5. Virology 369:389-99.
14. Barro, M., and J. T. Patton. 2005. Rotavirus nonstructural protein 1 subverts innate immune response by inducing degradation of IFN regulatory factor 3. Proc Natl Acad Sci U S A 102:4114-9.
15. Barro, M., and J. T. Patton. 2007. Rotavirus NSP1 inhibits expression of type I interferon by antagonizing the function of interferon regulatory factors IRF3, IRF5, and IRF7. J Virol 81:4473-81.
16. Bass, D. M., M. R. Baylor, C. Chen, E. M. Mackow, M. Bremont, and H. B. Greenberg. 1992. Liposome-mediated transfection of intact viral particles reveals that plasma membrane penetration determines permissivity of tissue culture cells to rotavirus. J Clin Invest 90:2313-20.

17. **Bastardo, J. W., and I. H. Holmes.** 1980. Attachment of SA-11 rotavirus to erythrocyte receptors. Infect Immun **29:**1134-40.
18. **Benureau, Y., J. C. Huet, A. Charpilienne, D. Poncet, and J. Cohen.** 2005. Trypsin is associated with the rotavirus capsid and is activated by solubilization of outer capsid proteins. J Gen Virol **86:**3143-51.
19. **Bergmann, C. C., D. Maass, M. S. Poruchynsky, P. H. Atkinson, and A. R. Bellamy.** 1989. Topology of the non-structural rotavirus receptor glycoprotein NS28 in the rough endoplasmic reticulum. Embo J **8:**1695-703.
20. **Berkova, Z., S. E. Crawford, S. E. Blutt, A. P. Morris, and M. K. Estes.** 2007. Expression of rotavirus NSP4 alters the actin network organization through the actin remodeling protein cofilin. J Virol **81:**3545-53.
21. **Berkova, Z., S. E. Crawford, G. Trugnan, T. Yoshimori, A. P. Morris, and M. K. Estes.** 2006. Rotavirus NSP4 induces a novel vesicular compartment regulated by calcium and associated with viroplasms. J Virol **80:**6061-71.
22. **Berkova, Z., A. P. Morris, and M. K. Estes.** 2003. Cytoplasmic calcium measurement in rotavirus enterotoxin-enhanced green fluorescent protein (NSP4-EGFP) expressing cells loaded with Fura-2. Cell Calcium **34:**55-68.
23. **Berois, M., C. Sapin, I. Erk, D. Poncet, and J. Cohen.** 2003. Rotavirus nonstructural protein NSP5 interacts with major core protein VP2. J Virol **77:**1757-63.
24. **Bican, P., J. Cohen, A. Charpilienne, and R. Scherrer.** 1982. Purification and characterization of bovine rotavirus cores. J Virol **43:**1113-7.
25. **Bishop, R. F., G. P. Davidson, I. H. Holmes, and B. J. Ruck.** 1973. Virus particles in epithelial cells of duodenal mucosa from children with acute non-bacterial gastroenteritis. Lancet **2:**1281-3.
26. **Blackhall, J., A. Fuentes, K. Hansen, and G. Magnusson.** 1997. Serine protein kinase activity associated with rotavirus phosphoprotein NSP5. J Virol **71:**138-44.
27. **Blackhall, J., M. Munoz, A. Fuentes, and G. Magnusson.** 1998. Analysis of rotavirus nonstructural protein NSP5 phosphorylation. J Virol **72:**6398-405.
28. **Blanchard, H., X. Yu, B. S. Coulson, and M. von Itzstein.** 2007. Insight into host cell carbohydrate-recognition by human and porcine rotavirus from crystal structures of the virion spike associated carbohydrate-binding domain (VP8*). J Mol Biol **367:**1215-26.
29. **Blutt, S. E., D. O. Matson, S. E. Crawford, M. A. Staat, P. Azimi, B. L. Bennett, P. A. Piedra, and M. E. Conner.** 2007. Rotavirus antigenemia in children is associated with viremia. PLoS Med **4:**e121.
30. **Boshuizen, J. A., J. W. Rossen, C. K. Sitaram, F. F. Kimenai, Y. Simons-Oosterhuis, C. Laffeber, H. A. Buller, and A. W. Einerhand.** 2004. Rotavirus enterotoxin NSP4 binds to the extracellular matrix proteins laminin-beta3 and fibronectin. J Virol **78:**10045-53.
31. **Both, G. W., L. J. Siegman, A. R. Bellamy, and P. H. Atkinson.** 1983. Coding assignment and nucleotide sequence of simian rotavirus SA11 gene segment 10: location of glycosylation sites suggests that the signal peptide is not cleaved. J Virol **48:**335-9.
32. **Bowman, G. D., I. M. Nodelman, O. Levy, S. L. Lin, P. Tian, T. J. Zamb, S. A. Udem, B. Venkataraghavan, and C. E. Schutt.** 2000. Crystal structure of the oligomerization domain of NSP4 from rotavirus reveals a core metal-binding site. J Mol Biol **304:**861-71.
33. **Boyce, M., C. C. Celma, and P. Roy.** 2008. Development of reverse genetics systems for bluetongue virus: recovery of infectious virus from synthetic RNA transcripts. J Virol **82:**8339-48.

34. **Boyce, M., and P. Roy.** 2007. Recovery of infectious bluetongue virus from RNA. J Virol **81:**2179-86.
35. **Boyle, J. F., and K. V. Holmes.** 1986. RNA-binding proteins of bovine rotavirus. J Virol **58:**561-8.
36. **Broome, R. L., P. T. Vo, R. L. Ward, H. F. Clark, and H. B. Greenberg.** 1993. Murine rotavirus genes encoding outer capsid proteins VP4 and VP7 are not major determinants of host range restriction and virulence. J Virol **67:**2448-55.
37. **Brottier, P., P. Nandi, M. Bremont, and J. Cohen.** 1992. Bovine rotavirus segment 5 protein expressed in the baculovirus system interacts with zinc and RNA. J Gen Virol **73 (Pt 8):**1931-8.
38. **Browne, E. P., A. R. Bellamy, and J. A. Taylor.** 2000. Membrane-destabilizing activity of rotavirus NSP4 is mediated by a membrane-proximal amphipathic domain. J Gen Virol **81:**1955-9.
39. **Brunet, J. P., J. Cotte-Laffitte, C. Linxe, A. M. Quero, M. Geniteau-Legendre, and A. Servin.** 2000. Rotavirus infection induces an increase in intracellular calcium concentration in human intestinal epithelial cells: role in microvillar actin alteration. J Virol **74:**2323-32.
40. **Bugarcic, A., and J. A. Taylor.** 2006. Rotavirus nonstructural glycoprotein NSP4 is secreted from the apical surfaces of polarized epithelial cells. J Virol **80:**12343-9.
41. **Burke, B., and U. Desselberger.** 1996. Rotavirus pathogenicity. Virology **218:**299-305.
42. **Cabral-Romero, C., and L. Padilla-Noriega.** 2006. Association of rotavirus viroplasms with microtubules through NSP2 and NSP5. Mem Inst Oswaldo Cruz **101:**603-11.
43. **Campagna, M., M. Budini, F. Arnoldi, U. Desselberger, J. E. Allende, and O. R. Burrone.** 2007. Impaired hyperphosphorylation of rotavirus NSP5 in cells depleted of casein kinase 1alpha is associated with the formation of viroplasms with altered morphology and a moderate decrease in virus replication. J Gen Virol **88:**2800-10.
44. **Campagna, M., and O. R. Burrone.** 2006. Fusion of tags induces spurious phosphorylation of rotavirus NSP5. J Virol **80:**8283-4; author reply 8284-5.
45. **Campagna, M., C. Eichwald, F. Vascotto, and O. R. Burrone.** 2005. RNA interference of rotavirus segment 11 mRNA reveals the essential role of NSP5 in the virus replicative cycle. J Gen Virol **86:**1481-7.
46. **Carpio, R. V., F. D. Gonzalez-Nilo, H. Jayaram, E. Spencer, B. V. Prasad, J. T. Patton, and Z. F. Taraporewala.** 2004. Role of the histidine triad-like motif in nucleotide hydrolysis by the rotavirus RNA-packaging protein NSP2. J Biol Chem **279:**10624-33.
47. **Charpilienne, A., M. J. Abad, F. Michelangeli, F. Alvarado, M. Vasseur, J. Cohen, and M. C. Ruiz.** 1997. Solubilized and cleaved VP7, the outer glycoprotein of rotavirus, induces permeabilization of cell membrane vesicles. J Gen Virol **78 (Pt 6):**1367-71.
48. **Charpilienne, A., J. Lepault, F. Rey, and J. Cohen.** 2002. Identification of rotavirus VP6 residues located at the interface with VP2 that are essential for capsid assembly and transcriptase activity. J Virol **76:**7822-31.
49. **Charpilienne, A., M. Nejmeddine, M. Berois, N. Parez, E. Neumann, E. Hewat, G. Trugnan, and J. Cohen.** 2001. Individual rotavirus-like particles containing 120 molecules of fluorescent protein are visible in living cells. J Biol Chem **276:**29361-7.
50. **Chemello, M. E., O. C. Aristimuno, F. Michelangeli, and M. C. Ruiz.** 2002. Requirement for vacuolar H+ -ATPase activity and Ca2+ gradient during entry of rotavirus into MA104 cells. J Virol **76:**13083-7.

51. Chen, D., M. Barros, E. Spencer, and J. T. Patton. 2001. Features of the 3'-consensus sequence of rotavirus mRNAs critical to minus strand synthesis. Virology 282:221-9.
52. Chen, D., C. L. Luongo, M. L. Nibert, and J. T. Patton. 1999. Rotavirus open cores catalyze 5'-capping and methylation of exogenous RNA: evidence that VP3 is a methyltransferase. Virology 265:120-30.
53. Chen, D., and J. T. Patton. 2000. De novo synthesis of minus strand RNA by the rotavirus RNA polymerase in a cell-free system involves a novel mechanism of initiation. Rna 6:1455-67.
54. Chen, D., and J. T. Patton. 1998. Rotavirus RNA replication requires a single-stranded 3' end for efficient minus-strand synthesis. J Virol 72:7387-96.
55. Chen, D., C. Q. Zeng, M. J. Wentz, M. Gorziglia, M. K. Estes, and R. F. Ramig. 1994. Template-dependent, in vitro replication of rotavirus RNA. J Virol 68:7030-9.
56. Chizhikov, V., and J. T. Patton. 2000. A four-nucleotide translation enhancer in the 3'-terminal consensus sequence of the nonpolyadenylated mRNAs of rotavirus. Rna 6:814-25.
57. Ciarlet, M., S. E. Crawford, E. Cheng, S. E. Blutt, D. A. Rice, J. M. Bergelson, and M. K. Estes. 2002. VLA-2 (alpha2beta1) integrin promotes rotavirus entry into cells but is not necessary for rotavirus attachment. J Virol 76:1109-23.
58. Ciarlet, M., and M. K. Estes. 1999. Human and most animal rotavirus strains do not require the presence of sialic acid on the cell surface for efficient infectivity. J Gen Virol 80 (Pt 4):943-8.
59. Clark, S. M., J. R. Roth, M. L. Clark, B. B. Barnett, and R. S. Spendlove. 1981. Trypsin enhancement of rotavirus infectivity: mechanism of enhancement. J Virol 39:816-22.
60. Clarke, M. L., L. J. Lockett, and G. W. Both. 1995. Membrane binding and endoplasmic reticulum retention sequences of rotavirus VP7 are distinct: role of carboxy-terminal and other residues in membrane binding. J Virol 69:6473-8.
61. Cohen, J., J. Laporte, A. Charpilienne, and R. Scherrer. 1979. Activation of rotavirus RNA polymerase by calcium chelation. Arch Virol 60:177-86.
62. Crawford, S. E., M. Labbe, J. Cohen, M. H. Burroughs, Y. J. Zhou, and M. K. Estes. 1994. Characterization of virus-like particles produced by the expression of rotavirus capsid proteins in insect cells. J Virol 68:5945-22.
63. Crawford, S. E., M. Labbe, J. Cohen, M. H. Burroughs, Y. J. Zhou, and M. K. Estes. 1994. Characterization of virus-like particles produced by the expression of rotavirus capsid proteins in insect cells. J Virol 68:5945-52.
64. Crawford, S. E., S. K. Mukherjee, M. K. Estes, J. A. Lawton, A. L. Shaw, R. F. Ramig, and B. V. Prasad. 2001. Trypsin cleavage stabilizes the rotavirus VP4 spike. J Virol 75:6052-61.
65. Cuadras, M. A., B. B. Bordier, J. L. Zambrano, J. E. Ludert, and H. B. Greenberg. 2006. Dissecting rotavirus particle-raft interaction with small interfering RNAs: insights into rotavirus transit through the secretory pathway. J Virol 80:3935-46.
66. Cuadras, M. A., and H. B. Greenberg. 2003. Rotavirus infectious particles use lipid rafts during replication for transport to the cell surface in vitro and in vivo. Virology 313:308-21.
67. Dector, M. A., P. Romero, S. Lopez, and C. F. Arias. 2002. Rotavirus gene silencing by small interfering RNAs. EMBO Rep 3:1175-80.
68. Delmas, O., M. Breton, C. Sapin, A. Le Bivic, O. Colard, and G. Trugnan. 2007. Heterogeneity of Raft-type membrane microdomains associated with VP4, the rotavirus spike protein, in Caco-2 and MA 104 cells. J Virol 81:1610-8.

69. **Delmas, O., A. M. Durand-Schneider, J. Cohen, O. Colard, and G. Trugnan.** 2004. Spike protein VP4 assembly with maturing rotavirus requires a postendoplasmic reticulum event in polarized caco-2 cells. J Virol **78:**10987-94.
70. **Delmas, O., A. Gardet, S. Chwetzoff, M. Breton, J. Cohen, O. Colard, C. Sapin, and G. Trugnan.** 2004. Different ways to reach the top of a cell. Analysis of rotavirus assembly and targeting in human intestinal cells reveals an original raft-dependent, Golgi-independent apical targeting pathway. Virology **327:**157-61.
71. **Delorme, C., H. Brussow, J. Sidoti, N. Roche, K. A. Karlsson, J. R. Neeser, and S. Teneberg.** 2001. Glycosphingolipid binding specificities of rotavirus: identification of a sialic acid-binding epitope. J Virol **75:**2276-87.
72. **Denisova, E., W. Dowling, R. LaMonica, R. Shaw, S. Scarlata, F. Ruggeri, and E. R. Mackow.** 1999. Rotavirus capsid protein VP5* permeabilizes membranes. J Virol **73:**3147-53.
73. **Dennehy, P. H.** 2008. Rotavirus vaccines: an overview. Clin Microbiol Rev **21:**198-208.
74. **Deo, R. C., C. M. Groft, K. R. Rajashankar, and S. K. Burley.** 2002. Recognition of the rotavirus mRNA 3' consensus by an asymmetric NSP3 homodimer. Cell **108:**71-81.
75. **Desselberger, U.** 1996. Genome rearrangements of rotaviruses. Arch Virol Suppl **12:**37-51.
76. **Desselberger, U., and M. A. McCrae.** 1994. The rotavirus genome. Curr Top Microbiol Immunol **185:**31-66.
77. **Diaz, Y., M. E. Chemello, F. Pena, O. C. Aristimuno, J. L. Zambrano, H. Rojas, F. Bartoli, L. Salazar, S. Chwetzoff, C. Sapin, G. Trugnan, F. Michelangeli, and M. C. Ruiz.** 2008. EXPRESSION OF NON STRUCTURAL ROTAVIRUS PROTEIN NSP4 MIMICKS Ca2+ HOMEOSTASIS CHANGES INDUCED BY ROTAVIRUS INFECTION IN CULTURED CELLS. J Virol.
78. **Dong, Y., C. Q. Zeng, J. M. Ball, M. K. Estes, and A. P. Morris.** 1997. The rotavirus enterotoxin NSP4 mobilizes intracellular calcium in human intestinal cells by stimulating phospholipase C-mediated inositol 1,4,5-trisphosphate production. Proc Natl Acad Sci U S A **94:**3960-5.
79. **Dormitzer, P. R., and H. B. Greenberg.** 1992. Calcium chelation induces a conformational change in recombinant herpes simplex virus-1-expressed rotavirus VP7. Virology **189:**828-32.
80. **Dormitzer, P. R., H. B. Greenberg, and S. C. Harrison.** 2000. Purified recombinant rotavirus VP7 forms soluble, calcium-dependent trimers. Virology **277:**420-8.
81. **Dormitzer, P. R., E. B. Nason, B. V. Prasad, and S. C. Harrison.** 2004. Structural rearrangements in the membrane penetration protein of a non-enveloped virus. Nature **430:**1053-8.
82. **Dormitzer, P. R., Z. Y. Sun, G. Wagner, and S. C. Harrison.** 2002. The rhesus rotavirus VP4 sialic acid binding domain has a galectin fold with a novel carbohydrate binding site. Embo J **21:**885-97.
83. **Dowling, W., E. Denisova, R. LaMonica, and E. R. Mackow.** 2000. Selective membrane permeabilization by the rotavirus VP5* protein is abrogated by mutations in an internal hydrophobic domain. J Virol **74:**6368-76.
84. **Eichwald, C., G. Jacob, B. Muszynski, J. E. Allende, and O. R. Burrone.** 2004. Uncoupling substrate and activation functions of rotavirus NSP5: phosphorylation of Ser-67 by casein kinase 1 is essential for hyperphosphorylation. Proc Natl Acad Sci U S A **101:**16304-9.
85. **Eichwald, C., J. F. Rodriguez, and O. R. Burrone.** 2004. Characterisation of rotavirus NSP2/NSP5 interaction and dynamics of viroplasms formation. J Gen Virol **85:**625-634.

86. **Eichwald, C., J. F. Rodriguez, and O. R. Burrone.** 2004. Characterization of rotavirus NSP2/NSP5 interactions and the dynamics of viroplasm formation. J Gen Virol **85:**625-34.
87. **Eichwald, C., F. Vascotto, E. Fabbretti, and O. R. Burrone.** 2002. Rotavirus NSP5: mapping phosphorylation sites and kinase activation and viroplasm localization domains. J Virol **76:**3461-70.
88. **Enouf, V., S. Chwetzoff, G. Trugnan, and J. Cohen.** 2003. Interactions of rotavirus VP4 spike protein with the endosomal protein Rab5 and the prenylated Rab acceptor PRA1. J Virol **77:**7041-7.
89. **Erk, I., J. C. Huet, M. Duarte, S. Duquerroy, F. Rey, J. Cohen, and J. Lepault.** 2003. A zinc ion controls assembly and stability of the major capsid protein of rotavirus. J Virol **77:**3595-601.
90. **Esparza, J., M. Gorziglia, F. Gil, and H. Romer.** 1980. Multiplication of human rotavirus in cultured cells: an electron microscopic study. J Gen Virol **47:**461-72.
91. **Estes, M., Kapikian, A.** 2007. Rotaviruses. In: Fields' Virology, 5th edition, P.H. DM Knipe, et al (Ed.), p. 1917-1974. Wolters Kluwer Health/Lippincott Williams & Wilkins, Philadelphia.
92. **Estes, M. K.** 2001. Rotaviruses and their replication. In: Fields' Virology, 4th edition, Knipe, D.M., Howley, P.M. et al (Ed), 1747-1785. Lippincott, Williams and Wilkins, Philadelphia.
93. **Estes, M. K., D. Y. Graham, C. P. Gerba, and E. M. Smith.** 1979. Simian rotavirus SA11 replication in cell cultures. J Virol **31:**810-5.
94. **Estes, M. K., D. Y. Graham, and B. B. Mason.** 1981. Proteolytic enhancement of rotavirus infectivity: molecular mechanisms. J Virol **39:**879-88.
95. **Estes, M. K., D. Y. Graham, E. M. Smith, and C. P. Gerba.** 1979. Rotavirus stability and inactivation. J Gen Virol **43:**403-9.
96. **Fabbretti, E., I. Afrikanova, F. Vascotto, and O. R. Burrone.** 1999. Two non-structural rotavirus proteins, NSP2 and NSP5, form viroplasm-like structures in vivo. J Gen Virol **80 (Pt 2):**333-9.
97. **Feng, N., J. A. Lawton, J. Gilbert, N. Kuklin, P. Vo, B. V. Prasad, and H. B. Greenberg.** 2002. Inhibition of rotavirus replication by a non-neutralizing, rotavirus VP6-specific IgA mAb. J Clin Invest **109:**1203-13.
98. **Fiore, L., H. B. Greenberg, and E. R. Mackow.** 1991. The VP8 fragment of VP4 is the rhesus rotavirus hemagglutinin. Virology **181:**553-63.
99. **Flewett, T. H., A. S. Bryden, and H. Davies.** 1973. Letter: Virus particles in gastroenteritis. Lancet **2:**1497.
100. **Fuentes-Panana, E. M., S. Lopez, M. Gorziglia, and C. F. Arias.** 1995. Mapping the hemagglutination domain of rotaviruses. J Virol **69:**2629-32.
101. **Fuerst, T. R., E. G. Niles, F. W. Studier, and B. Moss.** 1986. Eukaryotic transient-expression system based on recombinant vaccinia virus that synthesizes bacteriophage T7 RNA polymerase. Proc Natl Acad Sci U S A **83:**8122-6.
102. **Fukuhara, N., O. Yoshie, S. Kitaoka, and T. Konno.** 1988. Role of VP3 in human rotavirus internalization after target cell attachment via VP7. J Virol **62:**2209-18.
103. **Gajardo, R., P. Vende, D. Poncet, and J. Cohen.** 1997. Two proline residues are essential in the calcium-binding activity of rotavirus VP7 outer capsid protein. J Virol **71:**2211-6.
104. **Gallegos, C. O., and J. T. Patton.** 1989. Characterization of rotavirus replication intermediates: a model for the assembly of single-shelled particles. Virology **172:**616-27.

105. Gardet, A., M. Breton, P. Fontanges, G. Trugnan, and S. Chwetzoff. 2006. Rotavirus spike protein VP4 binds to and remodels actin bundles of the epithelial brush border into actin bodies. J Virol 80:3947-56.
106. Gardet, A., M. Breton, G. Trugnan, and S. Chwetzoff. 2007. Role for actin in the polarized release of rotavirus. J Virol 81:4892-4.
107. Golantsova, N. E., E. E. Gorbunova, and E. R. Mackow. 2004. Discrete domains within the rotavirus VP5* direct peripheral membrane association and membrane permeability. J Virol 78:2037-44.
108. Gonzalez, R. A., R. Espinosa, P. Romero, S. Lopez, and C. F. Arias. 2000. Relative localization of viroplasmic and endoplasmic reticulum-resident rotavirus proteins in infected cells. Arch Virol 145:1963-73.
109. Gonzalez, R. A., M. A. Torres-Vega, S. Lopez, and C. F. Arias. 1998. In vivo interactions among rotavirus nonstructural proteins. Arch Virol 143:981-96.
110. Gonzalez, S. A., and J. L. Affranchino. 1995. Assembly of double-layered virus-like particles in mammalian cells by coexpression of human rotavirus VP2 and VP6. J Gen Virol 76 (Pt 9):2357-60.
111. Gonzalez, S. A., and O. R. Burrone. 1989. Porcine OSU rotavirus segment II sequence shows common features with the viral gene of human origin. Nucleic Acids Res 17:6402.
112. Gonzalez, S. A., and O. R. Burrone. 1991. Rotavirus NS26 is modified by addition of single O-linked residues of N-acetylglucosamine. Virology 182:8-16.
113. Gonzalez, S. A., N. M. Mattion, R. Bellinzoni, and O. R. Burrone. 1989. Structure of rearranged genome segment 11 in two different rotavirus strains generated by a similar mechanism. J Gen Virol 70 (Pt 6):1329-36.
114. Gorziglia, M., C. Larrea, F. Liprandi, and J. Esparza. 1985. Biochemical evidence for the oligomeric (possibly trimeric) structure of the major inner capsid polypeptide (45K) of rotaviruses. J Gen Virol 66 (Pt 9):1889-900.
115. Gorziglia, M., K. Nishikawa, and N. Fukuhara. 1989. Evidence of duplication and deletion in super short segment 11 of rabbit rotavirus Alabama strain. Virology 170:587-90.
116. Graff, J. W., J. Ewen, K. Ettayebi, and M. E. Hardy. 2007. Zinc-binding domain of rotavirus NSP1 is required for proteasome-dependent degradation of IRF3 and autoregulatory NSP1 stability. J Gen Virol 88:613-20.
117. Graff, J. W., D. N. Mitzel, C. M. Weisend, M. L. Flenniken, and M. E. Hardy. 2002. Interferon regulatory factor 3 is a cellular partner of rotavirus NSP1. J Virol 76:9545-50.
118. Graham, A., G. Kudesia, A. M. Allen, and U. Desselberger. 1987. Reassortment of human rotavirus possessing genome rearrangements with bovine rotavirus: evidence for host cell selection. J Gen Virol 68 (Pt 1):115-22.
119. Graham, K. L., F. E. Fleming, P. Halasz, M. J. Hewish, H. S. Nagesha, I. H. Holmes, Y. Takada, and B. S. Coulson. 2005. Rotaviruses interact with alpha4beta7 and alpha4beta1 integrins by binding the same integrin domains as natural ligands. J Gen Virol 86:3397-408.
120. Graham, K. L., P. Halasz, Y. Tan, M. J. Hewish, Y. Takada, E. R. Mackow, M. K. Robinson, and B. S. Coulson. 2003. Integrin-using rotaviruses bind alpha2beta1 integrin alpha2 I domain via VP4 DGE sequence and recognize alphaXbeta2 and alphaVbeta3 by using VP7 during cell entry. J Virol 77:9969-78.
121. Graham, K. L., Y. Takada, and B. S. Coulson. 2006. Rotavirus spike protein VP5* binds alpha2beta1 integrin on the cell surface and competes with virus for cell binding and infectivity. J Gen Virol 87:1275-83.

122. **Graham, K. L., W. Zeng, Y. Takada, D. C. Jackson, and B. S. Coulson.** 2004. Effects on rotavirus cell binding and infection of monomeric and polymeric peptides containing alpha2beta1 and alphaxbeta2 integrin ligand sequences. J Virol **78:**11786-97.
123. **Gualtero, D. F., F. Guzman, O. Acosta, and C. A. Guerrero.** 2007. Amino acid domains 280-297 of VP6 and 531-554 of VP4 are implicated in heat shock cognate protein hsc70-mediated rotavirus infection. Arch Virol **152:**2183-96.
124. **Guerrero, C. A., D. Bouyssounade, S. Zarate, P. Isa, T. Lopez, R. Espinosa, P. Romero, E. Mendez, S. Lopez, and C. F. Arias.** 2002. Heat shock cognate protein 70 is involved in rotavirus cell entry. J Virol **76:**4096-102.
125. **Guerrero, C. A., E. Mendez, S. Zarate, P. Isa, S. Lopez, and C. F. Arias.** 2000. Integrin alpha(v)beta(3) mediates rotavirus cell entry. Proc Natl Acad Sci U S A **97:**14644-9.
126. **Guerrero, C. A., S. Zarate, G. Corkidi, S. Lopez, and C. F. Arias.** 2000. Biochemical characterization of rotavirus receptors in MA104 cells. J Virol **74:**9362-71.
127. **Guo, C. T., O. Nakagomi, M. Mochizuki, H. Ishida, M. Kiso, Y. Ohta, T. Suzuki, D. Miyamoto, K. I. Hidari, and Y. Suzuki.** 1999. Ganglioside GM(1a) on the cell surface is involved in the infection by human rotavirus KUN and MO strains. J Biochem (Tokyo) **126:**683-8.
128. **Halasz, P., F. E. Fleming, and B. S. Coulson.** 2005. Evaluation of specificity and effects of monoclonal antibodies submitted to the Eighth Human Leucocyte Differentiation Antigen Workshop on rotavirus-cell attachment and entry. Cell Immunol **236:**179-87.
129. **Hewish, M. J., Y. Takada, and B. S. Coulson.** 2000. Integrins alpha2beta1 and alpha4beta1 can mediate SA11 rotavirus attachment and entry into cells. J Virol **74:**228-36.
130. **Horie, Y., O. Nakagomi, Y. Koshimura, T. Nakagomi, Y. Suzuki, T. Oka, S. Sasaki, Y. Matsuda, and S. Watanabe.** 1999. Diarrhea induction by rotavirus NSP4 in the homologous mouse model system. Virology **262:**398-407.
131. **Hua, J., X. Chen, and J. T. Patton.** 1994. Deletion mapping of the rotavirus metalloprotein NS53 (NSP1): the conserved cysteine-rich region is essential for virus-specific RNA binding. J Virol **68:**3990-4000.
132. **Hua, J., and J. T. Patton.** 1994. The carboxyl-half of the rotavirus nonstructural protein NS53 (NSP1) is not required for virus replication. Virology **198:**567-76.
133. **Hwang, L. N., N. Englund, T. Das, A. K. Banerjee, and A. K. Pattnaik.** 1999. Optimal replication activity of vesicular stomatitis virus RNA polymerase requires phosphorylation of a residue(s) at carboxy-terminal domain II of its accessory subunit, phosphoprotein P. J Virol **73:**5613-20.
134. **Imataka, H., A. Gradi, and N. Sonenberg.** 1998. A newly identified N-terminal amino acid sequence of human eIF4G binds poly(A)-binding protein and functions in poly(A)-dependent translation. Embo J **17:**7480-9.
135. **Iturriza-Gomara, M., Desselberger, U., Gray, J.** 2003. Molecular epidemiology of rotaviruses: genetic mechanisms associated with diversity, p. 317-344. *In* U. D. J. G. (Eds) (ed.), Viral Gastroenteritis. Elsevier, Science, Amsterdam.
136. **Iturriza-Gomara, M., J. Green, D. W. Brown, U. Desselberger, and J. J. Gray.** 1999. Comparison of specific and random priming in the reverse transcriptase polymerase chain reaction for genotyping group A rotaviruses. J Virol Methods **78:**93-103.
137. **Jagannath, M. R., M. M. Kesavulu, R. Deepa, P. N. Sastri, S. S. Kumar, K. Suguna, and C. D. Rao.** 2006. N- and C-terminal cooperation in rotavirus enterotoxin: novel mechanism of

modulation of the properties of a multifunctional protein by a structurally and functionally overlapping conformational domain. J Virol **80:**412-25.

138. **Jayaram, H., Z. Taraporewala, J. T. Patton, and B. V. Prasad.** 2002. Rotavirus protein involved in genome replication and packaging exhibits a HIT-like fold. Nature **417:**311-5.
139. **Jiang, X., H. Jayaram, M. Kumar, S. J. Ludtke, M. K. Estes, and B. V. Prasad.** 2006. Cryoelectron microscopy structures of rotavirus NSP2-NSP5 and NSP2-RNA complexes: implications for genome replication. J Virol **80:**10829-35.
140. **Jolly, C. L., B. M. Beisner, and I. H. Holmes.** 2000. Rotavirus infection of MA104 cells is inhibited by Ricinus lectin and separately expressed single binding domains. Virology **275:**89-97.
141. **Jourdan, N., J. P. Brunet, C. Sapin, A. Blais, J. Cotte-Laffitte, F. Forestier, A. M. Quero, G. Trugnan, and A. L. Servin.** 1998. Rotavirus infection reduces sucrase-isomaltase expression in human intestinal epithelial cells by perturbing protein targeting and organization of microvillar cytoskeleton. J Virol **72:**7228-36.
142. **Jourdan, N., M. Maurice, D. Delautier, A. M. Quero, A. L. Servin, and G. Trugnan.** 1997. Rotavirus is released from the apical surface of cultured human intestinal cells through nonconventional vesicular transport that bypasses the Golgi apparatus. J Virol **71:**8268-78.
143. **Kabcenell, A. K., and P. H. Atkinson.** 1985. Processing of the rough endoplasmic reticulum membrane glycoproteins of rotavirus SA11. J Cell Biol **101:**1270-80.
144. **Kaljot, K. T., R. D. Shaw, D. H. Rubin, and H. B. Greenberg.** 1988. Infectious rotavirus enters cells by direct cell membrane penetration, not by endocytosis. J Virol **62:**1136-44.
145. **Kattoura, M. D., X. Chen, and J. T. Patton.** 1994. The rotavirus RNA-binding protein NS35 (NSP2) forms 10S multimers and interacts with the viral RNA polymerase. Virology **202:**803-13.
146. **Kirkwood, C. D., R. F. Bishop, and B. S. Coulson.** 1998. Attachment and growth of human rotaviruses RV-3 and S12/85 in Caco-2 cells depend on VP4. J Virol **72:**9348-52.
147. **Kobayashi, T., A. A. Antar, K. W. Boehme, P. Danthi, E. A. Eby, K. M. Guglielmi, G. H. Holm, E. M. Johnson, M. S. Maginnis, S. Naik, W. B. Skelton, J. D. Wetzel, G. J. Wilson, J. D. Chappell, and T. S. Dermody.** 2007. A plasmid-based reverse genetics system for animal double-stranded RNA viruses. Cell Host Microbe **1:**147-57.
148. **Kojima, K., K. Taniguchi, T. Urasawa, and S. Urasawa.** 1996. Sequence analysis of normal and rearranged NSP5 genes from human rotavirus strains isolated in nature: implications for the occurrence of the rearrangement at the step of plus strand synthesis. Virology **224:**446-52.
149. **Komoto, S., M. Kugita, J. Sasaki, and K. Taniguchi.** 2008. Generation of recombinant rotavirus with an antigenic mosaic of cross-reactive neutralization epitopes on VP4. J Virol **82:**6753-7.
150. **Komoto, S., J. Sasaki, and K. Taniguchi.** 2006. Reverse genetics system for introduction of site-specific mutations into the double-stranded RNA genome of infectious rotavirus. Proc Natl Acad Sci U S A **103:**4646-51.
151. **Kumar, M., H. Jayaram, R. Vasquez-Del Carpio, X. Jiang, Z. F. Taraporewala, R. H. Jacobson, J. T. Patton, and B. V. Prasad.** 2007. Crystallographic and biochemical analysis of rotavirus NSP2 with nucleotides reveals a nucleoside diphosphate kinase-like activity. J Virol **81:**12272-84.

152. **Labbe, M., P. Baudoux, A. Charpilienne, D. Poncet, and J. Cohen.** 1994. Identification of the nucleic acid binding domain of the rotavirus VP2 protein. J Gen Virol **75 (Pt 12):**3423-30.
153. **Labbe, M., A. Charpilienne, S. E. Crawford, M. K. Estes, and J. Cohen.** 1991. Expression of rotavirus VP2 produces empty corelike particles. J Virol **65:**2946-52.
154. **Laemmli, U. K.** 1970. Cleavage of structural proteins during the assembly of the head of bacteriophage T4. Nature **227:**680-5.
155. **LaMonica, R., S. S. Kocer, J. Nazarova, W. Dowling, E. Geimonen, R. D. Shaw, and E. R. Mackow.** 2001. VP4 differentially regulates TRAF2 signaling, disengaging JNK activation while directing NF-kappa B to effect rotavirus-specific cellular responses. J Biol Chem **276:**19889-96.
156. **Lawton, J. A., M. K. Estes, and B. V. Prasad.** 1999. Comparative structural analysis of transcriptionally competent and incompetent rotavirus-antibody complexes. Proc Natl Acad Sci U S A **96:**5428-33.
157. **Lawton, J. A., M. K. Estes, and B. V. Prasad.** 2001. Identification and characterization of a transcription pause site in rotavirus. J Virol **75:**1632-42.
158. **Lawton, J. A., M. K. Estes, and B. V. Prasad.** 2000. Mechanism of genome transcription in segmented dsRNA viruses. Adv Virus Res **55:**185-229.
159. **Lawton, J. A., M. K. Estes, and B. V. Prasad.** 1997. Three-dimensional visualization of mRNA release from actively transcribing rotavirus particles. Nat Struct Biol **4:**118-21.
160. **Lawton, J. A., C. Q. Zeng, S. K. Mukherjee, J. Cohen, M. K. Estes, and B. V. Prasad.** 1997. Three-dimensional structural analysis of recombinant rotavirus-like particles with intact and amino-terminal-deleted VP2: implications for the architecture of the VP2 capsid layer. J Virol **71:**7353-60.
161. **Lepault, J., I. Petitpas, I. Erk, J. Navaza, D. Bigot, M. Dona, P. Vachette, J. Cohen, and F. A. Rey.** 2001. Structural polymorphism of the major capsid protein of rotavirus. Embo J **20:**1498-507.
162. **Libersou, S., X. Siebert, M. Ouldali, L. F. Estrozi, J. Navaza, A. Charpilienne, P. Garnier, D. Poncet, and J. Lepault.** 2008. Geometric mismatches within the concentric layers of rotavirus particles: a potential regulatory switch of viral particle transcription activity. J Virol **82:**2844-52.
163. **Liu, M., and M. K. Estes.** 1989. Nucleotide sequence of the simian rotavirus SA11 genome segment 3. Nucleic Acids Res **17:**7991.
164. **Liu, M., N. M. Mattion, and M. K. Estes.** 1992. Rotavirus VP3 expressed in insect cells possesses guanylyltransferase activity. Virology **188:**77-84.
165. **Lopez, T., M. Camacho, M. Zayas, R. Najera, R. Sanchez, C. F. Arias, and S. Lopez.** 2005. Silencing the morphogenesis of rotavirus. J Virol **79:**184-92.
166. **Lopez, T., M. Rojas, C. Ayala-Breton, S. Lopez, and C. F. Arias.** 2005. Reduced expression of the rotavirus NSP5 gene has a pleiotropic effect on virus replication. J Gen Virol **86:**1609-17.
167. **Ludert, J. E., N. Feng, J. H. Yu, R. L. Broome, Y. Hoshino, and H. B. Greenberg.** 1996. Genetic mapping indicates that VP4 is the rotavirus cell attachment protein in vitro and in vivo. J Virol **70:**487-93.
168. **Lundgren, O., A. T. Peregrin, K. Persson, S. Kordasti, I. Uhnoo, and L. Svensson.** 2000. Role of the enteric nervous system in the fluid and electrolyte secretion of rotavirus diarrhea. Science **287:**491-5.

169. **Maass, D. R., and P. H. Atkinson.** 1994. Retention by the endoplasmic reticulum of rotavirus VP7 is controlled by three adjacent amino-terminal residues. J Virol **68**:366-78.
170. **Maass, D. R., and P. H. Atkinson.** 1990. Rotavirus proteins VP7, NS28, and VP4 form oligomeric structures. J Virol **64**:2632-41.
171. **Mackow, E. R., R. D. Shaw, S. M. Matsui, P. T. Vo, M. N. Dang, and H. B. Greenberg.** 1988. The rhesus rotavirus gene encoding protein VP3: location of amino acids involved in homologous and heterologous rotavirus neutralization and identification of a putative fusion region. Proc Natl Acad Sci U S A **85**:645-9.
172. **Martin, S., M. Lorrot, M. A. El Azher, and M. Vasseur.** 2002. Ionic strength- and temperature-induced K(Ca) shifts in the uncoating reaction of rotavirus strains RF and SA11: correlation with membrane permeabilization. J Virol **76**:552-9.
173. **Maruri-Avidal, L., S. Lopez, and C. F. Arias.** 2008. Endoplasmic reticulum chaperones are involved in the morphogenesis of rotavirus infectious particles. J Virol **82**:5368-80.
174. **Mathieu, M., I. Petitpas, J. Navaza, J. Lepault, E. Kohli, P. Pothier, B. V. Prasad, J. Cohen, and F. A. Rey.** 2001. Atomic structure of the major capsid protein of rotavirus: implications for the architecture of the virion. Embo J **20**:1485-97.
175. **Matthijnssens, J., M. Ciarlet, E. Heiman, I. Arijs, T. Delbeke, S. M. McDonald, E. A. Palombo, M. Iturriza-Gomara, P. Maes, J. T. Patton, M. Rahman, and M. Van Ranst.** 2008. Full Genome-Based Classification of Rotaviruses Reveals Common Origin between Human Wa-like and Porcine rotavirus strains and Human DS-1-like and Bovine Rotavirus strains. J Virol.
176. **Matthijnssens, J., M. Ciarlet, M. Rahman, H. Attoui, K. Banyai, M. K. Estes, J. R. Gentsch, M. Iturriza-Gomara, C. D. Kirkwood, V. Martella, P. P. Mertens, O. Nakagomi, J. T. Patton, F. M. Ruggeri, L. J. Saif, N. Santos, A. Steyer, K. Taniguchi, U. Desselberger, and M. Van Ranst.** 2008. Recommendations for the classification of group A rotaviruses using all 11 genomic RNA segments. Arch Virol **153**:1621-9.
177. **Mattion, N. M., J. Cohen, C. Aponte, and M. K. Estes.** 1992. Characterization of an oligomerization domain and RNA-binding properties on rotavirus nonstructural protein NS34. Virology **190**:68-83.
178. **Mattion, N. M., D. B. Mitchell, G. W. Both, and M. K. Estes.** 1991. Expression of rotavirus proteins encoded by alternative open reading frames of genome segment 11. Virology **181**:295-304.
179. **Mendez, E., C. F. Arias, and S. Lopez.** 1993. Binding to sialic acids is not an essential step for the entry of animal rotaviruses to epithelial cells in culture. J Virol **67**:5253-9.
180. **Meyer, J. C., C. C. Bergmann, and A. R. Bellamy.** 1989. Interaction of rotavirus cores with the nonstructural glycoprotein NS28. Virology **171**:98-107.
181. **Michelangeli, F., F. Liprandi, M. E. Chemello, M. Ciarlet, and M. C. Ruiz.** 1995. Selective depletion of stored calcium by thapsigargin blocks rotavirus maturation but not the cytopathic effect. J Virol **69**:3838-47.
182. **Mir, K. D., R. D. Parr, F. Schroeder, and J. M. Ball.** 2007. Rotavirus NSP4 interacts with both the amino- and carboxyl-termini of caveolin-1. Virus Res **126**:106-15.
183. **Mirazimi, A., K. E. Magnusson, and L. Svensson.** 2003. A cytoplasmic region of the NSP4 enterotoxin of rotavirus is involved in retention in the endoplasmic reticulum. J Gen Virol **84**:875-83.
184. **Mirazimi, A., M. Nilsson, and L. Svensson.** 1998. The molecular chaperone calnexin interacts with the NSP4 enterotoxin of rotavirus in vivo and in vitro. J Virol **72**:8705-9.

185. Mirazimi, A., and L. Svensson. 2000. ATP is required for correct folding and disulfide bond formation of rotavirus VP7. J Virol 74:8048-52.
186. Mirazimi, A., and L. Svensson. 1998. Carbohydrates facilitate correct disulfide bond formation and folding of rotavirus VP7. J Virol 72:3887-92.
187. Mirazimi, A., C. H. von Bonsdorff, and L. Svensson. 1996. Effect of brefeldin A on rotavirus assembly and oligosaccharide processing. Virology 217:554-63.
188. Mitchell, D. B., and G. W. Both. 1990. Completion of the genomic sequence of the simian rotavirus SA11: nucleotide sequences of segments 1, 2, and 3. Virology 177:324-31.
189. Mitchell, D. B., and G. W. Both. 1990. Conservation of a potential metal binding motif despite extensive sequence diversity in the rotavirus nonstructural protein NS53. Virology 174:618-21.
190. Mohan, K. V., J. Muller, and C. D. Atreya. 2003. The N- and C-terminal regions of rotavirus NSP5 are the critical determinants for the formation of viroplasm-like structures independent of NSP2. J Virol 77:12184-92.
191. Montero, H., C. F. Arias, and S. Lopez. 2006. Rotavirus Nonstructural Protein NSP3 is not required for viral protein synthesis. J Virol 80:9031-8.
192. Montero, H., M. Rojas, C. F. Arias, and S. Lopez. 2008. Rotavirus infection induces the phosphorylation of eIF2alpha but prevents the formation of stress granules. J Virol 82:1496-504.
193. Morris, A. P., J. K. Scott, J. M. Ball, C. Q. Zeng, W. K. O'Neal, and M. K. Estes. 1999. NSP4 elicits age-dependent diarrhea and Ca(2+)mediated I(-) influx into intestinal crypts of CF mice. Am J Physiol 277:G431-44.
194. Murphy, T. V., P. M. Gargiullo, M. S. Massoudi, D. B. Nelson, A. O. Jumaan, C. A. Okoro, L. R. Zanardi, S. Setia, E. Fair, C. W. LeBaron, M. Wharton, and J. R. Livengood. 2001. Intussusception among infants given an oral rotavirus vaccine. N Engl J Med 344:564-72.
195. Musalem, C., and R. T. Espejo. 1985. Release of progeny virus from cells infected with simian rotavirus SA11. J Gen Virol 66 (Pt 12):2715-24.
196. Nejmeddine, M., G. Trugnan, C. Sapin, E. Kohli, L. Svensson, S. Lopez, and J. Cohen. 2000. Rotavirus spike protein VP4 is present at the plasma membrane and is associated with microtubules in infected cells. J Virol 74:3313-20.
197. Newton, K., J. C. Meyer, A. R. Bellamy, and J. A. Taylor. 1997. Rotavirus nonstructural glycoprotein NSP4 alters plasma membrane permeability in mammalian cells. J Virol 71:9458-65.
198. Nickel, W. 2003. The mystery of nonclassical protein secretion. A current view on cargo proteins and potential export routes. Eur J Biochem 270:2109-19.
199. Obert, G., I. Peiffer, and A. L. Servin. 2000. Rotavirus-induced structural and functional alterations in tight junctions of polarized intestinal Caco-2 cell monolayers. J Virol 74:4645-51.
200. O'Brien, J. A., J. A. Taylor, and A. R. Bellamy. 2000. Probing the structure of rotavirus NSP4: a short sequence at the extreme C terminus mediates binding to the inner capsid particle. J Virol 74:5388-94.
201. Offit, P. A., R. D. Shaw, and H. B. Greenberg. 1986. Passive protection against rotavirus-induced diarrhea by monoclonal antibodies to surface proteins vp3 and vp7. J Virol 58:700-3.
202. Padilla-Noriega, L., O. Paniagua, and S. Guzman-Leon. 2002. Rotavirus protein NSP3 shuts off host cell protein synthesis. Virology 298:1-7.

203. **Parashar, U. D., C. J. Gibson, J. S. Bresse, and R. I. Glass.** 2006. Rotavirus and severe childhood diarrhea. Emerg Infect Dis **12:**304-6.
204. **Parr, R. D., S. M. Storey, D. M. Mitchell, A. L. McIntosh, M. Zhou, K. D. Mir, and J. M. Ball.** 2006. The rotavirus enterotoxin NSP4 directly interacts with the caveolar structural protein caveolin-1. J Virol **80:**2842-54.
205. **Patton, J., V. Chizhikov, Z. Taraporewala, and D.Y. Chen.** 2000. Virus replication. Rotaviruses. Methods and Protocols (J.Gray and U. Desselberger, Eds.). Humana Press, Totowa, NJ.:33-66.
206. **Patton, J. T.** 2001. Rotavirus RNA replication and gene expression. Novartis Found Symp **238:**64-77; discussion 77-81.
207. **Patton, J. T.** 1996. Rotavirus VP1 alone specifically binds to the 3' end of viral mRNA, but the interaction is not sufficient to initiate minus-strand synthesis. J Virol **70:**7940-7.
208. **Patton, J. T.** 1986. Synthesis of simian rotavirus SA11 double-stranded RNA in a cell-free system. Virus Res **6:**217-33.
209. **Patton, J. T., and D. Chen.** 1999. RNA-binding and capping activities of proteins in rotavirus open cores. J Virol **73:**1382-91.
210. **Patton, J. T., and C. O. Gallegos.** 1990. Rotavirus RNA replication: single-stranded RNA extends from the replicase particle. J Gen Virol **71 (Pt 5):**1087-94.
211. **Patton, J. T., and C. O. Gallegos.** 1988. Structure and protein composition of the rotavirus replicase particle. Virology **166:**358-65.
212. **Patton, J. T., M. T. Jones, A. N. Kalbach, Y. W. He, and J. Xiaobo.** 1997. Rotavirus RNA polymerase requires the core shell protein to synthesize the double-stranded RNA genome. J Virol **71:**9618-26.
213. **Patton, J. T., and E. Spencer.** 2000. Genome replication and packaging of segmented double-stranded RNA viruses. Virology **277:**217-25.
214. **Patton, J. T., Z. Taraporewala, D. Chen, V. Chizhikov, M. Jones, A. Elhelu, M. Collins, K. Kearney, M. Wagner, Y. Hoshino, and V. Gouvea.** 2001. Effect of intragenic rearrangement and changes in the 3' consensus sequence on NSP1 expression and rotavirus replication. J Virol **75:**2076-86.
215. **Patton, J. T., M. Wentz, J. Xiaobo, and R. F. Ramig.** 1996. cis-Acting signals that promote genome replication in rotavirus mRNA. J Virol **70:**3961-71.
216. **Perez-Vargas, J., P. Romero, S. Lopez, and C. F. Arias.** 2006. The peptide-binding and ATPase domains of recombinant hsc70 are required to interact with rotavirus and reduce its infectivity. J Virol **80:**3322-31.
217. **Pesavento, J. B., S. E. Crawford, E. Roberts, M. K. Estes, and B. V. Prasad.** 2005. pH-induced conformational change of the rotavirus VP4 spike: implications for cell entry and antibody neutralization. J Virol **79:**8572-80.
218. **Petrie, B. L., M. K. Estes, and D. Y. Graham.** 1983. Effects of tunicamycin on rotavirus morphogenesis and infectivity. J Virol **46:**270-4.
219. **Petrie, B. L., D. Y. Graham, H. Hanssen, and M. K. Estes.** 1982. Localization of rotavirus antigens in infected cells by ultrastructural immunocytochemistry. J Gen Virol **63:**457-67.
220. **Petrie, B. L., H. B. Greenberg, D. Y. Graham, and M. K. Estes.** 1984. Ultrastructural localization of rotavirus antigens using colloidal gold. Virus Res **1:**133-52.
221. **Pim, D., P. Massimi, S. M. Dilworth, and L. Banks.** 2005. Activation of the protein kinase B pathway by the HPV-16 E7 oncoprotein occurs through a mechanism involving interaction with PP2A. Oncogene **24:**7830-8.

222. **Pina-Vazquez, C., M. De Nova-Ocampo, S. Guzman-Leon, and L. Padilla-Noriega.** 2007. Post-translational regulation of rotavirus protein NSP1 expression in mammalian cells. Arch Virol **152:**345-68.
223. **Piron, M., T. Delaunay, J. Grosclaude, and D. Poncet.** 1999. Identification of the RNA-binding, dimerization, and eIF4GI-binding domains of rotavirus nonstructural protein NSP3. J Virol **73:**5411-21.
224. **Piron, M., P. Vende, J. Cohen, and D. Poncet.** 1998. Rotavirus RNA-binding protein NSP3 interacts with eIF4GI and evicts the poly(A) binding protein from eIF4F. Embo J **17:**5811-21.
225. **Pizarro, J. L., A. M. Sandino, J. M. Pizarro, J. Fernandez, and E. Spencer.** 1991. Characterization of rotavirus guanylyltransferase activity associated with polypeptide VP3. J Gen Virol **72 (Pt 2):**325-32.
226. **Poncet, D., C. Aponte, and J. Cohen.** 1993. Rotavirus protein NSP3 (NS34) is bound to the 3' end consensus sequence of viral mRNAs in infected cells. J Virol **67:**3159-65.
227. **Poncet, D., S. Laurent, and J. Cohen.** 1994. Four nucleotides are the minimal requirement for RNA recognition by rotavirus non-structural protein NSP3. Embo J **13:**4165-73.
228. **Poncet, D., P. Lindenbaum, R. L'Haridon, and J. Cohen.** 1997. In vivo and in vitro phosphorylation of rotavirus NSP5 correlates with its localization in viroplasms. J Virol **71:**34-41.
229. **Poruchynsky, M. S., and P. H. Atkinson.** 1991. Rotavirus protein rearrangements in purified membrane-enveloped intermediate particles. J Virol **65:**4720-7.
230. **Poruchynsky, M. S., D. R. Maass, and P. H. Atkinson.** 1991. Calcium depletion blocks the maturation of rotavirus by altering the oligomerization of virus-encoded proteins in the ER. J Cell Biol **114:**651-6.
231. **Poruchynsky, M. S., C. Tyndall, G. W. Both, F. Sato, A. R. Bellamy, and P. H. Atkinson.** 1985. Deletions into an NH2-terminal hydrophobic domain result in secretion of rotavirus VP7, a resident endoplasmic reticulum membrane glycoprotein. J Cell Biol **101:**2199-209.
232. **Prasad, B. V., J. W. Burns, E. Marietta, M. K. Estes, and W. Chiu.** 1990. Localization of VP4 neutralization sites in rotavirus by three-dimensional cryo-electron microscopy. Nature **343:**476-9.
233. **Prasad, B. V., and M. Estes.** 1997. Molecular Basis of Rotavirus Replication. Structure-Function Correlations., p. 239-268. *In* W. Chiu, R. M. Burnett, and G. R.L. (ed.), Structural Biology of Viruses. Oxford University Press, New York.
234. **Prasad, B. V., R. Rothnagel, C. Q. Zeng, J. Jakana, J. A. Lawton, W. Chiu, and M. K. Estes.** 1996. Visualization of ordered genomic RNA and localization of transcriptional complexes in rotavirus. Nature **382:**471-3.
235. **Prasad, B. V., G. J. Wang, J. P. Clerx, and W. Chiu.** 1988. Three-dimensional structure of rotavirus. J Mol Biol **199:**269-75.
236. **Predonzani, A., F. Arnoldi, A. Lopez-Requena, and O. R. Burrone.** 2008. In vivo site-specific biotinylation of proteins within the secretory pathway using a single vector system. BMC Biotechnol **8:**41.
237. **Preiss, T., and M. W. Hentze.** 1998. Dual function of the messenger RNA cap structure in poly(A)-tail-promoted translation in yeast. Nature **392:**516-20.
238. **Rainsford, E. W., and M. A. McCrae.** 2007. Characterization of the NSP6 protein product of rotavirus gene 11. Virus Res **130:**193-201.
239. **Ramig, R. F., and B. L. Petrie.** 1984. Characterization of temperature-sensitive mutants of simian rotavirus SA11: protein synthesis and morphogenesis. J Virol **49:**665-73.

240. **Ready, K. F., and M. Sabara.** 1987. In vitro assembly of bovine rotavirus nucleocapsid protein. Virology **157:**189-98.
241. **Richardson, S. C., L. E. Mercer, S. Sonza, and I. H. Holmes.** 1986. Intracellular localization of rotaviral proteins. Arch Virol **88:**251-64.
242. **Roner, M. R., and W. K. Joklik.** 2001. Reovirus reverse genetics: Incorporation of the CAT gene into the reovirus genome. Proc Natl Acad Sci U S A **98:**8036-41.
243. **Roner, M. R., I. Nepliouev, B. Sherry, and W. K. Joklik.** 1997. Construction and characterization of a reovirus double temperature-sensitive mutant. Proc Natl Acad Sci U S A **94:**6826-30.
244. **Ruggeri, F. M., and H. B. Greenberg.** 1991. Antibodies to the trypsin cleavage peptide VP8 neutralize rotavirus by inhibiting binding of virions to target cells in culture. J Virol **65:**2211-9.
245. **Ruiz, M. C., M. J. Abad, A. Charpilienne, J. Cohen, and F. Michelangeli.** 1997. Cell lines susceptible to infection are permeabilized by cleaved and solubilized outer layer proteins of rotavirus. J Gen Virol **78 (Pt 11):**2883-93.
246. **Ruiz, M. C., O. C. Aristimuno, Y. Diaz, F. Pena, M. E. Chemello, H. Rojas, J. E. Ludert, and F. Michelangeli.** 2007. Intracellular disassembly of infectious rotavirus particles by depletion of Ca2+ sequestered in the endoplasmic reticulum at the end of virus cycle. Virus Res **130:**140-50.
247. **Ruiz, M. C., A. Charpilienne, F. Liprandi, R. Gajardo, F. Michelangeli, and J. Cohen.** 1996. The concentration of Ca2+ that solubilizes outer capsid proteins from rotavirus particles is dependent on the strain. J Virol **70:**4877-83.
248. **Sabara, M., J. E. Gilchrist, G. R. Hudson, and L. A. Babiuk.** 1985. Preliminary characterization of an epitope involved in neutralization and cell attachment that is located on the major bovine rotavirus glycoprotein. J Virol **53:**58-66.
249. **Sabara, M., M. Parker, P. Aha, C. Cosco, E. Gibbons, S. Parsons, and L. A. Babiuk.** 1991. Assembly of double-shelled rotaviruslike particles by simultaneous expression of recombinant VP6 and VP7 proteins. J Virol **65:**6994-7.
250. **Sabara, M., K. F. Ready, P. J. Frenchick, and L. A. Babiuk.** 1987. Biochemical evidence for the oligomeric arrangement of bovine rotavirus nucleocapsid protein and its possible significance in the immunogenicity of this protein. J Gen Virol **68 (Pt 1):**123-33.
251. **Sanchez-San Martin, C., T. Lopez, C. F. Arias, and S. Lopez.** 2004. Characterization of rotavirus cell entry. J Virol **78:**2310-8.
252. **Sapin, C., O. Colard, O. Delmas, C. Tessier, M. Breton, V. Enouf, S. Chwetzoff, J. Ouanich, J. Cohen, C. Wolf, and G. Trugnan.** 2002. Rafts promote assembly and atypical targeting of a nonenveloped virus, rotavirus, in Caco-2 cells. J Virol **76:**4591-602.
253. **Sato, M., H. Suemori, N. Hata, M. Asagiri, K. Ogasawara, K. Nakao, T. Nakaya, M. Katsuki, S. Noguchi, N. Tanaka, and T. Taniguchi.** 2000. Distinct and essential roles of transcription factors IRF-3 and IRF-7 in response to viruses for IFN-alpha/beta gene induction. Immunity **13:**539-48.
254. **Schmid, S., D. Mayer, U. Schneider, and M. Schwemmle.** 2007. Functional characterization of the major and minor phosphorylation sites of the P protein of Borna disease virus. J Virol **81:**5497-507.
255. **Schuck, P., Z. Taraporewala, P. McPhie, and J. T. Patton.** 2001. Rotavirus nonstructural protein NSP2 self-assembles into octamers that undergo ligand-induced conformational changes. J Biol Chem **276:**9679-87.

256. Sen, A., N. Sen, and E. R. Mackow. 2007. The formation of viroplasm-like structures by the rotavirus NSP5 protein is calcium regulated and directed by a C-terminal helical domain. J Virol 81:11758-67.
257. Seo, N. S., C. Q. Zeng, J. M. Hyser, B. Utama, S. E. Crawford, K. J. Kim, M. Hook, and M. K. Estes. 2008. Inaugural article: integrins alpha1beta1 and alpha2beta1 are receptors for the rotavirus enterotoxin. Proc Natl Acad Sci U S A 105:8811-8.
258. Shahrabadi, M. S., L. A. Babiuk, and P. W. Lee. 1987. Further analysis of the role of calcium in rotavirus morphogenesis. Virology 158:103-11.
259. Shahrabadi, M. S., and P. W. Lee. 1986. Bovine rotavirus maturation is a calcium-dependent process. Virology 152:298-307.
260. Shaw, A. L., R. Rothnagel, D. Chen, R. F. Ramig, W. Chiu, and B. V. Prasad. 1993. Three-dimensional visualization of the rotavirus hemagglutinin structure. Cell 74:693-701.
261. Silvestri, L. S., Z. F. Taraporewala, and J. T. Patton. 2004. Rotavirus replication: plus-sense templates for double-stranded RNA synthesis are made in viroplasms. J Virol 78:7763-74.
262. Silvestri, L. S., M. A. Tortorici, R. Vasquez-Del Carpio, and J. T. Patton. 2005. Rotavirus glycoprotein NSP4 is a modulator of viral transcription in the infected cell. J Virol 79:15165-74.
263. Southern, J. A., D. F. Young, F. Heaney, W. K. Baumgartner, and R. E. Randall. 1991. Identification of an epitope on the P and V proteins of simian virus 5 that distinguishes between two isolates with different biological characteristics. J Gen Virol 72 (Pt 7):1551-7.
264. Spencer, E., and M. L. Arias. 1981. In vitro transcription catalyzed by heat-treated human rotavirus. J Virol 40:1-10.
265. Stacy-Phipps, S., and J. T. Patton. 1987. Synthesis of plus- and minus-strand RNA in rotavirus-infected cells. J Virol 61:3479-84.
266. Stirzaker, S. C., P. L. Whitfeld, D. L. Christie, A. R. Bellamy, and G. W. Both. 1987. Processing of rotavirus glycoprotein VP7: implications for the retention of the protein in the endoplasmic reticulum. J Cell Biol 105:2897-903.
267. Storey, S. M., T. F. Gibbons, C. V. Williams, R. D. Parr, F. Schroeder, and J. M. Ball. 2007. Full-length, glycosylated NSP4 is localized to plasma membrane caveolae by a novel raft isolation technique. J Virol 81:5472-83.
268. Suzuki, H., S. Kitaoka, T. Konno, T. Sato, and N. Ishida. 1985. Two modes of human rotavirus entry into MA 104 cells. Arch Virol 85:25-34.
269. Tafazoli, F., C. Q. Zeng, M. K. Estes, K. E. Magnusson, and L. Svensson. 2001. NSP4 enterotoxin of rotavirus induces paracellular leakage in polarized epithelial cells. J Virol 75:1540-6.
270. Taraporewala, Z., D. Chen, and J. T. Patton. 1999. Multimers formed by the rotavirus nonstructural protein NSP2 bind to RNA and have nucleoside triphosphatase activity. J Virol 73:9934-43.
271. Taraporewala, Z. F., X. Jiang, R. Vasquez-Del Carpio, H. Jayaram, B. V. Prasad, and J. T. Patton. 2006. Structure-function analysis of rotavirus NSP2 octamer by using a novel complementation system. J Virol 80:7984-94.
272. Taraporewala, Z. F., and J. T. Patton. 2001. Identification and characterization of the helix-destabilizing activity of rotavirus nonstructural protein NSP2. J Virol 75:4519-27.
273. Taraporewala, Z. F., P. Schuck, R. F. Ramig, L. Silvestri, and J. T. Patton. 2002. Analysis of a temperature-sensitive mutant rotavirus indicates that NSP2 octamers are the functional form of the protein. J Virol 76:7082-93.

274. **Tarun, S. Z., Jr., and A. B. Sachs.** 1995. A common function for mRNA 5' and 3' ends in translation initiation in yeast. Genes Dev **9**:2997-3007.
275. **Taylor, J. A., J. C. Meyer, M. A. Legge, J. A. O'Brien, J. E. Street, V. J. Lord, C. C. Bergmann, and A. R. Bellamy.** 1992. Transient expression and mutational analysis of the rotavirus intracellular receptor: the C-terminal methionine residue is essential for ligand binding. J Virol **66**:3566-72.
276. **Taylor, J. A., J. A. O'Brien, V. J. Lord, J. C. Meyer, and A. R. Bellamy.** 1993. The RER-localized rotavirus intracellular receptor: a truncated purified soluble form is multivalent and binds virus particles. Virology **194**:807-14.
277. **Taylor, J. A., J. A. O'Brien, and M. Yeager.** 1996. The cytoplasmic tail of NSP4, the endoplasmic reticulum-localized non-structural glycoprotein of rotavirus, contains distinct virus binding and coiled coil domains. Embo J **15**:4469-76.
278. **Tian, P., Y. Hu, W. P. Schilling, D. A. Lindsay, J. Eiden, and M. K. Estes.** 1994. The nonstructural glycoprotein of rotavirus affects intracellular calcium levels. J Virol **68**:251-7.
279. **Torres-Vega, M. A., R. A. Gonzalez, M. Duarte, D. Poncet, S. Lopez, and C. F. Arias.** 2000. The C-terminal domain of rotavirus NSP5 is essential for its multimerization, hyperphosphorylation and interaction with NSP6. J Gen Virol **81**:821-30.
280. **Tortorici, M. A., T. J. Broering, M. L. Nibert, and J. T. Patton.** 2003. Template recognition and formation of initiation complexes by the replicase of a segmented double-stranded RNA virus. J Biol Chem **278**:32673-82.
281. **Tortorici, M. A., B. A. Shapiro, and J. T. Patton.** 2006. A base-specific recognition signal in the 5' consensus sequence of rotavirus plus-strand RNAs promotes replication of the double-stranded RNA genome segments. Rna **12**:133-46.
282. **Towbin, H., T. Staehelin, and J. Gordon.** 1979. Electrophoretic transfer of proteins from polyacrylamide gels to nitrocellulose sheets: procedure and some applications. Proc Natl Acad Sci U S A **76**:4350-4.
283. **Trask, S. D., and P. R. Dormitzer.** 2006. Assembly of highly infectious rotavirus particles recoated with recombinant outer capsid proteins. J Virol **80**:11293-304.
284. **Valenzuela, S., J. Pizarro, A. M. Sandino, M. Vasquez, J. Fernandez, O. Hernandez, J. Patton, and E. Spencer.** 1991. Photoaffinity labeling of rotavirus VP1 with 8-azido-ATP: identification of the viral RNA polymerase. J Virol **65**:3964-7.
285. **Vascotto, F., M. Campagna, M. Visintin, A. Cattaneo, and O. R. Burrone.** 2004. Effects of intrabodies specific for rotavirus NSP5 during the virus replicative cycle. J Gen Virol **85**:3285-90.
286. **Vasquez, M., A. M. Sandino, J. M. Pizarro, J. Fernandez, S. Valenzuela, and E. Spencer.** 1993. Function of rotavirus VP3 polypeptide in viral morphogenesis. J Gen Virol **74 (Pt 5)**:937-41.
287. **Vasquez-Del Carpio, R., F. D. Gonzalez-Nilo, G. Riadi, Z. F. Taraporewala, and J. T. Patton.** 2006. Histidine triad-like motif of the rotavirus NSP2 octamer mediates both RTPase and NTPase activities. J Mol Biol **362**:539-54.
288. **Vasquez-del Carpio, R., J. L. Morales, M. Barro, A. Ricardo, and E. Spencer.** 2006. Bioinformatic prediction of polymerase elements in the rotavirus VP1 protein. Biol Res **39**:649-59.
289. **Vende, P., M. Piron, N. Castagne, and D. Poncet.** 2000. Efficient translation of rotavirus mRNA requires simultaneous interaction of NSP3 with the eukaryotic translation initiation factor eIF4G and the mRNA 3' end. J Virol **74**:7064-71.

290. Vende, P., Z. F. Taraporewala, and J. T. Patton. 2002. RNA-binding activity of the rotavirus phosphoprotein NSP5 includes affinity for double-stranded RNA. J Virol 76:5291-9.
291. Vende, P., M. A. Tortorici, Z. F. Taraporewala, and J. T. Patton. 2003. Rotavirus NSP2 interferes with the core lattice protein VP2 in initiation of minus-strand synthesis. Virology 313:261-73.
292. Vitour, D., P. Lindenbaum, P. Vende, M. M. Becker, and D. Poncet. 2004. RoXaN, a novel cellular protein containing TPR, LD, and zinc finger motifs, forms a ternary complex with eukaryotic initiation factor 4G and rotavirus NSP3. J Virol 78:3851-62.
293. Welch, S. K., S. E. Crawford, and M. K. Estes. 1989. Rotavirus SA11 genome segment 11 protein is a nonstructural phosphoprotein. J Virol 63:3974-82.
294. Wentz, M. J., J. T. Patton, and R. F. Ramig. 1996. The 3'-terminal consensus sequence of rotavirus mRNA is the minimal promoter of negative-strand RNA synthesis. J Virol 70:7833-41.
295. Whitfeld, P. L., C. Tyndall, S. C. Stirzaker, A. R. Bellamy, and G. W. Both. 1987. Location of sequences within rotavirus SA11 glycoprotein VP7 which direct it to the endoplasmic reticulum. Mol Cell Biol 7:2491-7.
296. Xu, A., A. R. Bellamy, and J. A. Taylor. 1998. BiP (GRP78) and endoplasmin (GRP94) are induced following rotavirus infection and bind transiently to an endoplasmic reticulum-localized virion component. J Virol 72:9865-72.
297. Xu, A., A. R. Bellamy, and J. A. Taylor. 2000. Immobilization of the early secretory pathway by a virus glycoprotein that binds to microtubules. Embo J 19:6465-74.
298. Xu, Y., Y. Xing, Y. Chen, Y. Chao, Z. Lin, E. Fan, J. W. Yu, S. Strack, P. D. Jeffrey, and Y. Shi. 2006. Structure of the protein phosphatase 2A holoenzyme. Cell 127:1239-51.
299. Yeager, M., J. A. Berriman, T. S. Baker, and A. R. Bellamy. 1994. Three-dimensional structure of the rotavirus haemagglutinin VP4 by cryo-electron microscopy and difference map analysis. Embo J 13:1011-8.
300. Yeager, M., K. A. Dryden, N. H. Olson, H. B. Greenberg, and T. S. Baker. 1990. Three-dimensional structure of rhesus rotavirus by cryoelectron microscopy and image reconstruction. J Cell Biol 110:2133-44.
301. Yoder, J. D., and P. R. Dormitzer. 2006. Alternative intermolecular contacts underlie the rotavirus VP5* two- to three-fold rearrangement. Embo J 25:1559-68.
302. Zambrano, J. L., Y. Diaz, F. Pena, E. Vizzi, M. C. Ruiz, F. Michelangeli, F. Liprandi, and J. E. Ludert. 2008. Silencing of rotavirus NSP4 or VP7 expression reduces alterations in Ca2+ homeostasis induced by infection of cultured cells. J Virol 82:5815-24.
303. Zarate, S., M. A. Cuadras, R. Espinosa, P. Romero, K. O. Juarez, M. Camacho-Nuez, C. F. Arias, and S. Lopez. 2003. Interaction of rotaviruses with Hsc70 during cell entry is mediated by VP5. J Virol 77:7254-60.
304. Zarate, S., R. Espinosa, P. Romero, C. A. Guerrero, C. F. Arias, and S. Lopez. 2000. Integrin alpha2beta1 mediates the cell attachment of the rotavirus neuraminidase-resistant variant nar3. Virology 278:50-4.
305. Zarate, S., R. Espinosa, P. Romero, E. Mendez, C. F. Arias, and S. Lopez. 2000. The VP5 domain of VP4 can mediate attachment of rotaviruses to cells. J Virol 74:593-9.
306. Zarate, S., P. Romero, R. Espinosa, C. F. Arias, and S. Lopez. 2004. VP7 mediates the interaction of rotaviruses with integrin alphavbeta3 through a novel integrin-binding site. J Virol 78:10839-47.

307. **Zeng, C. Q., M. K. Estes, A. Charpilienne, and J. Cohen.** 1998. The N terminus of rotavirus VP2 is necessary for encapsidation of VP1 and VP3. J Virol **72:**201-8.
308. **Zeng, C. Q., M. J. Wentz, J. Cohen, M. K. Estes, and R. F. Ramig.** 1996. Characterization and replicase activity of double-layered and single-layered rotavirus-like particles expressed from baculovirus recombinants. J Virol **70:**2736-42.
309. **Zhang, M., C. Q. Zeng, A. P. Morris, and M. K. Estes.** 2000. A functional NSP4 enterotoxin peptide secreted from rotavirus-infected cells. J Virol **74:**11663-70.

RINGRAZIAMENTI

Un sentito ringraziamento al mio supervisor Oscar Burrone per avermi concesso l'opportunità di realizzare questo progetto, per gli insegnamenti fondamentali in tutti questi anni di studio e lavoro e la costante e disponibile presenza.

Un grazie particolare al dottor Ulrich Desselberger per l'immancabile, gentile e prezioso sostegno, per avermi insegnato tanto ed essermi stato particolarmente vicino in ogni occasione.

Grazie a Roberta Contin per l'importante contributo a questo lavoro,
agli altri membri del "gruppo rotavirus", in particolare Michela Campagna, Fabio Rossi e Bartosz Muszynski, per lo stimolante e arricchente scambio di idee e consigli.

Un sentito ringraziamento al dottor Marco Bestagno, per la disponibilità e l'aiuto concreto in numerose occasioni.

Infine grazie a tutti gli amici del laboratorio, vicini e lontani, per aver condiviso con sincera amicizia molti momenti importanti della mia esperienza di dottorato,
alla mia famiglia e a Luca, per la costante presenza carica di fiducia e di affetto.